Med-X (2024) 2:28
https://doi.org/10.1007/s44258-024-00044-0

Med-X

REVIEW

Isolation of circulating tumor cells: recent progress and future perspectives

Ziheng Guo[1] · **Weiliang Xia**[1,2]

Received: 7 May 2024 / Revised: 13 October 2024 / Accepted: 22 October 2024

Abstract

Circulating tumor cells (CTCs) are cancer cells that shed from the primary tumor and enter into body fluids of the patient, where they travel to distant sites and ultimately form metastasis. Understanding the biology of CTCs, in particular at the critical stages of their itinerary, holds promises for better cancer cure. Since the beginning of this century, liquid biopsy has steadily grown to be a keen area of research due to its non-invasive features. As one of the most promising tumor biomarkers, CTCs have shown great potential in cancer diagnosis, prognosis, treatment response monitoring, and the exploration of biological mechanisms. Although various types of isolation and detection technologies emerge constantly, the rarity and heterogeneity of CTCs still pose huge challenges for these methods and make them inefficient. In addition, the clinical practice of different technologies still lacks reasonable and uniform standards. In this review, we provide a detailed overview of the isolation and enrichment strategies of CTCs, as well as their advantages and limitations. By summarizing the current status and suggesting future areas of CTCs research, we hope to continue the concerted effort for pushing forward the clinical application of CTCs, which may represent a paradigm shift for cancer theranostics in the future.

✉ Weiliang Xia
wlxia@sjtu.edu.cn

[1] School of Biomedical Engineering and Med-X Research Institute, Shanghai Jiao Tong University, Shanghai, China

[2] State Key Laboratory of Systems Medicine for Cancer, Renji Hospital, School of Medicine, Shanghai Jiao Tong University, Shanghai, China

Published online: 24 December 2024

Graphical Abstract

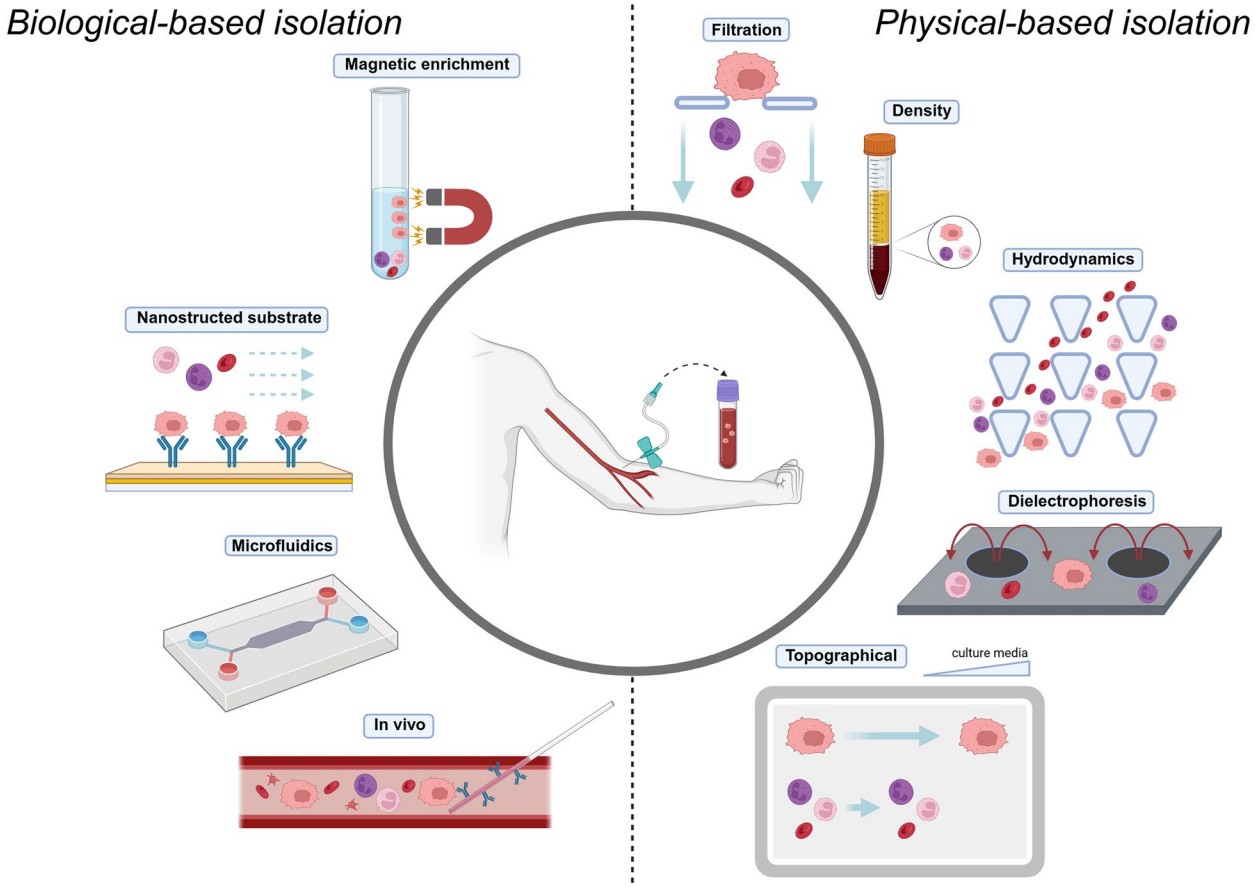

Highlights

- As seeds of metastasis, circulating tumor cells have shown great potential in cancer diagnosis, prognosis, and treatment.
- The rarity and heterogeneity of circulating tumor cells pose challenges for their isolation and detection technologies in clinical practice.
- This review summarizes and compares biological and physical isolation methods of circulating tumor cells.

Keywords Circulating tumor cells · Liquid biopsy · Tumor biomarker · Metastasis

Introduction

Cancer is a multifaceted and dynamic disease characterized by the unbridled proliferation and dissemination of aberrant cells within the human body. Despite advances in diagnosis and treatment, cancer still accounts for nearly 10 million and one in six deaths in 2020 according to World Health Organization (WHO) [1, 2]. Metastasis, a process by which tumor cells spread from primary site to other parts of the body through the bloodstream or lymphatic system, is the leading cause of death and indicates advanced stages and recurrence in cancer patients [3]. However, tumor may not show any noticeable symptoms in the early stages, which makes it difficult to detect with current medical imaging techniques and finally results in more cases of advanced stages and metastasis with lower five-year survival rate. On the other hand, even as the gold standard of clinical cancer diagnosis, tissue biopsy also has many limitations, such as invasiveness, inconvenience, and expensiveness. Moreover, the tumor heterogeneity could not be reflected comprehensively [4].

In the past two decades, liquid biopsy, as a non-invasive to obtain valuable information from patient body fluids such as blood, sputum, and pleural effusion, has become a hot area of research. Among liquid biopsy, CTCs, circulating tumor DNA (ctDNA), and exosomes are the most commonly detected biomarkers [4]. CTCs are tumor cells which detach from primary and metastatic tumors and enter the

bloodstream or lymphatic system. These cells can travel to distant sites, and finally form metastasis. ctDNA and EVs are tumor-derived DNA and lipid-bound nanovesicles, respectively, which are freely circulating in the blood of cancer patients. Compared to ctDNA and EVs, CTC is the most specific hallmark of cancer with complete genomes, transcriptomes, and proteomes, which can be utilized to better analyze the tumor heterogeneity [5]. Moreover, As the seed of cancer metastasis, CTCs can be used to dynamically monitor treatment response, indicate recurrence and prognosis, study drug resistance mechanism as well, which make them the best alternative to tissue biopsy. However, rare CTCs (1 ~ 1000 CTCs per mL) among a high background of blood cells [6] in the bloodstream makes their isolation and detection challenging [7]. In addition, the tumor heterogeneity between different patients and even within the same patient affects the capture efficiency and purity of CTCs isolation methods.

Nowadays, more and more techniques have been developed or upgraded for the sensitive and specific isolation of CTCs, which could be classified into three categories: (1) Biological-based isolation technologies, (2) Physical-based isolation technologies, and (3) Combined isolation technologies. In this review, we provide a detailed and complete summarization of those strategies and compare their advantages and disadvantages. In the end, we outline the bottlenecks and propose future directions of CTCs development.

Biological-based isolation technologies

Biological-based CTCs isolation technologies utilize specific ligands like antibodies or aptamers that bind to antigens on the surface of CTCs and then separate them from the patient blood. The most outstanding advantages of biological-based technologies are the good specificity and low false-positive rate. In this section, we generalize three methods for biological-based CTCs isolation: magnetic enrichment, nanostructured substrate, and microfluidics (Table 1), as well as their merits and limitations (Table 2).

Magnetic enrichment

Magnetic enrichment methods use magnetic beads coated with antibodies or aptamers to capture CTCs or leukocytes, which can be divided into positive enrichment and negative enrichment. For positive enrichment, CTCs bound to magnetic beads are retained with external magnet while the rest of the blood components are washed away. For negative enrichment, leukocytes bound to magnetic beads are retained with external magnet so that CTCs in the solution can be recovered.

Magnetic enrichment methods have many advantages such as simplicity, convenience, and high specificity. Nevertheless, these methods are limited by expensiveness, low cell viability, dependence on expressed proteins, difficulty in automation. In this section, we summarize magnetic enrichment methods, including antibody-based technologies and aptamer-based technologies.

Antibody-based technologies

Antibody, conjugated with magnetic microbeads, can identify the target proteins expressed on the surface of CTCs and separate CTCs from blood samples. Among these target proteins, *E*pithelial *C*ellular *A*dhesion *M*olecule (EpCAM), which is highly expressed on the surface of epithelial cells, is the most common biomarkers for CTCs isolation. As the "gold standard" of CTCs separation and detection methods, Cellsearch® system (Menarini Silicon Biosystems, Italy) is the first technology approved by the US Food and Drug Administration (FDA) which utilizes the magnetic beads coated with anti-EpCAM antibodies to capture CTCs from whole blood samples, and followed by verification with fluorescence-labeled antibodies including the anti-cytokeratins (CK 8,18 and 19) antibody and anti-CD45 antibody, together with the nuclear dye 4′,6-diamidino-2-phenylindole (DAPI). With Cellsearch® system, Allard et al. found that the recovery of SKBR-3 cells was 85% and 0 ~ 23,618 per 7.5 mL of blood (mean, 60 ± 693 CTCs per 7.5 mL of blood) CTCs (defined as CK^+, $DAPI^+$, $CD45^-$ and round or oval cell morphology) were captured and detected in 2,183 blood samples from 964 metastatic carcinoma patients [8]. Likewise, MACS® (Miltenyi Biotech GmbH) uses anti-CK/anti-EpCAM magnetic microbeads to isolate CTCs and identify them by immunofluorescence staining. For clinical tests, Katharina et al. have shown that CTCs (defined as CK^+, $DAPI^+$, $CD45^-$ and round or oval cell morphology) were isolated in 23 of 69 patients (33.3%) ranging from 1 to 19 per sample with MACS® technology [9].

To improve the purity and throughput of CTCs capture, Talasaz et al. designed the MagSweeper™ (Stanford University), which uses a magnetic rod to capture CTCs labeled with magnetic beads and then moves them to a wash station to remove other unwanted cells. Finally, CTCs are released in a release well with external magnets (Fig. 1A) [11]. Their study has shown that MagSweeper™ could successfully process 9 mL blood per hour and capture 62% ± 7% of MCF7 cells in spiking experiments with a purity of 51% ± 18%. Moreover, 12 ± 23 CTCs per 9 mL of blood were isolated in 47 of 47 patient samples. Further, Xiong et al. developed a biomimetic immuno-magnetosome (IMS), decorated with the leukocyte membrane and anti-EpCAM antibodies on a magnetic nanocluster (Fig. 1B) [15]. Due to the property of the leukocyte membrane, IMS could successfully

Table 1 Summary of biological-based CTCs isolation technologies

Technology	Company	Principle of capture	Capture efficiency	Recovery	Purity	Viability	Throughput	Cancer type	Volume of blood (mL)	Positive rate of patients	Range (*n*)	CTCs definition in the referred study
Magnetic enrichment (antibody-based)												
CellSearch® [8]	Menarini-Silicon Biosystems	EpCAM	N/A	≥ 85%	N/A	N/A	N/A	Breast colo-rectal prostate	7.5	71.4% (35/49)	0 ~ 23,618	CK^+, $DAPI^+$, $CD45^-$round or oval cell morphology (immunofluorescence)
MACS® [9, 10]	Miltenyi Biotech	EpCAM, CK	N/A	N/A	N/A	N/A	N/A	NSCLC breast pancreatic	7.5	33.3% (23/69)	1 ~ 19	CK^+, $DAPI^+$, $CD45^-$round or oval cell morphology (immunofluorescence)
MagSweeper™ [11, 12]	Stanford University	EpCAM	N/A	55 ~ 69%	51% ± 18%	N/A	9 mL/h	Breast colo-rectal prostate	9	100% (17/17)	12 ± 23	N/A
AdnaTest® [13, 14]	AdnaGen AG	EpCAM	N/A	N/A	N/A	N/A	N/A	Breast colon ovarian prostate	5	30% (13/43) 62% (34/55)	N/A	$EpCAM^+$ or CEA^+ or $EGFR^+$ or $HER2^+$ or $MUC1^+$(RT-PCR)
Immuno-magnetosomes [15]	N/A	EpCAM	84 ~ 100%	N/A	N/A	viable	N/A	N/A	N/A	N/A	N/A	N/A
Neutrophil membrane-coated immunomagnetic nanoparticles [16]	N/A	EpCAM	96.82%	N/A	90.68%	viable	N/A	breast	1	95% (19/20)	0 ~ 15	CK^+, $DAPI^+$, $CD45^-$(immunofluorescence)
Lipid magnetic spheres [17]	N/A	EpCAM Vimentin GPC3	98.64% in PBS 97.17% in simulated blood	98.12%	N/A	N/A	N/A	HCC	2	100% (17/17)	24.15 ± 4.47	CK^+, $DAPI^+$, $CD45^-$obvious cellular morphology (immunofluorescence)
N/A [18]	N/A	MUC16	> 95%	N/A	> 85%	92%	N/A	N/A	N/A	N/A	N/A	N/A
EasySep® [19]	STEMCELL Technologies	CD45	N/A	57 ~ 94%	1%	N/A	N/A	variety; melanoma	10	56% (47/84); 53% (17/32)	1 ~ 55; 1 ~ 551	$EpCAM^+$, CK^+, $CD45^-$; $MCSP^+$, $CD45^-$(flow cytometry)
Cyttel® [20, 21]	Cyttel Biosciences	CD45	N/A	N/A	N/A	N/A	N/A	NSCLC; colorectal	3.2	84.3% (107/127); 83.1% (49/59)	0 ~ 80; 2 ~ 46	centromere of chromosome 8^+, $DAPI^+$ and $CD45^-$(FISH)
DynaBeads® [22]	ThermoFisher Scientific	CD45	N/A	44 ± 23%	N/A	N/A	N/A	N/A	N/A	N/A	N/A	N/A
Magnetic enrichment (aptamer-based)												
NanoOctopus [23]	N/A	PTK7	88 ± 6%	N/A	97%	94%	N/A	AML	0.5 ~ 1	100% (33/33)	0 ~ 450	$PTK7^+$, $DAPI^+$, $CD45^-$(immunofluorescence)
Double-sided tape [24]	N/A	EpCAM	85 ± 10%	N/A	70 ± 10%	N/A	N/A	breast	0.5 ~ 1	100% (20/20)	0 ~ 120	$EpCAM^+$, CK^+, $CD45^-$(immunofluorescence)

Table 1 (continued)

Technology	Company	Principle of capture	Capture efficiency	Recovery	Purity	Viability	Throughput	Cancer type	Volume of blood (mL)	Positive rate of patients	Range (*n*)	CTCs definition in the referred study
HM-Fe3O4@SiO2/multi-DNA-Ag2S NDs [25]	N/A	MUC1	97.63%	96.24% in lysed blood 90.25% in whole blood	96.96%	N/A	N/A	breast	1	100% (8/8)	6 ~ 10	HM-Fe3O4@SiO2/Tetra-DNA-Ag2S nanobioprobe^{+}, CD45^{-}, Hoechst^{+}(immunofluorescence)
CoFe2O4@Ag magnetic nano-hybrids [26]	N/A	HER2	N/A	93.00 ~ 105.22%	N/A	> 80%	1 mL/75 min	N/A	1	N/A	N/A	N/A
Nanostructured substrate (antibody-based)												
3D silicon-nanopillar array [27]	N/A	EpCAM	45 ~ 65%	N/A	N/A	84 ~ 91%	N/A	N/A	N/A	N/A	N/A	N/A
TiO2 nanofibers substrate [28]	N/A	EpCAM	N/A	45%	N/A	N/A	N/A	Colorectal gastric	0.5	66.7% (2/3) 100% (7/7)	0 ~ 2 3 ~ 19	DAPI^{+}/ CK^{+}/ CD45^{-}30 μm > cell sizes > 10 μm (immunofluorescence)
PLGA nanofiber-NanoVelcro Chip [29]	N/A	EpCAM	75%	N/A	N/A	> 80%	0.5 mL/h	prostate	6	100% (1/1)	39 ~ 95	PSMA^{+}, CK^{+}, CD45^{-}, DAPI^{+}(immunofluorescence)
FAuNSs Fractal nanostructures [30]	N/A	EpCAM	62 ± 13%	> 50%	N/A	95%	N/A	N/A	N/A	N/A	N/A	N/A
Nanostructured substrate (aptamer-based)												
Chitosan [31]	N/A	EpCAM	45 ~ 60%	N/A	97%	95%	N/A	N/A	1	N/A	N/A	N/A
BSA-TiO2 nanorod array [32]	N/A	EpCAM	85 ~ 95%	85%	N/A	N/A	N/A	N/A	1	N/A	N/A	N/A
Gold nanowire array [33]	N/A	PTK7	50 ~ 61%	(50 ~ 61%) *96.2%	N/A	90%	N/A	N/A	N/A	N/A	N/A	N/A
Microfluidics (magnetic enrichment-based)												
IsoFlux™ System [34]	Fluxion	EpCAM	N/A	74 ~ 85%	1.40%	viable	N/A	Prostate colorectal	7.5	95% (21/22) 86.7% (13/15)	0 ~ 600	CK^{+}, CD45^{-}, Hoechest^{+}morphologically intact (immunofluorescence)
LiquidBiopsy® [35]	Cynvenio	EpCAM	N/A	82 ± 10% 86 ± 6% 89 ± 19%	11 ± 4% 77 ± 5% 70 ± 13%	N/A	N/A	N/A	8	N/A	N/A	N/A
Magnetic ranking cytometry [36]	N/A	EpCAM	N/A	95 ± 5% 93 ± 4% 91 ± 6% 94 ± 5%	N/A	98%	500 μL/h	mCRPC prostate	10	100% (24/24)	9 ~ 48 16 ~ 95	CK^{+}, DAPI^{+}, CD45^{-}(immunofluorescence)
Microfluidics (nanostructured substrate-based)												
OncoCEE™ [37, 38]	Biocept	cocktail	> 70%	> 75%	N/A	N/A	18 μL/min	breast	10; 20 (30)	89% (17/19); 80% (43/54)	0 ~ 166; 0 ~ 319	DAPI^{+}, CD45^{-}(immunofluorescence) HER2^{+}(FISH)

Table 1 (continued)

Technology	Company	Principle of capture	Capture efficiency	Recovery	Purity	Viability	Throughput	Cancer type	Volume of blood (mL)	Positive rate of patients	Range (*n*)	CTCs definition in the referred study
CTC-Chip [39]	N/A	EpCAM	65%	> 65% in PBS > 60% in whole blood	50%	Viable	1 ~ 2 mL/h	Lung Prostate Pancreatic Breast colon	0.9 ~ 5.1	99% (115/116)	5 ~ 1,281	CK^+, $DAPI^+$, $CD45^-$(immunofluorescence)
HTMSU [40]	N/A	EpCAM	> 97%	N/A	N/A	N/A	> 1.62 mL/h	N/A	1	N/A	N/A	N/A
Herringbone-chip [41]	N/A	EpCAM	91.8 ± 5.2%	N/A	14.0 ± 0.1%	95 ± 0.6%	1.5 ~ 2.5 mL/h	prostate	4	93% (14/15)	48 ~ 12,668	$PSMA^+$, $CD45^-$, $DAPI^+$(immunofluorescence)
Silicon nanopillar platform [42]	N/A	EpCAM	> 95%	> 95%	N/A	N/A	1 mL/h	prostate	1	77% (20/26)	0 ~ 33	CK^+, $CD45^-$, $DAPI^+$40 μm > diameter > 10 μm (immunofluorescence)
GO chip [43]	N/A	EpCAM	> 82.3%	65 ~ 94.2%	N/A	N/A	1 mL/h	Pancreatic Breast lung	1	100% (20/20)	2 ~ 23	CK^+, $DAPI^+$, $CD45^-$(immunofluorescence)
Geometrically enhanced mixing chip [44]	N/A	EpCAM	> 90%	92% in lysed blood 89% in whole blood	> 84%	> 86%	3.6 mL/h	pancreatic	N/A	94.4% (17/18)	0 ~ 7/mL	CK^+, $DAPI^+$, $CD45^-$ appropriate size and morphology (immunofluorescence)
DNA aptamer-enabled, micropillar-based microfluidic device [45]	N/A	cocktail	> 95%	N/A	81 ± 3%	93%	600 nL/s	N/A	1	N/A	N/A	N/A
Silicon nanowire substrate [46]	N/A	cocktail	> 50%	N/A	N/A	N/A	N/A	NSCLC	3, 4	100% (23/23)	1 ~ 71	CK^+, $DAPI^+$, $CD45^-$(immunofluorescence)
Nanoparticle herringbone-chip [47]	N/A	EpCAM, HER2, EGFR	68 ± 29.2% 72 ± 26.4%	(68 ± 29.2%) *91% (72 ± 26.4%) *92%	N/A	78% 87%	1 mL/h	breast	3.5	100% (4/4)	21 ~ 42	$DAPI^+$, $CD45^-$, $EpCAM^+$, cadherin 11 $(CDH11)^+$ (immunofluorescence)
In vivo												
CellCollector® [48]	GILUPI	EpCAM	N/A	N/A	N/A	N/A	30 min	NSCLC breast	N/A	83.3% (10/12) 100% (12/12)	0 ~ 50 2 ~ 515	$EpCAM^+$, CK^+, $DAPI^+$, $CD45^-$(immunofluorescence)

Abbreviations: *EpCAM* epithelial cell adhesion molecule, *CK* cytokeratin, *PTK7* protein tyrosine kinase 7, *MUC1* mucin 1, *MUC16* mucin16, *HER2* human epidermal growth factor receptor 2, *EGFR* epidermal growth factor receptor, *CEA* carcinoembryonic antigen, *MCSP* melanoma-associated chondroitin sulfate proteoglycan, *GPC3* Glypican-3, *NSCLC* non-small cell lung cancer, *HCC* hepatocellular carcinoma, *AML* acute myeloid system, *m-CRPC* metastic castrate-resistant prostate cancer, *RT-PCR* reverse transcriptase–polymerase chain reaction, *FISH* immunostaining and fluorescence in situ hybridization, *N/A* not available; # approved or cleared by Food and Drug Administration (FDA)

Table 2 Strengths and limitations of biological-based CTCs isolation technologies

Technology	Strengths	Limitations
Magnetic enrichment (antibody-based)		
CellSearch® [8][#]	high specificity convenient simple appropriate for all epithelial CTCs	omitting CTCs expressing low levels of EpCAM large blood volumes demand CTCs appear to be damaged magnetic beads may attach to the tube walls
MACS® [9, 10]	high specificity convenient simple appropriate for epithelial CTCs	omitting CTCs expressing low levels of EpCAM and CK CTCs appear to be damaged large blood volumes demand magnetic beads may attach to the tube walls
MagSweeper™ [11, 12]	high specificity higher throughput and purity than CellSearch® appropriate for epithelial CTCs	omitting CTCs expressing low levels of EpCAM CTCs appear to be damaged large blood volumes demand magnetic beads may attach to the tube walls
AdnaTest® [13, 14]	high specificity convenient simple appropriate for epithelial CTCs	omitting CTCs expressing low levels of EpCAM CTCs appear to be damaged magnetic beads may attach to the tube walls
Immuno-magnetosomes [15]	almost all of the captured cells were still viable low background leukocytes appropriate for epithelial CTCs	omitting CTCs expressing low levels of EpCAM expensive low throughput magnetic beads may attach to the tube walls lack of clinical data support
Neutrophil membrane-coated immunomagnetic nanoparticles [16]	high capture efficiency and purity high cell viability	low throughput magnetic beads may attach to the tube walls 1 mL blood might not contain CTCs
Lipid magnetic spheres [17]	high capture efficiency high sensitivity and specificity	magnetic beads may attach to the tube walls low purity low throughput
N/A [18]	high capture efficiency and purity high cell viability	magnetic beads may attach to the tube walls lack of clinical data support not applicable for pan-cancer low throughput
EasySep® [19]	high sensitivity and throughput high cell viability for downstream analysis	CTCs expressing CD45 may be removed low purity
Cyttel® [20, 21]	high sensitivity high throughput	CTCs expressing CD45 may be removed low purity erythrocyte lysis may cause damage to CTCs
DynaBeads® [22]	higher specificity and purity than CellSearch®	CTCs expressing CD45 may be removed only 3 types of DynaBeads are available magnetic beads may attach to the tube walls lack of clinical data support
Magnetic enrichment (aptamer-based)		
NanoOctopus [23]	high capture efficiency and purity simple quick high cell viability for downstream analysis cost-effectiveness	omitting CTCs expressing low levels of PTK7 low throughput magnetic beads may attach to the tube walls 1 mL blood might not contain CTCs
Double-sided tape [24]	reducing non-specific cellular uptake of ligand-MNPs by CTCs	omitting CTCs expressing low levels of EpCAM 1 mL blood might not contain CTCs low throughput
HM-Fe3O4@SiO2/multi-DNA-Ag2S NDs [25]	high recovery low background leukocytes simple	omitting CTCs expressing low levels of MUC1 1 mL blood might not contain CTCs low throughput

Table 2 (continued)

Technology	Strengths	Limitations
CoFe2O4@Ag magnetic nanohybrids [26]	high recovery and viability cheap and fast	omitting CTCs expressing low levels of HER2 1 mL blood might not contain CTCs lack of clinical data support high false positive rate
Nanostructured substrate (antibody-based)		
3D silicon-nanopillar array [27]	high specificity convenient high cell viability	omitting CTCs expressing low levels of EpCAM low throughput lack of clinical data support
TiO2 nanofibers substrate [28]	high specificity convenient	omitting CTCs expressing low levels of EpCAM 1 mL blood might not contain CTCs
PLGA nanofiber-NanoVelcro Chip [29]	high specificity and purity high cell viability isolating single CTCs for downstream analysis	omitting CTCs expressing low levels of EpCAM low throughput
FAuNSs Fractal nanostructures [30]	high specificity efficient release of CTCs with little damage	omitting CTCs expressing low levels of EpCAM low throughput lack of clinical data support
Nanostructured substrate (aptamer-based)		
Chitosan [31]	high specificity high purity high cell viability	omitting CTCs expressing low levels of EpCAM low throughput lack of clinical data support 1 mL blood might not contain CTCs
BSA-TiO2 nanorod array [32]	highly capture specificity and sensitivity	omitting CTCs expressing low levels of EpCAM low throughput lack of clinical data support 1 mL blood might not contain CTCs
Gold nanowire array [33]	high cell viability	omitting CTCs expressing low levels of PTK7 low throughput lack of clinical data support
Microfluidics (magnetic enrichment-based)		
IsoFlux™ System [34]	high recovery than CellSearch® of low EpCAM expression of CTCs controlling flow and improve isolate efficiency	omitting CTCs expressing low levels of EpCAM complex process and equipment
LiquidBiopsy® [35]	high throughput and specificity no rigid adherence to the EpCAM marker system	omitting CTCs expressing low levels of EpCAM complex process and equipment lack of clinical data support
Magnetic ranking cytometry [36]	high specificity enabling the sensitive capture of CTCs of different phenotypes	large blood volumes demand complicated manufacturing
Microfluidics (nanostructured substrate-based)		
OncoCEE™ [37, 38]	capture various subtypes of CTCs high sensitivity	large blood volumes demand expensive complex process and equipment
CTC-Chip [39]	high specificity high throughput capturing viable CTCs without pre-dilution, pre-labelling, and pre-fixation	omitting CTCs expressing low levels of EpCAM complex process and equipment
HTMSU [40]	high capture efficiency and specificity high throughput	omitting CTCs expressing low levels of EpCAM lack of clinical data support 1 mL blood might not contain CTCs

Table 2 (continued)

Technology	Strengths	Limitations
Herringbone-chip [41]	high capture efficiency high throughput high cell viability for downstream analysis capturing CTCs clusters	omitting CTCs expressing low levels of EpCAM complicated manufacturing
Silicon nanopillar platform [42]	high capture efficiency and sensitivity	omitting CTCs expressing low levels of EpCAM complicated manufacturing 1 mL blood might not contain CTCs
GO chip [43]	high capture efficiency and sensitivity	omitting CTCs expressing low levels of EpCAM complicated manufacturing 1 mL blood might not contain CTCs
Geometrically enhanced mixing chip [44]	high capture efficiency, purity, throughput and cell viability	complicated manufacturing erythrocyte lysis cause damage to CTCs 1 mL blood might not contain CTCs lack of clinical data support
DNA aptamer-enabled, micropillar-based microfluidic device [45]	high capture efficiency, purity, throughput and cell viability no pretreatment of blood samples	complex process and equipment lack of clinical data support
Silicon nanowire substrate [46]	capturing various subtypes of CTCs high sensitivity	low purity low throughput expensive
Nanoparticle herringbone-chip [47]	high capture efficiency and recover of various subtypes of CTCs high release ability and cell viability for downstream analysis	Expensive complicated manufacturing low throughput
In vivo		
CellCollector® [48]	overcoming sample blood volume limitations a large number of CTCS can be detected	omitting CTCs expressing low levels of EpCAM invasive

[#] approved or cleared by Food and Drug Administration (FDA)

capture 84% ~ 100% of MCF7 cells in spiking experiments while WBCs were almost undetectable. Moreover, Wu et al. functionalized immunomagnetic nanoparticles (IMNs) with neutrophil membranes in order to enhance the capture efficiency (from 41.36% to 96.82%) and purity (from 40.25% to 90.68%) of CTCs isolation, when compared to bare IMNs (Fig. 1C) [16]. Additionally, CTCs (defined as CK^+, $DAPI^+$ and $CD45^-$) were captured and detected in 19 out of total 20 breast cancer patients with a range of 0 ~ 15 per sample.

In fact, there are also some other epitopes, which have been used for CTCs isolation. For instance, Huang et al. designed the lipid magnetic spheres modified with three antibodies including EpCAM, vimentin, and Glypican-3 (GPC3), which presented a good specificity (96.94%), high sensitivity (98.12%) and excellent capture efficiency (98.64%) in spiking tests of Huh7 cells [17]. Their clinical experiments also showed that CTCs (CK^+, $DAPI^+$ and $CD45^-$ and obvious cellular morphology) were detected in 100% (17/17) hepatocellular carcinoma (HCC) patients with the number of 24.15 ± 4.47 per 2 mL of blood. In addition, Feely et al. used magnetic nanoparticles targeting mucin16 (MUC16), which is highly expressed in ≈90% of ovarian cancers, and achieved high yield (> 95%), high purity (> 85%) and high viability (92%) in spiking experiments of CA125 [18].

Except the immunofluorescence staining, AdnaTest® (AdnaGen AG) utilizes multiplex reverse transcriptase–polymerase chain reaction (RT-PCR) to detect the tumor-associated transcripts of CTCs based on the tumor type, such as epidermal growth factor receptor (EGFR), carcinoembryonic antigen (CEA), mucin 1 (MUC1), human epidermal growth factor receptor 2 (HER2) and EpCAM. For clinical tests, Tobias et al. found that 13 out of 43 (30%) patients had at least one CTC (CTCs are positively identified if at least one of the multiplex PCR markers was detected) [13]. Later, Danila et al. discovered that 34 out of 55 (62%) analyzed patients were positive for CTCs [14].

Immunomagnetic negative enrichment methods use specific antibodies targeting normal blood cells, such as anti-CD45, to eliminate them and reduce the background noise. For instance, EasySep® (STEMCELL Technologies) enriches CTCs by CD45 depletion and the remainder is stained with EpCAM and CK 7/8 (CTCs are defined as $EpCAM^+$, CK^+, and $CD45^-$ by flow cytometry). Liu et al.

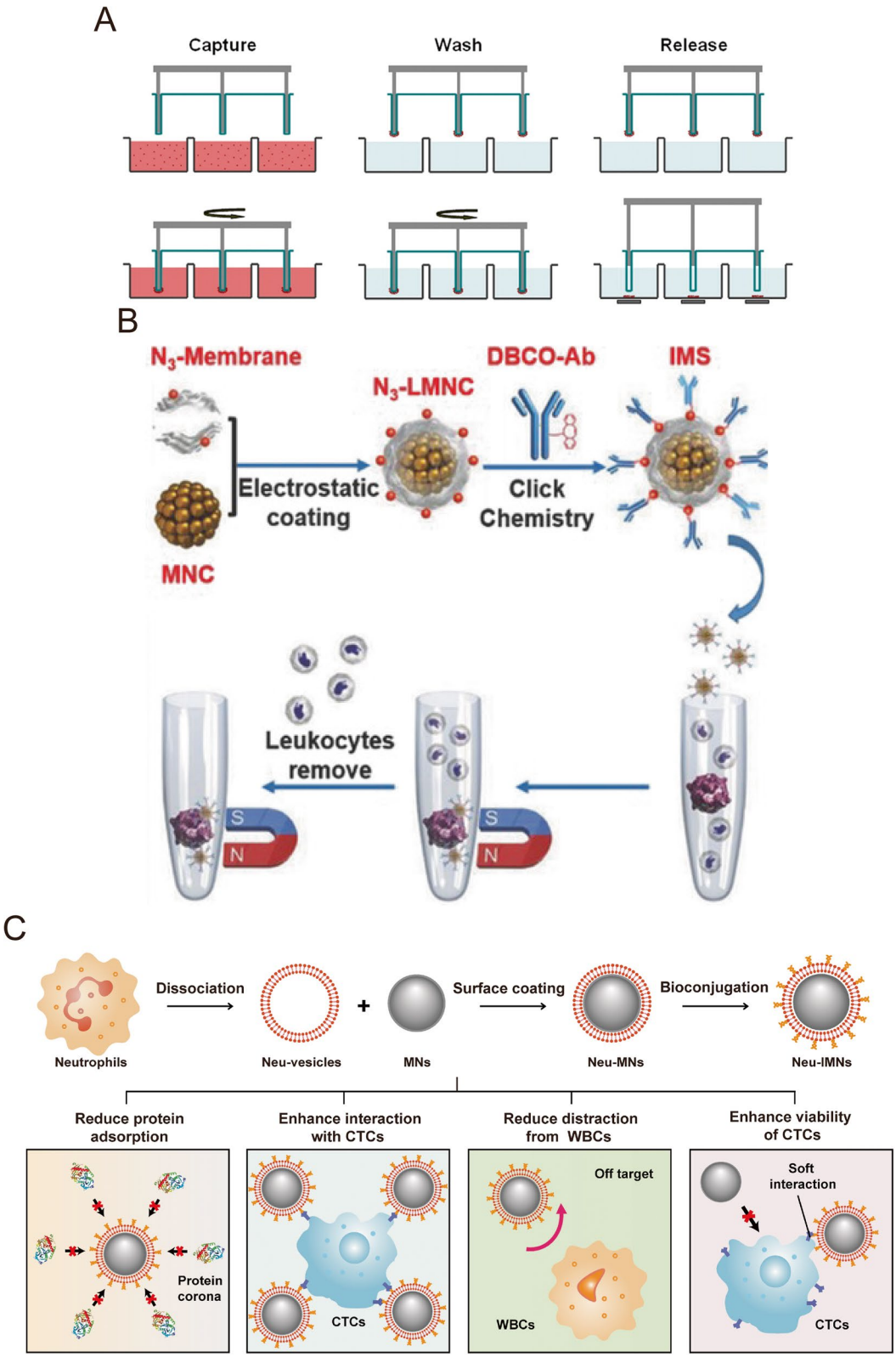

Fig. 1 Magnetic enrichment (antibody-based) CTCs isolation. **A** MagSweeper™ [11]. A magnetic rod which can capture CTCs labeled with magnetic beads, remove other unwanted cells in a wash station, and release CTCs in a release well. Copyright 2009, Proceedings of the National Academy of Sciences of the United States of America. **B** Immuno-magnetosomes [15]. A magnetic nanocluster decorated with the leukocyte membrane and anti-EpCAM antibodies. Copyright 2016, John Wiley and Sons. **C** Neutrophil membrane-coated immunomagnetic nanoparticles [16]. Immunomagnetic nanoparticles functionalized with neutrophil membranes in order to enhance the capture efficiency and purity of CTCs isolation. Copyright 2022, with permission from Elsevier

have shown that the recovery of SW620 cells ranged from 57 to 94% (median 69%) and 1 ~ 55 CTCs per 10 mL of blood were isolated in 47 of 84 (56%) samples [19]. Furthermore, Dynabeads® (ThermoFisher Scientific) system integrates the depletion of leukocytes with anti-CD45 magnetic beads and positive selection of CTCs with anti-EpCAM. Arik et al. reported that the recovery of Dynabeads® was a mean of 44 ± 23% compared to the EasySep™ system with a mean recovery of 24% ± 19% [22].

Abnormal chromosome numbers (aneuploidy) have been recognized as a common feature of malignant tumor. Therefore, Cyttel® (Cyttel Biosciences) combines erythrocyte lysis, CD45 subtraction enrichment, immunostaining and fluorescence in situ hybridization (FISH) to isolate and detect CTCs from blood samples. Bing et al. have illustrated that 0 ~ 80 CTCs (centromere of chromosome 8^+, $DAPI^+$ and $CD45^-$) per 3.2 mL of blood were detected in 107 of 127 Non-Small Cell Lung Carcinoma (NSCLC) patients [20]. Additionally, Yu et al. have found that 2 ~ 46 CTCs per 3.2 mL of blood were detected in 49 of 59 colorectal cancer patients [21].

Aptamer-based technologies

Aptamers are short, single-stranded RNA or DNA molecules that can specifically bind to target molecules. Therefore, aptamers can be designed to capture CTCs from blood samples when conjugated to microbeads.

In order to improve the capture efficiency, Chen et al. established the "NanoOctopus" with long aptamer DNA strands immobilized on magnetic microparticle and targeted the protein tyrosine kinase 7 (PTK7) receptors by mimicking the structure of octopus (Fig. 2A) [23]. The spiking experiments of CCRF-CEM cells showed the excellent capture efficiency (88 ± 6%) and purity (96.7%). In addition, their clinical results found that 0 ~ 450 per sample CTCs ($PTK7^+$, $CD45^-$, $DAPI^+$) were captured in 33 out of 33 Acute Myeloid System (AML) patients' blood. Since magnetic nanoparticles (MNPs) uptake will affect the viability and purity of CTCs, this group also designed a double-sided tape (DST), which makes CTCs interact with the ligand-MNPs with multiple copies of aptamers indirectly (Fig. 2B) [24]. With the DST method, CTCs (CK^+, $EpCAM^+$, $CD45^-$), with numbers ranging from 0 to 120 per sample, were captured in 20 of 20 breast cancer patients (100%).

Similar to IMS, Ding et al. have developed a nanoplatform which combines near-infrared (NIR) multivalent aptamer targeting MUC1, functionalized Ag2S nanodots, and hybrid cell membrane-coated MNPs to further reduce the background noise (Fig. 2C) [25]. Their study reported that MCF-7 cells were captured with the capture efficiency of 97.63% and the purity of 96.96% in spiking experiments and CTCs (HM-Fe3O4@SiO2/Tetra-DNA-Ag2S nanobioprobe$^+$, $CD45^-$, $Hoechst^+$) were identified and enumerated with a range of 6 ~ 10 mL^{-1} in the blood samples of eight cancer patients. Moreover, Fereshteh et al. integrated CoFe2O4@Ag magnetic nanohybrids and MXenes to isolate and detect CTCs with the recovery of 93.00–105.22% and more than 80% of CTCs being viable (Fig. 2D) [26].

Nanostructured substrate

Nanostructured substrate has become a popular method to be designed and modified with specific antibodies or aptamers to recognize and bind target cells. Since the specialized nanostructured surface provides a larger contact surface, the interaction between CTCs and the substrate will be enhanced, allowing for more efficient capture.

Nanostructured substrate-based isolation has many virtues. First, nanostructured surface has good specificity of CTCs capture which could reduce false-positive results. Additionally, this method increases the contact area and thus improves the capture efficiency. However, the process is time-consuming and the cost of producing and functionalizing is also a limiting factor. In this section, we summarize nanostructured substrate related methods, including antibody-based technologies and aptamer-based technologies.

Antibody-based technologies

In 2009, Wang et al. designed a 3D silicon-nanopillar (SiNP) array coated with anti-EpCAM antibodies, which achieved the capture efficiency of 45 ~ 65% and maintained the cell viability of 84 ~ 91% (Fig. 3A) [27]. Later, Nangang Zhang et al. constructed an electrospun TiO2 nanofibers (TiNFs)-deposited substrate modified with anti-EpCAM (Fig. 3B) [28]. Their results showed that the TiNFs enabled more than 45% recovery of spiked HCT116 cells. Furthermore, 0 ~ 2 and 3 ~ 19 CTCs per 0.5 mL of blood were captured in 2 of 3 colorectal cancer and 7 of 7 gastric cancer patients, respectively (CTCs: $DAPI^+$/ CK^+/ $CD45^-$, 30 μm > cell sizes > 10 μm).

To improve the purity and isolate single prostate CTC for downstream molecular analysis, Zhao et al. designed a PLGA nanofiber-NanoVelcro Chip, which integrates the NanoVelcro Chip with ArcturusXT laser capture microdissection (LCM) technology to capture, detect and isolate single CTC (Fig. 3C) [29]. The spiking experiments of PC3, C4-2 and LNCaP cells proved the good capture efficiency (74.7%) and viability (> 80%). In addition, more than 39 CTCs [prostate-specific membrane antigen $(PSMA)^+$, CK^+, $CD45^-$, $DAPI^+$] per 6 mL of blood were captured in one prostate patient.

Moreover, since cancer cell has a higher fractal dimension than normal cell and prefers to interact with fractal

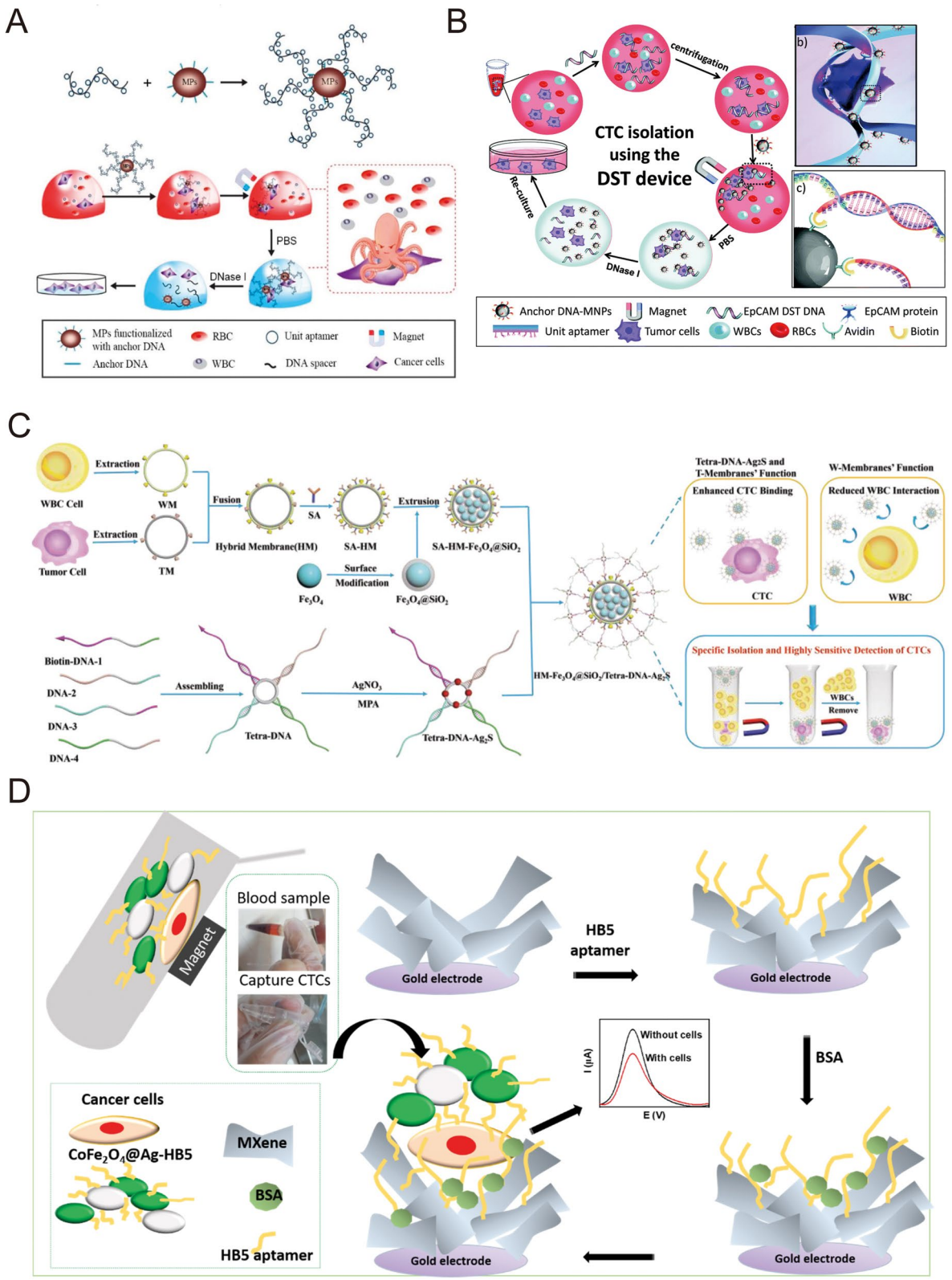

Fig. 2 Magnetic enrichment (aptamer-based) CTCs isolation. **A** NanoOctopus [23]. A technique with long aptamer DNA strands immobilized on magnetic microparticle and targeted PTK7 receptors by mimicking the structure of octopus. Copyright 2019, American Chemical Society. **B** Double-sided tape [24]. A DNA device which makes CTCs interact with the ligand-MNPs with multiple copies aptamers indirectly. Copyright 2019, Royal Society of Chemistry. **C** HM-Fe3O4@SiO2/Tetra-DNA-Ag2S [25]. A nanoplatform which combines near-infrared (NIR) multivalent aptamer targeting MUC1, functionalized Ag2S nanodots, and hybrid cell membrane-coated MNPs. Copyright 2020, John Wiley and Sons. **D** CoFe2O4@Ag magnetic nanohybrids [26]. A device which integrates CoFe2O4@Ag magnetic nanohybrids modified with HB5 aptamers and MXenes to isolate and detect CTCs. Copyright 2019, with permission from Elsevier

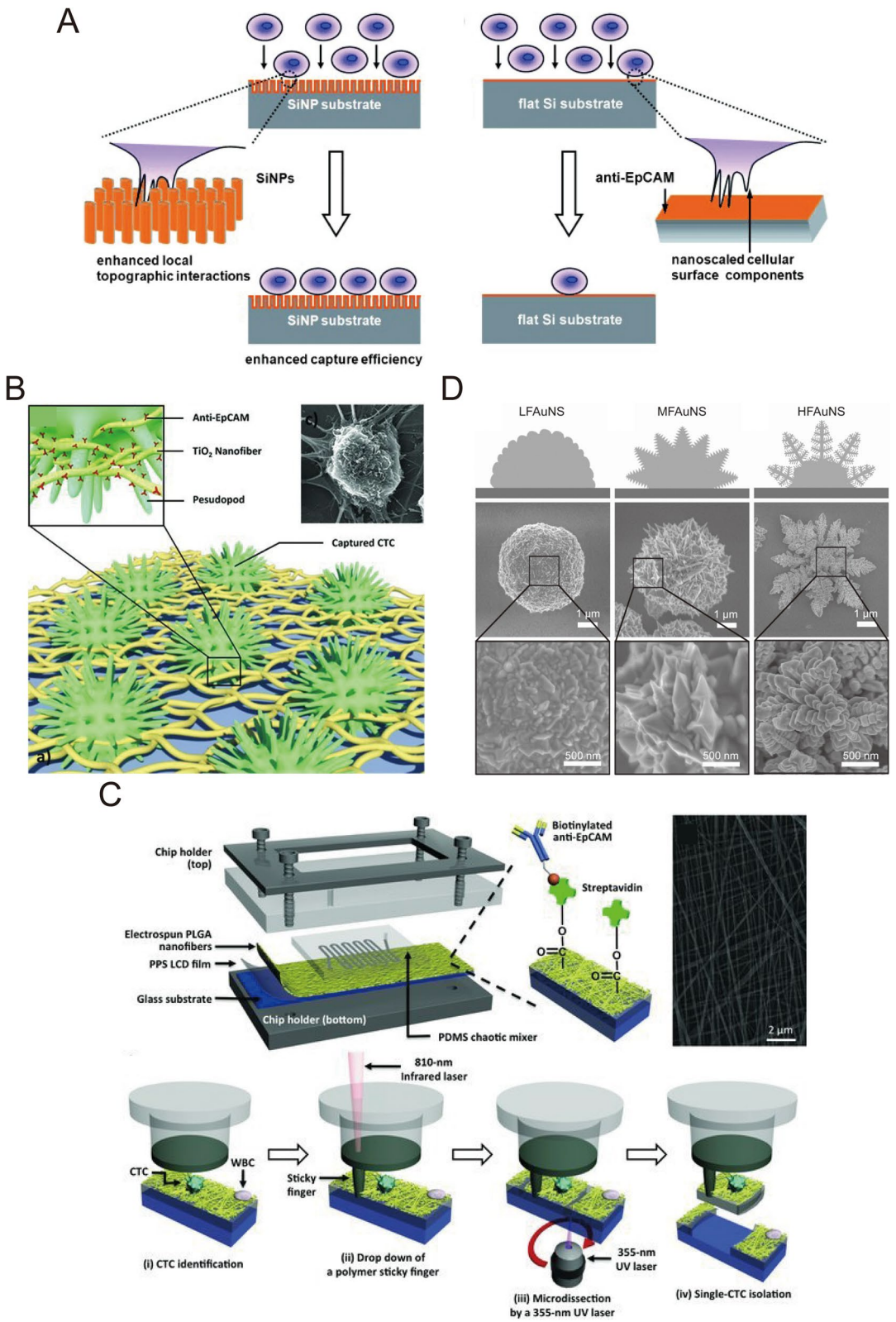

Fig. 3 Nanostructured substrate (antibody-based) CTCs isolation. **A** 3D silicon-nanopillar array [27]. A nanostructured substrate coated with anti-EpCAM. Copyright 2009, John Wiley and Sons. **B** TiO2 nanofibers substrate [28]. A nanostructured platform combined the electrospun TiO2 nanofibers (TiNFs)-deposited substrate and anti-EpCAM antibodies. Copyright 2012, John Wiley and Sons. **C** PLGA nanofiber-NanoVelcro Chip [29]. A device which integrates the NanoVelcro Chip with ArcturusXT laser capture microdissection (LCM) technology to capture, detect and isolate single CTC. Copyright 2013, John Wiley and Sons. **D** Fractal gold nanostructures [30]. A nanostructured substrate which can capture and release CTCs efficiently. Copyright 2013, John Wiley and Sons

nanostructures by enhanced topographic interactions, Zhang et al. designed the fractal gold nanostructures (FAuNSs) which can capture and release CTCs efficiently (Fig. 3D) [30]. Using the anti-EpCAM coated FAuNS interfaces, more than 50% recovery was achieved and 95% of CTCs were viably released through an electrochemical process.

Aptamer-based technologies

Similar to antibodies, aptamers can also be conjugated to nanostructured substrates to capture CTCs. In 2015, Sun et al. constructed a chitosan nanoparticle surface which is modified with polyethylene glycol (PEG) and DNA aptamer by electrospray to capture CTCs (Fig. 4A) [31]. Their spiking experiments reported that the capture efficiency of MCF-7 cells was 45 ~ 60% from 1 mL whole blood with the purity of 97% and the viability of 95%. Further, this group fabricated a multiscale TiO_2 nanorod array modified with bovine serum albumin (BSA) and DNA aptamer targeting EpCAM with high CTCs capture yield (85% ~ 95%) (Fig. 4B) [32].

To further improve the capture efficiency and reduce the nonspecific adsorption, Zhai et al. designed the gold nanowire arrays (AuNWs), modified with aptamer-sgc8c, PEG, and BSA by electrochemical deposition using anodic aluminum oxide (AAO) as template (Fig. 4C) [33]. They have found that spiked CCRF-CEM cells can be captured and released from AuNWs efficiently and keep excellent cell viability (90%).

Microfluidics

Microfluidic technologies can manipulate fluids at microliter or even nanoliter scale, using channels with dimensions of tens to hundreds of micrometers [49]. Due to the rarity of CTCs in the bloodstream, microfluidics has become promising systems which could control flow rate and isolate CTCs from blood samples as many as possible.

Biological-based microfluidics also utilizes antibodies or aptamers targeting specific surface protein of CTCs and separates them from other blood cells with many advantages, including good sensitivity, high efficiency and precise fluid manipulation. In this section, we sum up the biological-based microfluidics-related methods, including magnetic enrichment-based technologies and nanostructured substrate-based technologies.

Magnetic enrichment-based technology

In 2013, Wael et al. constructed the IsoFlux™ System (Fluxion Biosciences), which integrates microfluidics and magnetic enrichment method to isolate CTCs in an isolation zone (Fig. 5A) [34]. The spiking experiments have shown that the recovery of MDAMB-231, PC3 and SKBR3 cells was 74 ~ 85%. In addition, viable CTCs (CK^+, $CD45^-$, $Hoechest^+$ and morphologically intact) were captured in 21 of 22 (95%) prostate cancer patients and 13 of 15 (86.7%) colorectal cancer patients with numbers ranging from 0 to 600 per sample for downstream KRAS mutation analysis.

To capture CTCs of different phenotypes, Mahla et al. developed the magnetic ranking cytometry (MagRC), which could create high magnetic field gradients and capture CTCs in accordance with their expression of specific surface markers, such as EpCAM, by integrating microfluidics and X-shaped micromagnets (Fig. 5B) [36]. Their research reported the high recoveries of the spiked tumor cells (MCF-7 95 ± 5%, SKBR3 93 ± 4%, PC-3 91 ± 6%, MDA-MB-231 94 ± 5%) and the viability of captured cells (98%). Moreover, CTCs (CK^+, $CD45^-$, $DAPI^+$) were captured in 24 of 24 (100%) prostate cancer patients with numbers ranging from 9 to 95 per sample using the MagRC system.

Nanostructured substrate-based technology

In 2007, Sunitha et al. developed the CTC-chip which is capable of separating a large quantity of viable CTCs from blood samples with anti-EpCAM coated microposts under precisely controlled laminar flow conditions (Fig. 6A) [39]. The CTC-chip successfully recovered > 65% and > 60% spiked tumor cells in phosphate buffered saline (PBS) and whole blood, respectively. For clinical trials, CTCs (CK^+, $CD45^-$, $DAPI^+$) were isolated and detected in 115 of 116 (99%) blood samples of metastatic lung, prostate, pancreatic, breast and colon cancer patients with a range of 5 ~ 1,281 CTCs mL^{-1} per sample. To further enhance the interaction between CTCs and the antibody-coated device, Stott et al. constructed the herringbone-chip (HB-Chip), a high-throughput microfluidic mixing device that makes use of microvortices and surface ridges to disrupt blood streamline and increase the collisions between CTCs and the EpCAM-coated walls (Fig. 6B) [41]. Using the HB-Chip, PC3 cells were successfully recovered (91.8 ± 5.2%) with excellent cell viability (95 ± 0.6%) in spiking experiments. Furthermore, CTCs ($PSMA^+$, $CD45^-$, $DAPI^+$) were separated and detected in 14 of 15 (93%) prostate cancer patients with a range of 48 ~ 12,668 per sample (median = 63 CTCs/mL, mean = 386 ± 238 CTCs/mL). Later, in order to smoothly release captured CTCs, Park et al. coated gold nanoparticle on the surface of herringbone microfluidics chip, termed NP-HBCTC-Chip (Fig. 6C) [47], and their results showed that the average capture efficiency of spiked MDA-MD-231 and PC3 cells was 68 ± 29.2% and 72 ± 26.4%, respectively. In addition, clinical research found that CTCs [$DAPI^+$, $CD45^-$, $EpCAM^+$, cadherin 11 (CDH11) $^+$] were detected in 4 of

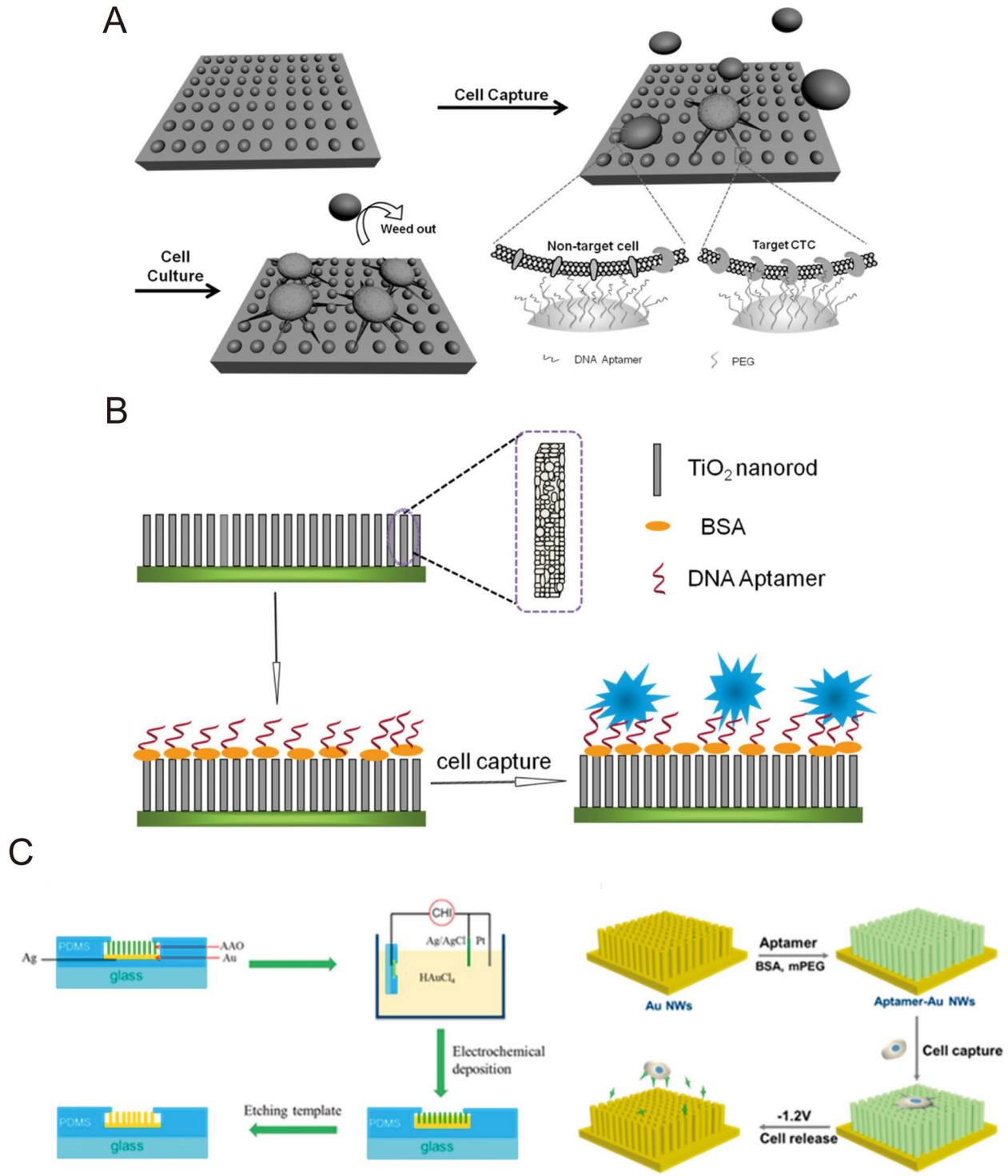

Fig. 4 Nanostructured substrate (aptamer-based) CTCs isolation. **A** Chitosan [31]. A nanoparticle surface fabricated by electrospray to specific capture rare CTCs. Copyright 2015, John Wiley and Sons. **B** BSA-TiO2 nanorod array [32]. A nanorod array modified with bovine serum albumin (BSA) and DNA aptamer targeting EpCAM. Copyright 2016, American Chemical Society. **C** Gold nanowire array [33]. An array modified with aptamer-sgc8c, PEG, and BSA by electrochemical deposition using anodic aluminum oxide (AAO) as template. Copyright 2017, American Chemical Society

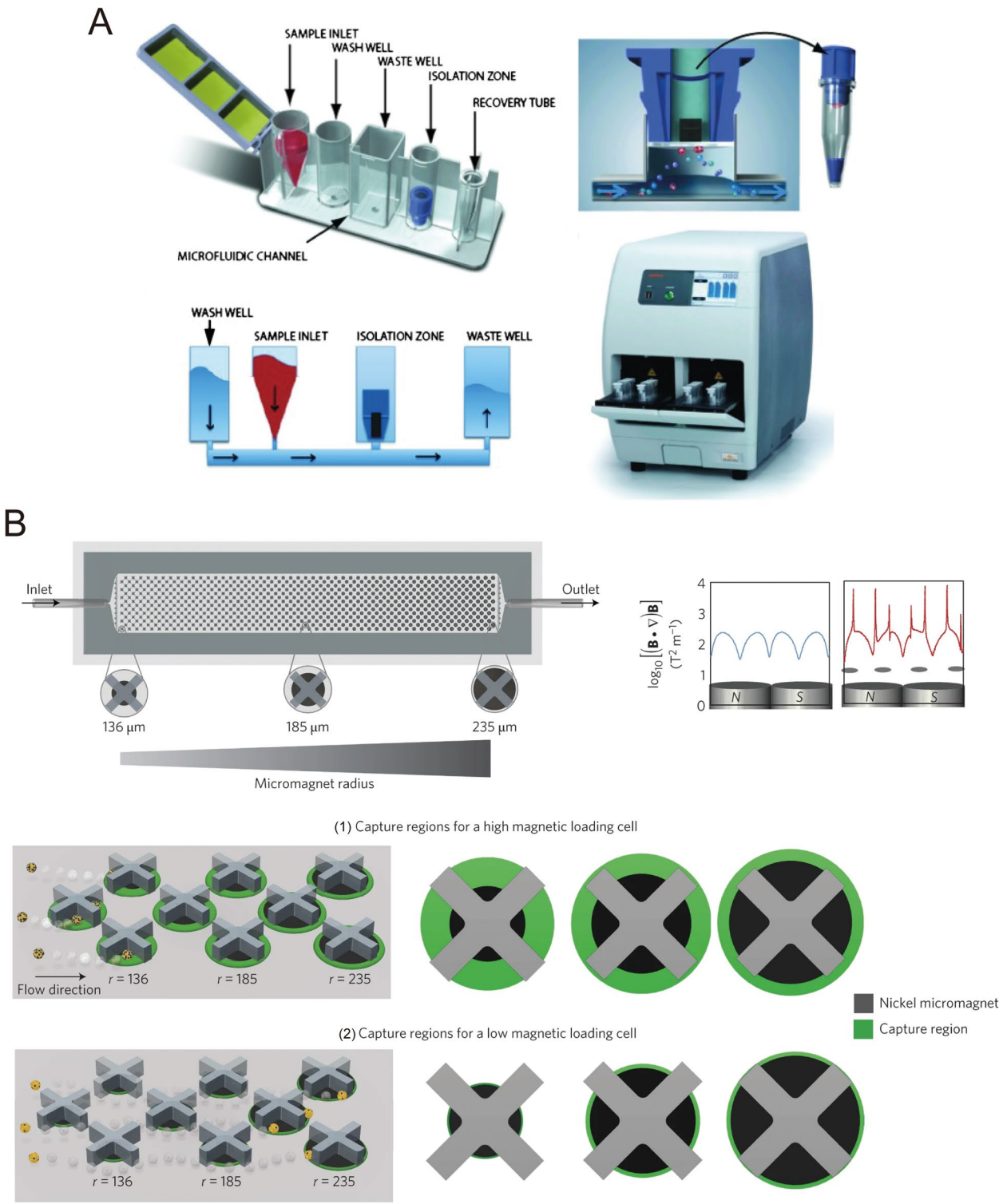

Fig. 5 Microfluidics (magnetic enrichment-based) CTCs isolation. **A** IsoFlux™ System [34]. A system which integrates microfluidics and magnetic enrichment method to isolate CTCs in an isolation zone. Copyright 2013, with permission from Elsevier. **B** Magnetic ranking cytometry [36]. A device which could create high magnetic field gradients and capture CTCs in accordance with their expression of specific surface markers, such as EpCAM, by integrating microfluidics and X-shaped micromagnets. Copyright 2017, Springer Nature

4 (100%) breast cancer patients ranging from 6 to 12 mL^{-1} of blood using the NP-HBCTC-Chip.

In addition to immunofluorescence staining and flow cytometry, Adams et al. fabricated a polymer-based HTMSU system, using anti-EpCAM antibodies to capture CTCs and single-cell conductivity sensor to enumerate CTCs, which achieved outstanding capture efficiency (> 97%) and high throughput (> 1.62 mL/h) [40].

In order to increase the contact frequency and further improve the capture efficiency and recovery of CTCs, Wang et al. reported a CTC-capture platform that integrates anti-EpCAM coated silicon nanopillar (SiNP) substrates with overlaid polydimethylsiloxane (PDMS) microfluidic chaotic mixers (Fig. 6D) [42]. In fact, more than 95% MCF7 cells were recovered in spiking experiments and 0 ~ 23 per sample CTCs (CK^+, $CD45^-$, $DAPI^+$, 40 μm > cell sizes > 10 μm) were captured in 20 of 26 prostate cancer patients in clinical tests. Further, Yoon et al. established a GO chip using functional graphene oxide nanosheets on a patterned gold surface and a PDMS layer as a microfluidic chamber to isolate CTCs effectively [43]. Their results showed the recovery was greater than 73% for high EpCAM expressing MCF-7 cells and more than 65% for low EpCAM expressing PC-3 cells in spiking experiments. Moreover, CTCs (CK^+, $CD45^-$, $DAPI^+$) with numbers ranging from 2 to 23 per sample were captured in 20 of 20 lung cancer patients with GO chip.

To improve the capture efficiency, purity, cell viability and throughput especially for rare target cells, Sheng et al. designed a geometrically enhanced mixing (GEM) chip based on geometrically optimized micromixer structures, which enhances the interaction between CTCs and anti-EpCAM substrates by transverse flow and flow folding (Fig. 6E) [44]. The GEM chip demonstrated good capture efficiency (> 90%), purity (> 84%), cell viability (86%) and high throughput (3.6 mL/h). In addition, their clinical experiments showed that CTCs (CK^+, $CD45^-$, $DAPI^+$, appropriate size and morphology) were captured in 17 of 18 pancreatic cancer patients ranging from 0 to 7 mL^{-1} of blood.

In addition to antibodies, aptamers have also been used for microfluidic-based CTCs separation. For instance, Sheng et al. designed a micropillar-based microfluidic device modified with aptamer cocktail which is able to efficiently isolate CTCs from whole blood with excellent capture efficiency (95%), good purity (81%) and also high cell viability (93%) [45]. Besides, Zhao et al. developed a silicon nanowire substrate (SiNS) embedded microfluidic chip to capture CTCs, modified with rational aptamer cocktail which presented > 50% capture performance across all five NSCLC cell lines (Fig. 6F) [46]. Clinical results revealed that CTCs (CK^+, $CD45^-$, $DAPI^+$) were captured in 23 out of 23 NSCLC samples with a range of 1 ~ 71 per sample.

In vivo method

To overcome the volume limitation of blood samples and capture a larger number of CTCs, Saucedo-Zeni et al. proposed an in vivo method, which uses functionalized and structured medical Seldinger guidewirews (FSMW) coated with anti-EpCAM to capture CTCs from peripheral blood vessels for 30 min [48]. Clinical results showed that FSMW successfully captured CTCs ($EpCAM^+$, CK^+, $CD45^-$, $DAPI^+$) from 10 of 12 breast cancer patients with a median of 5.5(0 ~ 50) per sample and 12 of 12 NSCLC patients with a median of 16(2 ~ 515) per sample.

In conclusion, biological-based methods mainly rely on the specific biomarkers expressed on tumor cell surfaces, such as EpCAM. However, depending on the type, stage, anatomical location and other factors of tumor, CTCs have a wide range of the expression level of EpCAM, based on the two recent studies (Fig. 7) [36, 50]. Furthermore, some metastatic tumor cells undergo epithelial-to-mesenchymal transition (EMT), decreasing the expression of epithelial markers typically used for detection. Therefore, to enhance the capture sensitivity of CTCs, some researchers used an antibody or aptamer cocktail targeting multiple markers, such as EpCAM, CK, and Vimentin. In this review, we describe six examples, including MACS® [9], Lipid magnetic spheres [17], OncoCEE™ [37, 38], DNA aptamer-enabled, micropillar-based microfluidic device [45], Silicon nanowire substrate [46], and Nanoparticle herringbone-chip [47], which take advantage of at least two epitopes to enrich CTCs. Nevertheless, this method increases the cost and may also compromise the purity since more epitopes mean more possibilities to capture part of WBCs with similar expression level.

Physical-based isolation technologies

Physical-based CTCs isolation technologies utilize the differences in biophysical properties between tumor cells and other blood cells, including size, density, deformability, dielectric property and surface adhesion to separate CTCs from whole blood. Physical-based isolation methods have many strengths, such as high throughput and the ability to isolate intact and viable CTCs, allowing for downstream analysis and characterization. In this section, we generalize filtration, density, hydrodynamics, dielectrophoresis and topographical techniques for CTCs isolation (Table 3), as well as their merits and limitations (Table 4).

Filtration

Since tumor cells are generally larger than most blood cells, filtration-based isolation methods use filters with pores of

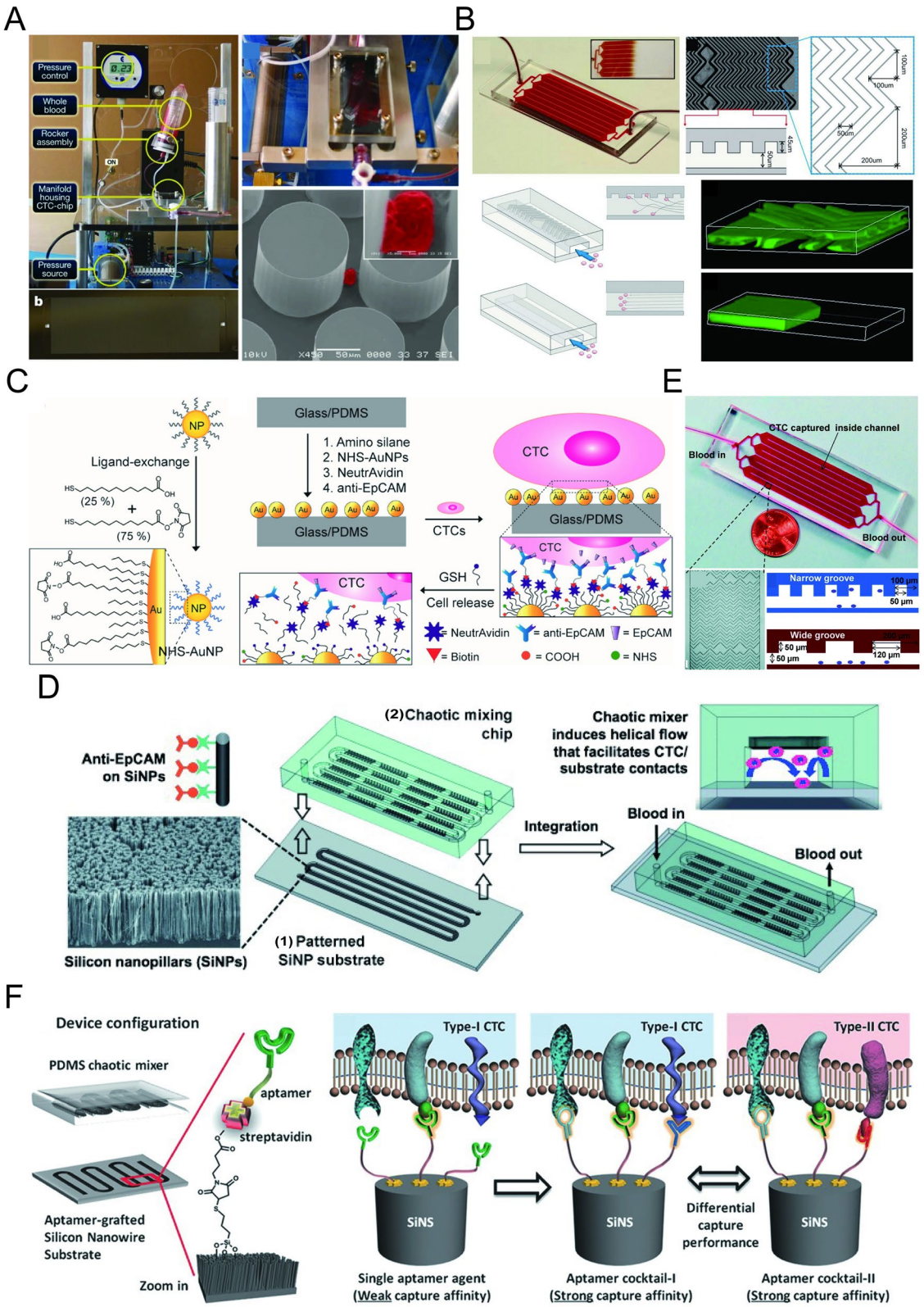
A
Pressure control
Whole blood
Rocker assembly
Manifold housing CTC-chip
Pressure source
B
C
Glass/PDMS
1. Amino silane
2. NHS-AuNPs
3. NeutrAvidin
4. anti-EpCAM
Ligand-exchange
(25 %)
(75 %)
NHS-AuNP
CTCs
GSH
Cell release
CTC
= NeutrAvidin
= anti-EpCAM
= EpCAM
= Biotin
= COOH
= NHS
D
Anti-EpCAM on SiNPs
Silicon nanopillars (SiNPs)
(1) Patterned SiNP substrate
(2)Chaotic mixing chip
Chaotic mixer induces helical flow that facilitates CTC/ substrate contacts
Integration
Blood in
Blood out
E
CTC captured inside channel
Blood in
Blood out
Narrow groove
Wide groove
F
Device configuration
PDMS chaotic mixer
aptamer
streptavidin
Aptamer-grafted Silicon Nanowire Substrate
Zoom in
Type-I CTC
Type-I CTC
Type-II CTC
SiNS
SiNS
SiNS
Differential capture performance
Single aptamer agent (Weak capture affinity)
Aptamer cocktail-I (Strong capture affinity)
Aptamer cocktail-II (Strong capture affinity)

◂**Fig. 6** Microfluidics (nanostructured substrate-based) CTCs isolation. **A** CTC-chip [39]. A microfluidic platform which is capable of separating a number of viable CTCs from blood samples with anti-EpCAM coated microposts under precisely controlled laminar flow conditions. Copyright 2007, Springer Nature. **B** Herringbone-chip [41]. A high-throughput microfluidic mixing device which makes use of microvortices and surface ridges to disrupt blood streamline and increase the collisions between CTCs and the EpCAM-coated walls. Copyright 2016, Proceedings of the National Academy of Sciences of the United States of America. **C** Nanoparticle herringbone-chip [47]. A chip which utilizes a chemical ligand-exchange reaction to release cells attached to a gold nanoparticle coating bound to HB-Chip. Copyright 2017, American Chemical Society. **D** Silicon nanopillar platform [42]. A CTC-capture platform that integrates anti-EpCAM coated SiNP substrates with overlaid polydimethylsiloxane (PDMS) microfluidic chaotic mixers. Copyright 2011, John Wiley and Sons. **E** Geometrically enhanced mixing chip [44]. A chip based on geometrically optimized micromixer structures, which enhances the interaction between CTCs and anti-EpCAM substrates by transverse flow and flow folding. Copyright 2014, Royal Society of Chemistry. **F** Silicon nanowire substrate [46]. A microfluidic chip which is modified with rational aptamer cocktail designed by cell-SELEX. Copyright 2016, John Wiley and Sons

specific size to separate CTCs. When blood samples pass through the filter, CTCs are retained while other smaller blood cells pass through.

Filtration-based approaches offer a few advantages in CTCs isolation, such as simplicity, inexpensiveness, and high throughput. However, there are also some shortcomings. For example, due to the size heterogeneity of tumor cells, some CTCs may be small and flexible, leading to their loss during the isolation. As reflected in Fig. 7, despite the fact that the diameters of most WBCs are below 13.9 μm (dot-dashed line), there is still an overlap of size between CTCs (ranging from 5.5 μm to 27 μm) and WBCs, resulting in low purity since some large leukocytes may be captured and misjudged as CTCs [50].

In 2000, Vona et al. developed the ISET® (Rare-cells Diagnostics) system, which utilizes a calibrated, 8-μm-diameter, cylindrical pores to separate CTCs from blood or diagnostic leukapheresis (DLA) samples with many advantages, such as high throughput and cell viability for downstream analysis [51]. Moreover, the clinical results of Tamminga et al. found that ISET® successfully isolated CTCs (TTF1/p40$^+$ or EpCAM$^+$, CD45$^-$) from 14 out of 16 NSCLC patients, with a range of 1.3 ~ 4 CTCs per mL of DLA [52]. Later, Desitter et al. constructed the ScreenCell® system which uses a filter with 7.5 ± 0.36 μm or 6.5 ± 0.33 μm circular pores to separate fixed or live cells, respectively (Fig. 8A) [53]. In spiking experiments, the recovery of H2030 cells was 91.2% or 74%, respectively. In addition, Kulasinghe et al. found that 0 ~ 3 CTCs (EGFR$^+$, CK$^+$, CD45$^-$, intact nuclei and morphologically different from leucocytes) per sample and clusters (5 or more CTCs) were detected in 13/28 (46.4%) advanced stage head and neck cancer (HNC) patients with ScreenCell® [54].

Since track-etch filters cannot overcome the problems of low porosity (3–5%) and non-uniform randomly distributed pores for CTCs isolation [53, 89, 90], Adams et al. utilized photolithographic technique to design a high porosity microfilters with an optimal diameter of 7 μm (CellSieve™, Creatv Microtech) which captured spiked MCF-7 cells at a rate of 98 ± 2% [57]. Furthermore, their clinical results showed that CTCs (CK$^+$, DAPI$^+$, CD45$^-$) were found in 10/10 breast patients with a range of 12 ~ 120 per sample.

In order to achieve precise fluid manipulation, Hvichia et al. constructed a FDA-cleared Parsortix™ cell separation system (ANGLE), which integrates microfluidics and stepped physical structures to separate CTCs with high capture efficiency (42 ~ 70%) of spiked PANC-1 cells and perfect cell viability (99%) (Fig. 8B) [58]. What's more, their clinical studies found that 0 ~ 26 CTCs (CK$^+$, DAPI$^+$, CD45$^-$) per sample were detected in 10 out of 26 cancer patients.

To improve the recovery of CTCs, Kim et al. utilized the fluid-assisted separation technology (FAST) and track-etched polycarbonate membrane with 8 μm pores to isolate CTCs from whole blood, which offers notable merits that include clog-free, high sensitivity (95.9 ± 3.1%), good specificity (> 2.5 log depletion of white blood cells), and excellent throughput (> 3 mL/min) (Fig. 8C) [59]. For clinical trials, the system successfully captured CTCs (CK$^+$/EpCAM$^+$, DAPI$^+$, CD45$^-$) in 83.3% (15/18) breast cancer patients (counts: 0 ~ 540 cells/7.5 mL blood), 82.9% (63/76) stomach cancer patients (counts: 2 ~ 485/7.5 mL blood), and 68.6% (24/35) lung cancer patients (counts: 0 ~ 62/7.5 mL blood). To further improve the capture efficiency and purity of CTCs, Tan et al. fabricated a crescent-shaped trap with three 5 μm gaps to isolate CTCs from whole blood, which achieved good isolation efficiency (> 80%) (Fig. 8D) [60]. Later, they developed a versatile label free biochip on the basis of the crescent-shaped trap and their clinical tests demonstrated that CTCs (CK$^+$, DAPI$^+$, CD45$^-$) were captured in 5 out of 5 lung cancer samples ranging from 20 to 85 per 2 mL of blood [61].

In addition to immunofluorescence staining, telomerase activation is a distinct feature of cancer cells which can also be used to detect CTCs. Therefore, Xu et al. used the real-time PCR-based telomeric repeat amplification protocol (TRAP) to measure telomerase activity from live CTCs captured on a parylene-C slot microfilter (6 μm) and patients were defined as positive if Ct values were below the threshold of 33 [62]. The microfilter platform achieved high capture efficiency (90%), high throughput (12 mL/h), and high cell viability (90%) for downstream analysis. Furthermore, clinical experiments showed that CTCs were detected in 6 out of 13 prostate cancer patients.

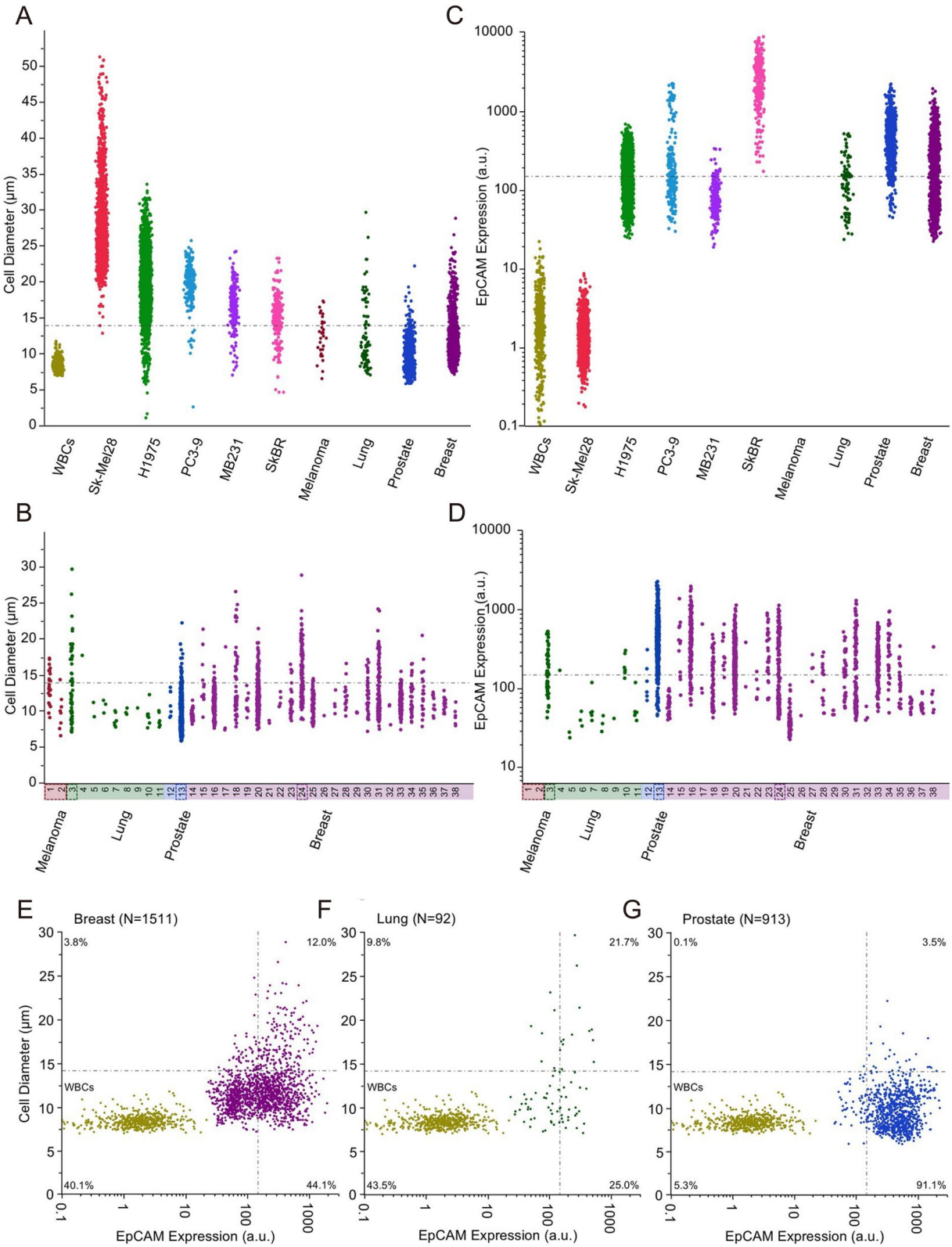
A
Cell Diameter (μm)
WBCs
Sk-Mel28
H1975
PC3-9
MB231
SkBR
Melanoma
Lung
Prostate
Breast
C
EpCAM Expression (a.u.)
B
D
E
Breast (N=1511)
3.8%
12.0%
WBCs
40.1%
44.1%
F
Lung (N=92)
9.8%
21.7%
43.5%
25.0%
G
Prostate (N=913)
0.1%
3.5%
5.3%
91.1%

◂**Fig. 7** Comparison of size and EpCAM expression between cell lines, WBCs and patient CTCs [50]. **A** The size distributions of the WBCs, cancer cell lines, including melanoma (SK-Mel28), lung (H1975), prostate (PC3-9) and breast (MB231 and SkBR) and CTCs of four cancer types obtained via monolithic chip. There are only 0.1% of WBCs, of which size are over the horizontal line at 13.9 μm. **B** The size distributions of CTCs derived from patients of four cancer types. **C** The EpCAM expression distributions of WBCs, cancer cell lines, including melanoma (SK-Mel28), lung (H1975), prostate (PC3-9) and breast (MB231 and SkBR) and CTCs of four cancer types. The horizontal line at 147 a.u. indicates the estimated CellSearch® threshold for capture. **D** The EpCAM expression distributions of CTCs derived from patients of four cancer types. The comparative distribution of EpCAM expression and size for single CTCs and WBCs in (**E**) breast cancer, (**F**) lung cancer and (**G**) prostate cancer patient. Note: the horizontal and vertical dotted and dashed lines are defined as the size of 13.9 μm and the EpCAM expression of 147 a.u. respectively. Copyright 2017, Springer Nature

To optimize the diameter and flow rate of the microcavities without clogging, Hosokawa et al. designed a circular size-selective microcavity array (MCA) with 9 μm in diameter, and achieved high capture efficiency (more than 80%), viability (98%) and throughput (200 – 1000 μL/min) for CTCs separation (Fig. 8E) [63]. Later, Yagi et al. developed a rectangular microcavity array (MCA) with sizes of 8 μm in width and 100 μm in length, and this MCA could recover more than 70% spiked NSCLC cells [64]. In addition, the system captured 0 ~ 46 CTCs (CK^+, $DAPI^+$, $CD45^-$) per 3 mL of blood in 80% (40/50) lung cancer patients.

Beyond that, Zhou et al. designed a separable bilayer (SB) microfilter with pores of 40 μm on the upper layer and 8 μm on the bottom layer for size-based CTCs capture (Fig. 8F) [65]. The SB microfilter demonstrated high capture efficiency (78 ~ 83%), high cell viability (71 ~ 74%) and captured CTCs in one colorectal cancer sample successfully.

Density

Density-based isolation methods separate CTCs from other blood components by gradient centrifugation. During centrifugation, CTCs and mononuclear cells (MNCs) migrate to a specific layer, which can be collected for subsequent identification and further analysis.

There are many advantages for density-based CTCs isolation. First, it is very simple, inexpensive, and rapid, requiring only needs one-step enrichment of CTCs by simple centrifugation. Second, it allows for the processing of large volumes of blood samples, increasing the number of captured CTCs. However, there are also a few limitations, such as low sensitivity and purity due to the overlap of density between CTCs and other blood cells, leading to CTCs loss or co-isolation.

Ficoll® (Biochrom, Berlin, Germany) and OncoQuick® (Greiner BioOne, Frickenhausen, Germany) are commonly used methods of density centrifugation. In 2002, Rosenberg et al. compared the capture efficiency between these two methods and found that the mean recovery of spiked tumor cells were 87% for OncoQuick® and 84% for Ficoll® [66]. In addition, they utilized OncoQuick® to capture CTCs in 11 out of 37 gastrointestinal cancer patients that were successfully detected by CK-20 RT-PCR.

Likewise, the AccuCyte®– CyteFinder® system also separates nucleated cells from the blood by density centrifugation and transfers them to microscopic slides for immunofluorescence staining and enumeration. The study by Campton et al. reported the excellent recovery of spiked tumor cells (90 ~ 91%) achieved by the AccuCyte®– CyteFinder® system, which outperformed Cellsearch® in a panel of 10 patients with advanced breast, prostate or colorectal cancer [68]. Moreover, van der Toom et al. also reported that CTCs ($DAPI^+$, CK^+ or $EpCAM^+$, $CD45/CD66b/CD11b/CD14/CD34^-$, diameter ≥ 4 μm) were captured in 8 out of 15 prostate patients, counting from 0 to 20 per sample by the AccuCyte® – CyteFinder® system [69].

Hydrodynamics

Hydrodynamics-based isolation methods take advantage of the physical properties such as size, shape, and deformability to separate CTCs from other blood components, which can be divided into four types: deterministic lateral displacement (DLD), dean flow fractionation (DFF), microfluidic vortex, and inertial migration.

Hydrodynamics-based CTCs isolation has notable merits: (1) capture efficiency, (2) CTCs viability and intactness, and (3) easy integration with other CTC capture or analysis technologies. Nevertheless, there are still disadvantages associated with hydrodynamics-based CTCs isolation. The specificity and sensitivity of CTCs separation are affected by the overlap of physical properties between some CTCs and leukocytes.

Deterministic lateral displacement

In 2012, Loutherback et al. developed a microfluidic device using DLD array to isolate CTCs from other background cells with high capture efficiency (> 85%), high throughput (10 mL/min), and high cell viability (> 95%) for downstream analysis (Fig. 9A) [70]. Later, Park et al. utilized tapered micrometer scale constrictions and oscillatory flow which could generate a ratcheting effect to separate CTCs from other blood cells based on the size and deformation properties (Fig. 9B) [71]. In spiking experiments, > 90% tumor cells were captured by this microfluidic device with the viability of 99.1%. For clinical tests, CTCs (CK^+, $DAPI^+$, $CD45^-$) were isolated from 19 out of 20 prostate patients, with a median of 178 CTCs per 7.5 mL of blood.

Table 3 Summary of physical-based CTCs isolation technologies

Technology	Company	Principle	Capture efficiency	Recovery	Purity	Viability	Throughput	Cancer type	Sample volume (mL)	Positive rate of patients	Range (*n*)	CTCDefinition
Filtration												
ISET® [51, 52]	Rarecells	size	N/A	N/A	N/A	N/A	N/A	NSCLC	10 DLA	88% (14/16)	1.3 ~ 4/mL	TTF1/p40$^+$ or EpCAM$^+$, CD45$^-$
ScreenCell® [53, 54]	Screen-Cell	size	N/A	74 ~ 91.2%	N/A	N/A	N/A	HNC	3	46.4% (13/28)	0 ~ 3 & CTC clusters	EGFR$^+$, CK$^+$, CD45$^-$, intact nuclei and morphologically different from leucocytes
MetaCell® system [55, 56]	MetaCell	size	N/A	N/A	N/A	viable	N/A	pancreatic	8	66.7% (16/24)	N/A	N/A
CellSieve™ [57]	Creatv Micro-tech Inc	size	98 ± 2% for fixed cells 89 ± 6% for unfixed cells	N/A	1.7 ± 1.4%	N/A	N/A	Breast NSCLC	7.5	100% (10/10)	56 ± 35	CK$^+$, CD45$^-$, DAPI$^+$
Parsortix™ [58, 59]#	ANGLE	size deform-ability	42 ~ 70%	(42 ~ 70%) * (54 ~ 69%)	N/A	99%	N/A	Breast Colon lung	4	38.5% (10/26)	0 ~ 26	CK$^+$, CD45$^-$, DAPI$^+$
Fluid-assisted separation technology [59]	Clinomics	size	96%	96.2 ± 2.6%	> 2.5 log depletion of WBCs	viable	180 mL/h	Breast Stomach lung	3	83.3% (15/18) 82.9% (63/76) 68.6% (24/35)	0 ~ 540/7.5 mL 2 ~ 485/7.5 mL 0 ~ 62/7.5 mL	CK$^+$/EpCAM$^+$, CD45$^-$, DAPI$^+$
Crescent-shaped trap [60, 61]	N/A	size	> 80%	87 ~ 103%	89%	viable	0.7 mL/h	lung	2	100% (5/5)	20 ~ 84	CK$^+$, CD45$^-$, DAPI$^+$
Parylene-C slot microfilter [62]	N/A	size	90%	N/A	N/A	90%	12 mL/h	prostate	7.5	46.2% (6/13)	N/A	N/A
Microcavity array (circular/rectangular) [63, 64]	N/A	size	80 ~ 97%	> 70%	N/A	98%	200 ~ 1000 μL/min	lung	3	80% (40/50)	0 ~ 46	CK$^+$, CD45$^-$, DAPI$^+$
Separable bilayer [65]	N/A	size	74 ~ 86%	N/A	N/A	62 ~ 80%	N/A	colorectal	1	100% (1/1)	N/A	N/A
Density												
Ficoll® [66, 67]	Biochrom	density	N/A	84%	N/A	N/A	N/A	breast cancer brain metastasis	7.5	32.6% (15/44)	0 ~ 40	CK$^+$, CD45$^-$, DAPI$^+$
OncoQuick® [66]	Greiner Bio-One	density size	N/A	87%	N/A	N/A	N/A	gastrointestinal	20	30% (11/37)	N/A	N/A
AccuCyte® [68, 69]	RareCyte	density	N/A	90 ~ 91%	N/A	N/A	> 1 sample/7 h	Prostate Breast colorectal; prostate	7.5	80% (8/10); 53% (8/15)	0 ~ 175; 0 ~ 20	EpCAM$^+$/CK$^+$, counterstain channel$^-$, DAPI$^+$diameter ≥ 4 μm
Hydrodynamics												
Deterministic Lateral Displacement (DLD)												
DLD microfluidic device [70]	N/A	size	> 85%	N/A	N/A	> 95%	10 mL/min	N/A	N/A	N/A	N/A	N/A

Table 3 (continued)

Technology	Company	Principle	Capture efficiency	Recovery	Purity	Viability	Throughput	Cancer type	Sample volume (mL)	Positive rate of patients	Range (*n*)	CTCDefinition
Microfluidic ratchet mechanism [71]	N/A	size deformability	> 90%	N/A	N/A	99%	1 mL/h	prostate	2	95% (19/20)	median 178/7.5 mL	CK^+, $CD45^-$, $DAPI^+$
Two-stage continuous microfluidic chip [72]	N/A	size asymmetry	N/A	98.7 ± 2.4% (large) 65.5 ± 6.5% (small)	N/A	91.7 ± 2.5%	0.5 mL/h	N/A	N/A	N/A	N/A	N/A
Hydrodynamics Dean Flow Fractionation (DFF)												
ClearCell® FX [73, 74]	Clearbridge BioMedics	size	N/A	N/A	N/A	> 90%	> 7.5 mL/h	Colon Lung Breast Stomach Liver prostate; melanoma	7.5; 8; 10	80.4% (45/56); 94% (15/16)	N/A	N/A
Slanted spiral microfluidics [75]	N/A	size	> 80%	> 80%	~4 log depletion of WBCs	> 90%	56.25 mL/h	Lung breast	7.5	100% (10/10)	3 ~ 125/mL 6 ~ 57/mL	CK^+, $CD45^-$, $DAPI^+$
Labyrinth [76]	N/A	size	> 90%	> 90%	600 WBCs/mL	viable	2.5 mL/min	Pancreatic breast	7.5	100% (20/20) 95% (52/56)	51.6 ± 25.5/mL 0 ~ 31/mL	CK^+, $CD45^-$, $DAPI^+$
Hydrodynamics Microfluidic vortex												
Vortex Chip [77]	N/A	size	25.8%	N/A	57 ~ 94%	85.7%	7.5 mL/20 min	Lung breast	7.5	100%(8/8) 100%(4/4)	23 ~ 317 25 ~ 51	Circular CK^+, $CD45^-$, $DAPI^+$30 μm > diameter > 10 μm
High Throughput Vortex Chip [78]	N/A	size	83%	N/A	80% in spiked tests 19.8% ± 13.9% in clinical tests	83.9 ± 4.0%	8 mL/min of 10 × diluted blood 0.8 mL/min of whole blood	Lung breast	8	80%(12/15) 86%(19/22)	0.5 ~ 24.2/mL 0.75 ~ 23.25/mL	CK^+, $CD45^-$, $DAPI^+$ or $DAPI^+$ with a large nucleus (> 9 μm) and N:C ratio (> 0.8)
Hydrodynamics Inertial migration												
Multi-flow straight channel [79]	N/A	size	N/A	> 83%	> 87%	N/A	300 μL/min	NSCLC	2	75% (6/8)	median 12/mL	CK^+, $CD45^-$, $DAPI^+$high N:C ratio morphologically larger than leukocytes
Dielectrophoresis												
Apostream® [80, 81]	ApoCell	dielectric	N/A	75.4 ± 3.1% 71.2 ± 1.6% 68.3 ± 10.4%	N/A	> 97%	N/A	NSCLC Breast Ovarian squamous lung	7.5	100% (5/5) 95% (19/20) 83.3% (5/6) 33.3 (2/6)	47 ~ 216 0 ~ 36 0 ~ 5 0 ~ 4	CK^+, $CD45^-$, $DAPI^+$
DEPArray™ [82, 83]	Menarini Silicon Biosystems	dielectric	N/A	99.7%	100%	viable	N/A	breast	20	90.9% (10/11)	0 ~ 6	CK^+, $EpCAM^+$, $CD45^-$, $DAPI^+$
Wireless bipolar electrode array [84]	N/A	Size dielectric	N/A	N/A	N/A	viable	> 5.5 mL/h	N/A	N/A	N/A	N/A	N/A

Table 3 (continued)

Technology	Company	Principle	Capture efficiency	Recovery	Purity	Viability	Throughput	Cancer type	Sample volume (mL)	Positive rate of patients	Range (*n*)	CTCDefinition
Topographical												
Collagen adhesion matrix assay [85]	N/A	Adhesion invasiveness	N/A	54 ± 9%	0.5 ~ 35%	99.9 ± 0.1%	N/A	metastic breast Stage I–III breast	3	100% (10/10) 52% (28/54)	18 ~ 256/mL	$EpCAM^+$, CAM^+, $CD34^-$, $CD45^-$, $7AAD^-$
Nanoroughened Surfaces [86]	N/A	adhesion	> 80%	> 90%	< 14%	N/A	N/A	N/A	N/A	N/A	N/A	N/A
An integrated microfluidic system [87]	N/A	Size invasiveness	74.00 ± 14.05% ~ 88.17 ± 9.10%	N/A	83.93 ± 0.63%	viable	0.6 mL/h	Colorectal Kidney bladder	1.5	100% (28/28)	1 ~ 13	$EpCAM^+$, $CD45^-$, $DAPI^+$
CTC-Race assay [88]	N/A	Size motility	11.5%	N/A	97.85%	> 96%	N/A	lung	N/A	100% (4/4)	N/A	$EpCAM^+$ or Vim^+, $CD45^-$, $DAPI^+$

Abbreviations: *NSCLC* non-small cell lung cancer, *HNC* head and neck cancer, *N:C ratio* nucleus to cytoplasmic ratio, *N/A* not available, *DLA* diagnostic leukapheresis, counterstain channel, CD45/CD66b/CD11b/CD14/$CD34^-$; 7AAD, 7-aminoactinomycin D; Vim, Vimentin; # approved or cleared by Food and Drug Administration (FDA). All CTC definitions were conducted by immunofluorescence staining

Table 4 Strengths and limitations of physical-based CTCs isolation technologies

Technology	Strengths	Limitations
Filtration		
ISET® [51, 52]	low-cost high throughput high cell viability for downstream analysis	losing CTCs due to the morphology and size heterogeneity of CTCs low purity due to larger leukocytes may be captured clog
ScreenCell® [53, 54]	high capture efficiency low-cost high throughput high cell viability for downstream analysis ability to work on living and fixed cells	losing CTCs due to the morphology and size heterogeneity of CTCs low purity due to larger leukocytes may be captured clog erythrocyte lysis may cause damage to CTCs
MetaCell® system [55, 56]	low-cost high throughput keeping CTCs viable for downstream analysis and cell culture	losing CTCs due to the morphology and size heterogeneity of CTCs low purity due to larger leukocytes may be captured clog
CellSieve™ [57]	high capture efficiency low-cost high throughput high cell viability for downstream analysis	losing CTCs due to the morphology and size heterogeneity of CTCs low purity due to larger leukocytes may be captured clog
Parsortix™ [58, 59][#]	high capture efficiency low-cost high throughput high cell viability for downstream analysis	losing CTCs due to the morphology and size heterogeneity of CTCs low purity due to larger leukocytes may be captured complex process and equipment
Fluid-assisted separation technology [59]	clog-free high sensitivity high capture efficiency low-cost high throughput high cell viability for downstream analysis	losing CTCs due to the morphology and size heterogeneity of CTCs low purity due to larger leukocytes may be captured complex process and equipment
Crescent-shaped trap [60, 61]	high sensitivity high capture efficiency low-cost high cell viability for downstream analysis	losing CTCs due to the morphology and size heterogeneity of CTCs low purity due to larger leukocytes may be captured complex process and equipment
Parylene-C slot microfilter [62]	high sensitivity high throughput low-cost high cell viability for downstream analysis	losing CTCs due to the morphology and size heterogeneity of CTCs low purity due to larger leukocytes may be captured clog centrifugation results in cell loss complex process and equipment
Microcavity array (circular/rectangular) [63, 64]	high sensitivity high throughput low-cost high cell viability for downstream analysis	losing CTCs due to the morphology and size heterogeneity of CTCs low purity due to larger leukocytes may be captured clog
Separable bilayer [65]	high capture efficiency low-cost high cell viability simultaneously act as a capture analysis and culture platform	losing CTCs due to the morphology and size heterogeneity of CTCs low purity due to larger leukocytes may be captured clog

Table 4 (continued)

Technology	Strengths	Limitations
Density		
Ficoll® [66, 67]	high throughput inexpensive one-step enrichment of CTCs by simple centrifugation post-CTC detection and analysis is possible	low specificity and purity due to the overlap of density between some CTCs and other blood cells additional techniques are needed platelet contamination
OncoQuick® [66]	high throughput inexpensive one-step enrichment of CTCs by simple centrifugation post-CTC detection and analysis is possible	low specificity and purity due to the overlap of density between some CTCs and other blood cells additional techniques are needed platelet contamination
AccuCyte® [68, 69]	high recovery high throughput inexpensive no-wash no-lysis collection and transfer of nucleated cells to slides	low specificity and purity due to the overlap of density between some CTCs and other blood cells platelet contamination
Hydrodynamics Deterministic Lateral Displacement (DLD)		
DLD microfluidic device [70]	high capture efficiency high throughput high cell viability for downstream analysis allow for isolating CTCs clusters	losing CTCs due to the deformability and size heterogeneity of CTCs low purity due to larger leukocytes may be captured lack of clinical data support complex process and equipment
Microfluidic ratchet mechanism [71]	high capture efficiency high cell viability for downstream analysis clog-free	losing CTCs due to the deformability and size heterogeneity of CTCs low purity due to larger leukocytes may be captured throughput limitation complex process and equipment
Two-stage continuous microfluidic chip [72]	high capture efficiency high cell viability sorting large and small CTCs clusters into different output streams	losing CTCs due to the deformability and size heterogeneity of CTCs low purity due to larger leukocytes may be captured lack of clinical data support complex process and equipment
Hydrodynamics Dean Flow Fractionation (DFF)		
ClearCell® FX [73, 74]	high throughput high cell viability for downstream analysis	losing CTCs due to the size heterogeneity of CTCs low purity due to larger leukocytes may be captured erythrocyte lysis may cause damage to CTCs complex process and equipment
Slanted spiral microfluidics [75]	high capture efficiency high throughput high cell viability for downstream analysis clog-free	losing CTCs due to the size heterogeneity of CTCs low purity due to larger leukocytes may be captured erythrocyte lysis may cause damage to CTCs complex process and equipment
Labyrinth [76]	high capture efficiency high throughput high cell viability for downstream analysis clog-free capable of both isolating heterogeneous single CTCs and clusters of CTCs	losing CTCs due to the size heterogeneity of CTCs low purity due to larger leukocytes may be captured complex process and equipment

Table 4 (continued)

Technology	Strengths	Limitations
Hydrodynamics Microfluidic vortex		
Vortex Chip [77]	low cost high throughput high purity high cell integrity and viability clog free	low recovery losing CTCs due to the size heterogeneity of CTCs low purity due to larger leukocytes may be captured
High Throughput Vortex Chip [78]	low cost maximizing throughput high capture efficiency high purity in cell line hastening downstream analyses to concentrate cells from any volume to ~ 200μL	losing CTCs due to the size heterogeneity of CTCs low purity in clinical tests due to larger leukocytes may be captured
Hydrodynamics Inertial migration		
Multi-flow straight channel [79]	high capture efficiency and purity high throughput isolation of circulating tumor microemboli (CTM) can be readily accomplished	losing CTCs due to the size heterogeneity of CTCs low purity due to larger leukocytes may be captured
Dielectrophoresis		
Apostream® [80, 81]	good recovery high cell viability clog free	may cause cellular damage larger leukocytes with similar dielectric property like CTCs may get captured CTCs of the same size as leukocytes may not be captured complex process and equipment centrifugation results in cell loss
DEPArray™ [82, 83]	high recovery high purity high cell viability single cell isolation for downstream analysis	low throughput limited volume complex process and equipment centrifugation results in cell loss
Wireless bipolar electrode array [84]	high cell viability single cell isolation for downstream analysis high throughput than other DEP devices	larger leukocytes with similar dielectric property like CTCs may get captured lack of clinical data support complex process and equipment
Topographical		
Collagen adhesion matrix assay [85]	Simple efficient in the recovery of invasive CTCs that have strong avidity to the ECM high cell viability for subsequent culture	low purity lose CTCs due to the size heterogeneity of CTCs 1 mL blood tested might not contain CTC low throughput
Nanoroughened Surfaces [86]	simple, high capture efficiency and sensitivity applicable to many different cancer cell types	the adhesion strength of cancer cells might be affected by various factors may cause cellular damage low purity low throughput lack of clinical data support
An integrated microfluidic system [87]	high capture efficiency and purity high cell viability applicable to many different cancer cell types allowing for analysis of metastasis	low throughput and time consuming low purity due to larger leukocytes may be captured complex process and equipment
CTC-Race assay [88]	can isolate metastatic CTCs high cell viability and purity	low throughput and time consuming complex process and equipment only obtain a little percentage of CTCs

[#] approved or cleared by Food and Drug Administration (FDA)

Furthermore, to obtain and study the clinical significance of CTCs clusters, Au et al. presented a two-stage DLD strategy composed of cylindrical micropillars to mainly recover large clusters at the first stage and asymmetrical pillars to mainly extract smaller clusters at the second stage (Fig. 9C) [72]. In spiking experiments, this system isolated

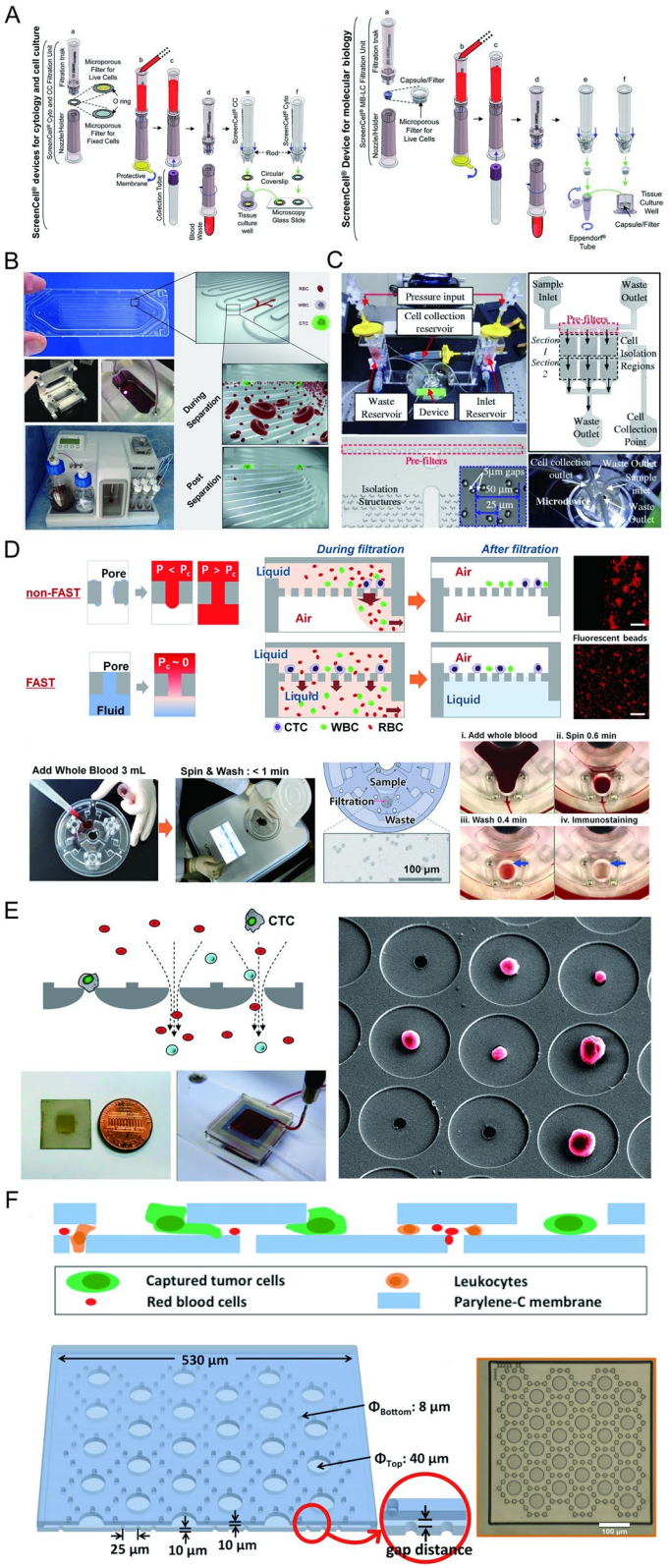
A
ScreenCell® devices for cytology and cell culture
Microporous Filter for Live Cells
O ring
Microporous Filter for Fixed Cells
Protective Membrane
Collection Tube
Blood Sample
Tissue culture well
Circular Coverslip
Microscopy Glass Slide
Rod
ScreenCell® Device for molecular biology
Capsule/Filter
Microporous Filter for Live Cells
Tissue Culture Well
Eppendorf® Tube
B
During Separation
Post Separation
C
Pressure input
Cell collection reservoir
Waste Reservoir
Device
Inlet Reservoir
Sample Inlet
Waste Outlet
Pre-filters
Section 1
Section 2
Cell Isolation Regions
Cell Collection Point
Isolation Structures
50 µm
25 µm
Cell collection outlet
Microdevice
D
non-FAST
FAST
Pore
Fluid
P < Pc
P > Pc
Pc ~ 0
During filtration
After filtration
Liquid
Air
Fluorescent beads
CTC
WBC
RBC
Add Whole Blood 3 mL
Spin & Wash : < 1 min
Sample
Filtration
Waste
100 µm
i. Add whole blood
ii. Spin 0.6 min
iii. Wash 0.4 min
iv. Immunostaining
E
CTC
F
Captured tumor cells
Red blood cells
Leukocytes
Parylene-C membrane
530 µm
ΦBottom: 8 µm
ΦTop: 40 µm
25 µm
10 µm
10 µm
gap distance
100 µm

◂**Fig. 8** Filtration-based CTCs isolation. **A** ScreenCell® [53]. A system which uses a filter with 7.5 ± 0.36 μm or 6.5 ± 0.33 μm circular pores to separate fixed or live cells, respectively. Copyright 2011, Anticancer Research. **B** Parsortix™ [58]. A microfluidic platform which integrates microfluidics and stepped physical structures to separate CTCs with high capture efficiency. Copyright 2016, John Wiley and Sons. **C** Fluid-assisted separation technology [59]. A system which utilizes FAST and tracketched polycarbonate membrane with 8 μm pores to isolate CTCs from whole blood. Copyright 2017, American Chemical Society. **D** Crescent-shaped trap [60]. A platform with three 5 μm gaps to isolate CTCs from whole blood, which achieved good isolation efficiency. Copyright 2019, Springer Link. **E** Microcavity array [63]. A circular size-selective device with the diameter of 9 μm, which achieved high capture efficiency (more than 80%), viability (98%) and rapid (200−1000 μL/min) for CTCs separation. Copyright 2010, American Chemical Society. **F** Separable bilayer [65]. A microfilter with pores of 40 μm on the upper layer and 8 μm on the bottom layer for size-based CTCs capture. Copyright 2014, Springer Nature

98.7 ± 2.4% large clusters and 65.5 ± 6.5% small clusters with good cell viability (91.7 ± 2.45%) at a flow rate of 0.5 mL/h in artificial blood.

Dean flow fractionation

DFF is another example of hydrodynamic method, which is based on the parabolic feature of the laminar velocity distribution [91]. In 2014, Warkiani et al. designed a slanted spiral microfluidic device which makes use of the principle of DFF to focus larger CTCs close to the inner wall and smaller blood cells towards the outer wall by inertial lift forces in the Dean vortex flows (Fig. 10A) [75]. The technique achieved high capture efficiency (> 80%), high purity (~4 log depletion of WBCs), high cell viability (> 90%), and high throughput (7.5 mL/8 min). Moreover, clinical results showed that CTCs (CK^+, $DAPI^+$, $CD45^-$) were isolated and detected from 100% patient samples ($n = 10$) with advanced stage metastatic breast and lung cancer in a range of 6 ~ 57 mL^{-1} and 3 ~ 125 mL^{-1} of blood, respectively. Thereafter, Lin et al. developed the "Labyrinth", a structure made up of long loops and sharp corners, which also utilizes the balance between inertial lift forces and dean flow to separate CTCs from other blood cells with high capture yield (> 90%) and purity (600 WBCs/mL) at a flow rate of 2.5 mL/min (Fig. 10B) [76]. In addition, clinical findings demonstrated that CTCs (CK^+, $DAPI^+$, $CD45^-$) were found in 20 out of 20 pancreatic cancer patients (counts: 51.6 ± 25.5 CTCs mL^{-1} of blood) and 52 out of 56 breast cancer samples (counts: 0 ~ 31 CTCs mL^{-1} of blood).

Microfluidic vortex

Microfluidic vortex takes advantage of inertial force by employing the structure of sudden expansion and contraction [91]. Based on this principle, Sollier et al. designed a Vortex chip which combines the micro-scale vortices and inertial focusing achieving high purity (57 ~ 94%), high throughput (7.5 mL/20 min), and high cell integrity and viability (85.7%) (Fig. 11A) [77]. For clinical experiments, CTCs (circular, CK^+, $DAPI^+$, $CD45^-$, 30 μm > diameter > 30 μm) were successfully separated from 4 out of 4 breast cancer patients with a range of 25 ~ 51 per sample and 8 out of 8 lung cancer patients with a range of 23 ~ 317 per sample. To further improve the capture efficiency and throughput, Che et al. constructed the High Throughput Vortex Chip (Vortex HT Chip), which is upgraded with 2 × more parallel channels and 1.5 × more serial reservoirs than Vortex Chip and reflow the sample waste at the same time (Fig. 11B) [78]. In spiking experiments, high capture efficiency (83%) was achieved with good purity (80%) and excellent viability (83.9 ± 4.0%). Moreover, the clinical results demonstrated that more CTCs [CK^+, $DAPI^+$, $CD45^-$ or only $DAPI^+$ with a large nucleus (> 9 μm) and N:C ratio (> 0.8)] were found in 12 out of 15 lung cancer patients with a range of 0.5 ~ 24.2 mL^{-1} of blood and 19 out of 22 breast cancer patients with a range of 0.75 ~ 23.25 mL^{-1} of blood than 10 healthy donors with a range of 0 ~ 1.25 mL^{-1} of blood.

Inertial migration

Since rotation-induced lift force is the predominant inertial force for cell migration, Zhou et al. constructed a multi-flow microfluidic device based on size-dependent inertial migration with a good recovery rate (> 83%) and excellent purity (> 87%) at a flow rate of 300 μL/min (Fig. 11C) [79, 92]. In addition, CTCs ($DAPI^+$, $CD45^-$, CK^+, with high nucleus to cytoplasmic ratio and morphologically larger than background leukocytes) were successfully isolated from 6 out of 8 NSCLC patients (median: 12 CTCs per mL of blood) in clinical tests.

Dielectrophoresis

Dielectrophoresis-based isolation methods utilize the differences in dielectric property between CTCs and other blood cells to separate them when subjected to non-uniform electric field, which induces polarization and generates forces on cells based on their dielectric properties, such as size, shape, membrane roughness and conductivity.

There are several virtues of dielectrophoresis-based isolation. Firstly, it could gently separate CTCs, minimizing the risk of cell damage. Furthermore, it allows for single CTC isolation which is suitable for downstream analysis, such as single cell sequencing. Despite this, the heterogeneity of CTCs still affects their response to the electric field and the purity may be influenced since large leukocytes may have similar dielectric property like CTCs.

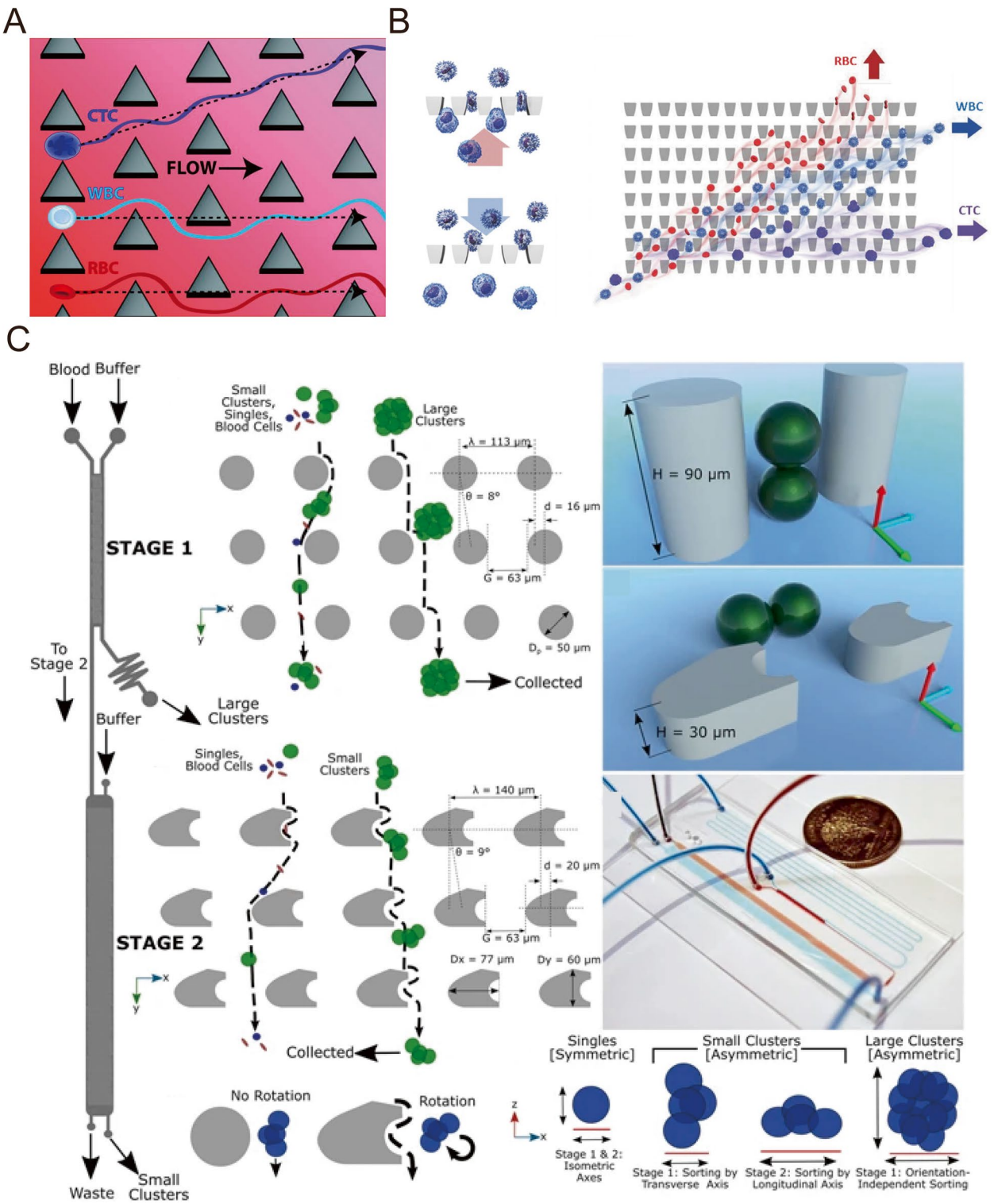

Fig. 9 Deterministic lateral displacement-based CTCs isolation. **A** Deterministic lateral displacement microfluidic device [70]. A microfluidic device using DLD arrays to isolate CTCs from other background cells with high capture efficiency, high throughput, and high cell viability. Copyright 2012, AIP Publishing. **B** Microfluidic ratchet mechanism [71]. A device with tapered micrometer scale constrictions and oscillatory flow which can generate a ratcheting effect to separate CTCs from other blood cells. Copyright 2016, John Wiley and Sons. **C** Two-stage continuous microfluidic chip [72]. A device composed of cylindrical micropillars to mainly recover large clusters at first stage and asymmetrical pillars to mainly extract smaller clusters at second stage. Copyright 2017, Springer Nature

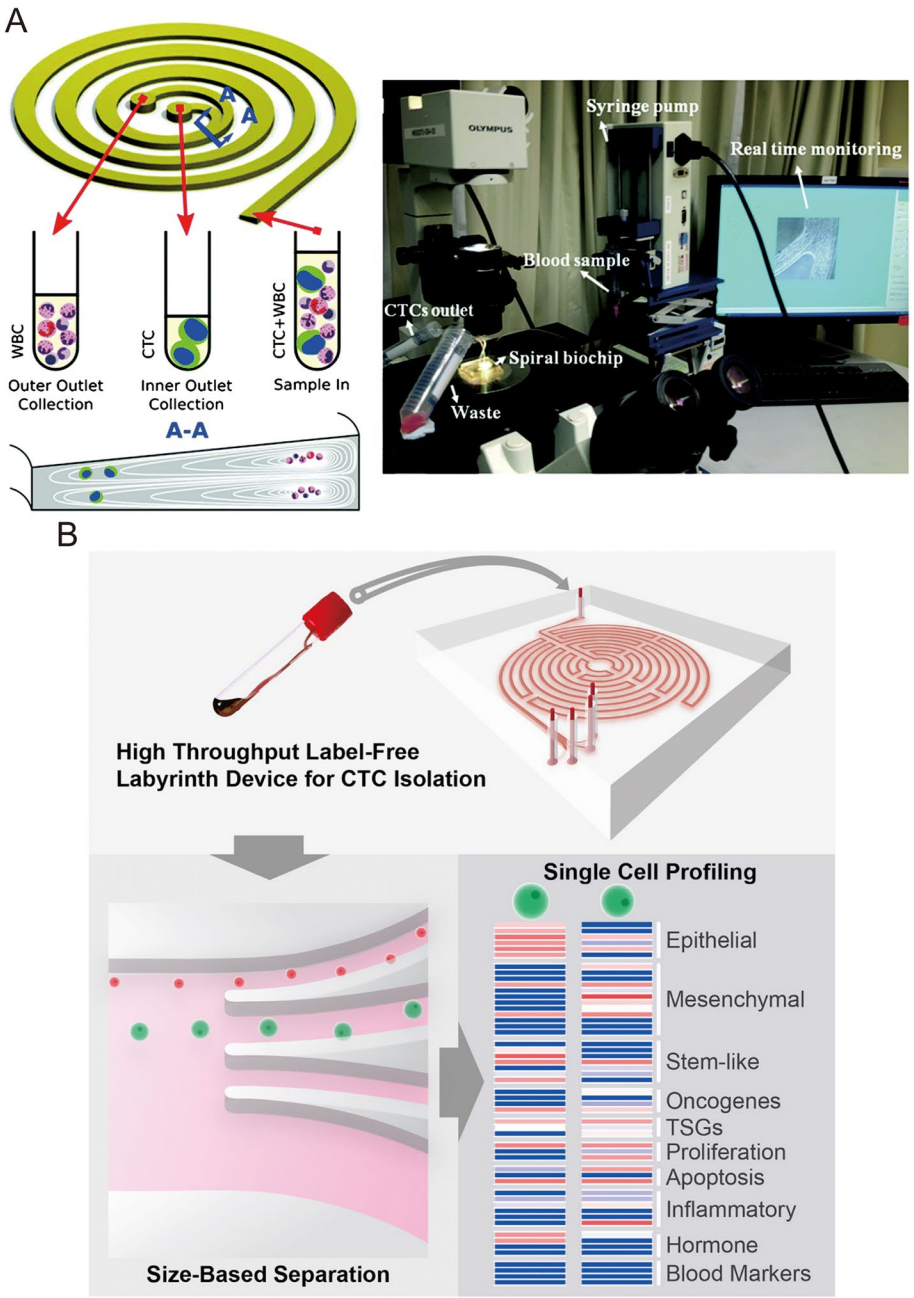

Fig. 10 Dean flow fractionation-based CTCs isolation. **A** Slanted spiral microfluidics [75]. A device which makes use of the principle of DFF to focus larger CTCs close to the inner wall and smaller blood cells towards the outer wall by inertial lift forces in the Dean vortex flows. Copyright 2014, Royal Society of Chemistry. **B** Labyrinth [76]. A device made up of long loops and sharp corners, which utilizes the balance between inertial lift forces and dean flow to separate CTCs from other blood cells. Copyright 2017, with permission from Elsevier

Additionally, the throughput of this method needs to be further improved.

In 2012, Gupta et al. developed the ApoStream® (ApoCell, Inc.) technology, which utilizes positive dielectrophoretic (DEP) forces to push CTCs towards the electrode plane while other blood components are attracted by negative DEP into the hydrodynamic flow velocity profile (Fig. 12A) [80]. The spiking experiments shown that the recovery of SKOV3 and MDA-MB-231 tumor cells was $75.4 \pm 3.1\%$ and $71.2 \pm 1.6\%$, respectively. Moreover, the research by O'Shannessy et al. found that CTCs (CK^+, $DAPI^+$, $CD45^-$)

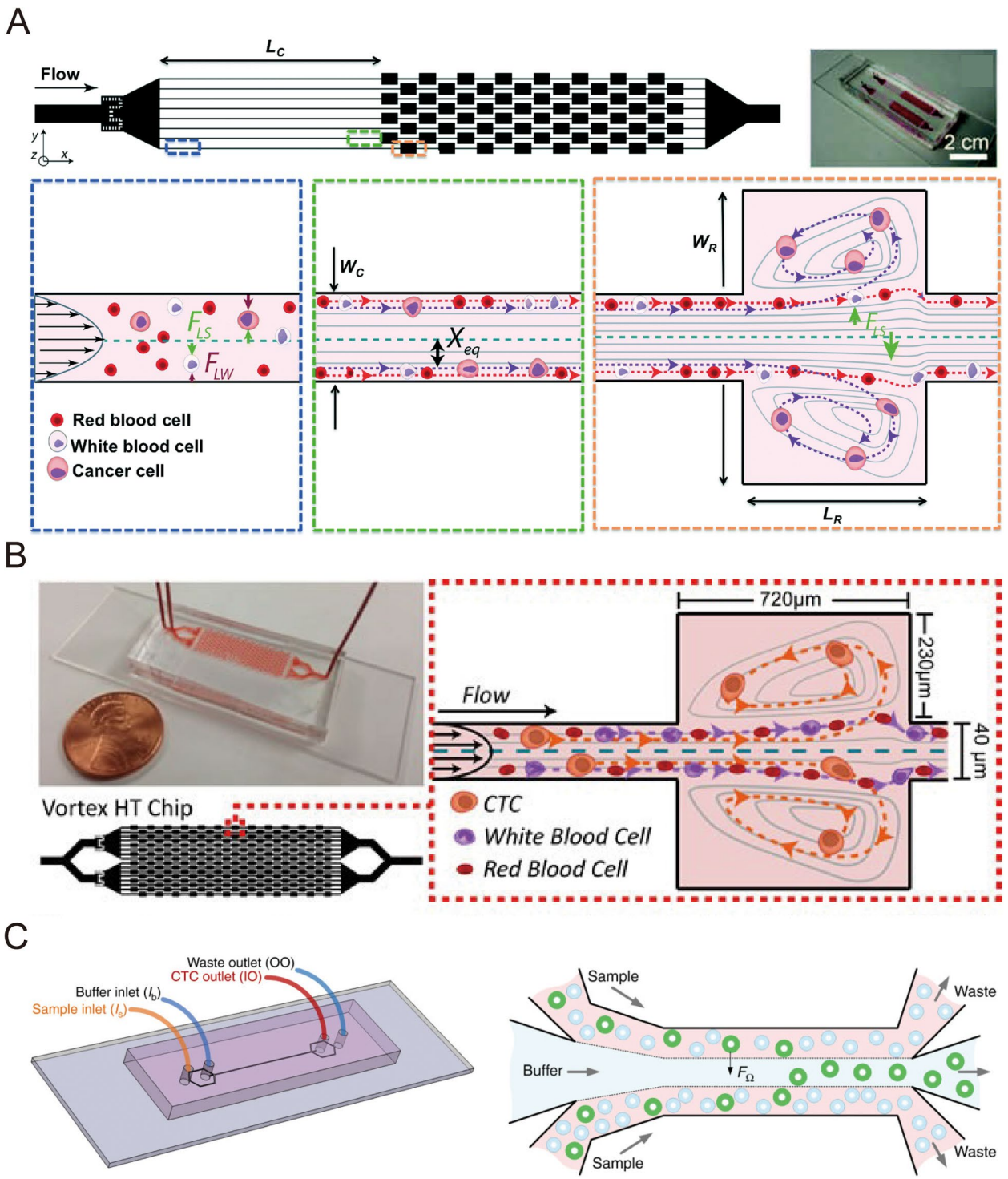

Fig. 11 Microfluidic vortex and inertial migration-based CTCs isolation. **A** Vortex Chip [77]. A chip which combines the micro-scale vortices and inertial focusing with high purity, high throughput, and high cell integrity and viability. Copyright 2014, Royal Society of Chemistry. **B** High Throughput Vortex Chip [78]. A chip which is upgraded with 2x more parallel channels and 1.5x more serial reservoirs than Vortex Chip and reflow the sample waste at the same time. Copyright 2016, Oncotarget. **C** Multiflow straight channel [79]. A multi-flow microfluidic device based on the size-dependent inertial migration. Copyright 2019, Springer Nature

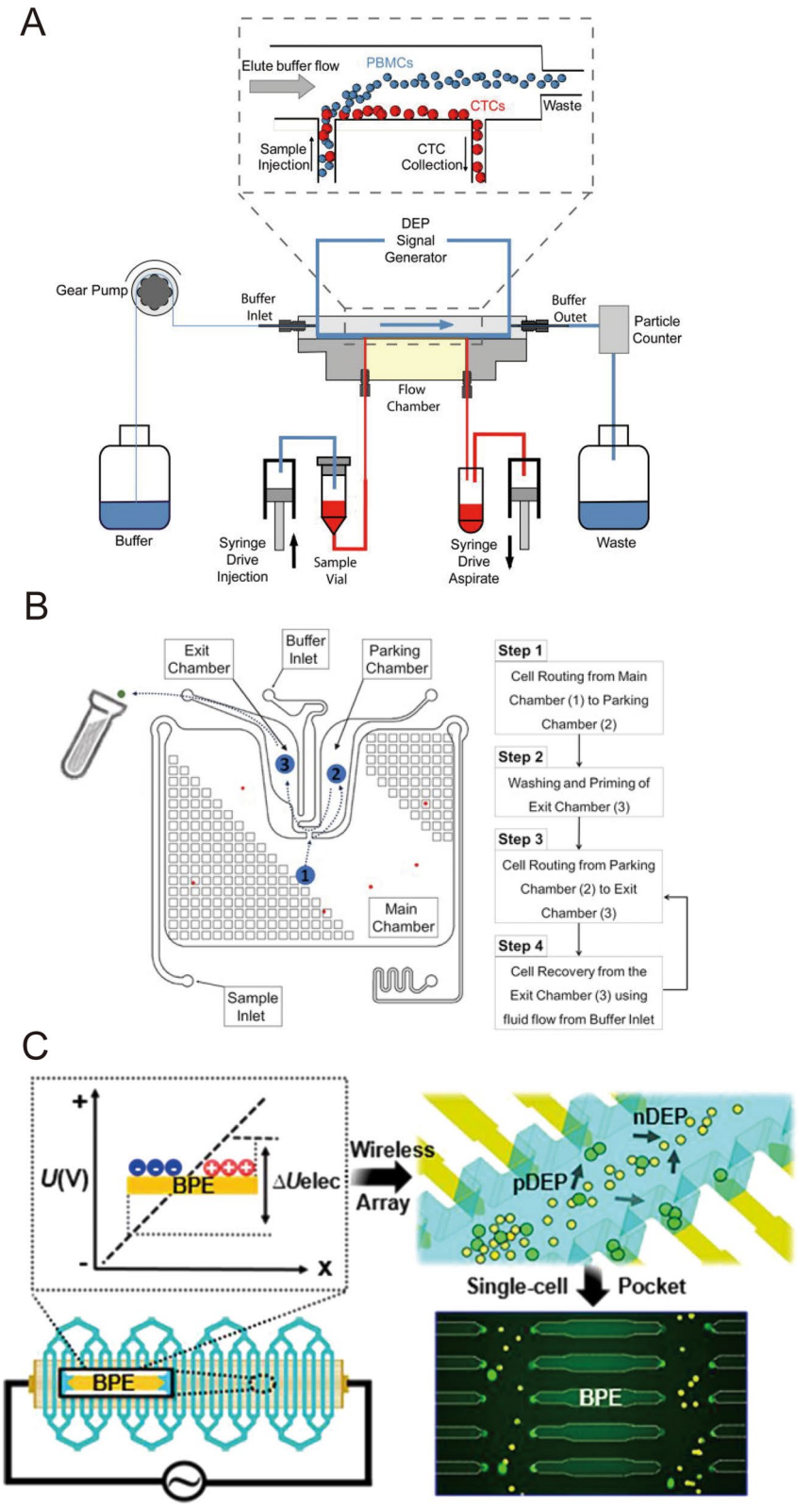

Fig. 12 Dielectrophoresis-based CTCs isolation. **A** ApoStream® [80]. A device which utilizes positive DEP forces to push CTCs towards the electrode plane while other blood components are attracted by negative DEP into the hydrodynamic flow velocity profile. Copyright 2012, AIP Pubilishing. **B** DEPArray™ [82]. A technology which combines the CellSearch® enrichment and the nonuniform electric field to attract and isolate single CTC with matchless purity. Copyright 2018, John Wiley and Sons. **C** Wireless bipolar electrode array [84]. A DEP device which attracts and traps CTCs at the electric field maxima around the BPE tips along both x- and y- directions while other blood cells remain in fluid flow. Copyright 2017, American Chemical Society

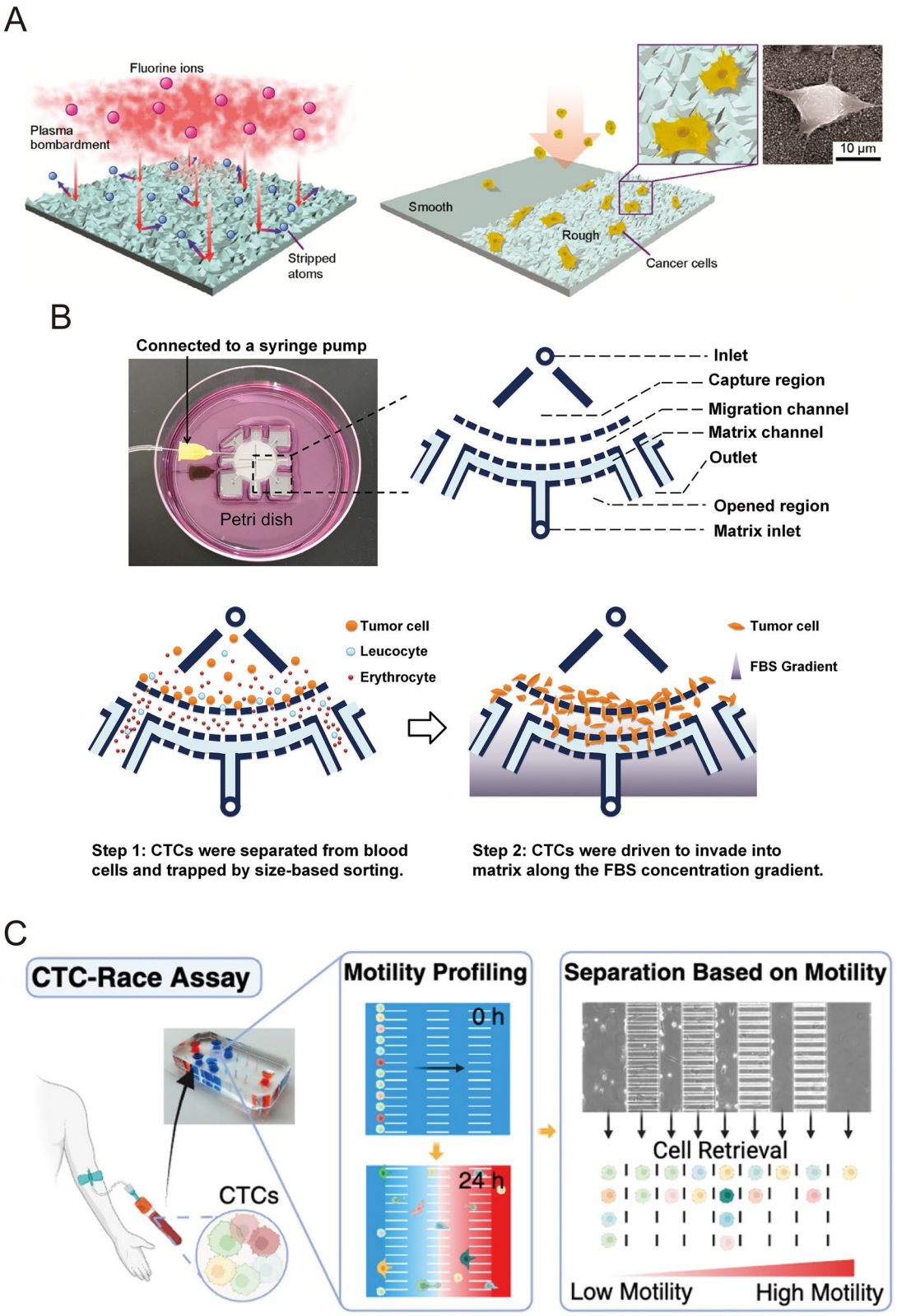

Fig. 13 Topographical-based CTCs isolation. **A** Nanoroughened surfaces [86]. A simple strategy, which takes advantage of the differential adhesion preference between tumor cells and other blood cells to capture CTCs with high capture efficiency. Copyright 2013, American Chemical Society. **B** An integrated microfluidic system [87]. A technique, which combines size-based enrichment and invasiveness-based analysis, providing a fetal bovine serum (FBS) ingredient to isolate and analyze the metastasis potential of CTCs. Copyright 2023, with permission from Elsevier. **C** CTC-Race assay [88]. An assay that separates a small percentage of CTCs (11.5%) of high motility with excellent purity and viability. Copyright 2024, American Chemical Society

were isolated from 31 out of 37 cancer patients with numbers ranging from 0 to 216 per sample [81].

In order to isolate single CTC with high purity, Di Trapani et al. designed the DEPArray™ (Menarini Silicon Biosystems, S.p.A., Italy) technology, combined with the CellSearch® enrichment, which utilizes the nonuniform electric field to attract and isolate single CTC with matchless purity (100%) (Fig. 12B) [82]. What's more, Rossi et al. integrated OncoQuick® for enrichment and DEPArray™ for CTCs isolation [83]. Their results showed that CTCs ($DAPI^+/EpCAM^+/CK^+/CD45^-$) enumerated from 0 to 6 per sample were found in 10 out of 11 breast cancer patients before surgery in clinical tests.

To further enhance the isolation throughput, Li et al. developed a wireless bipolar electrode (BPE) array which attracts and traps CTCs at the electric field maxima around the BPE tips along both *x*- and *y*- directions while other blood cells remain in fluid flow. (Fig. 12C) [84].

Topographical

Topographical-based isolation methods make use of the special ultrastructure (longer filopodia and more microvilli) of CTCs to separate them from other blood components when blood samples pass through the specific topological substrate [93].

Topographical-based isolation is able to recover multiple subtypes of CTCs which show strong adhesion and invasiveness to the specific surface. But it also faces some challenges. For instance, the purity and throughput need to be improved and the adhesion property of CTCs might be affected by various factors.

Based on this principle, in 2010, Lu et al. developed a collagen adhesion matrix (CAM) assay which successfully captured spiked tumor cells with the recovery of $54 \pm 9\%$ and the purity of 0.5–35% [85]. In addition, their clinical experiments demonstrated that CTCs [$EpCAM^+$, CAM^+, $CD34^-$, $CD45^-$, 7-aminoactinomycin D (7AAD) $^-$] were detected in 10 out of 10 metastatic breast patients (range: 18 ~ 256 CTCs per mL of blood) and 28 out of 54 stage I–III breast cancer patients (mean: 61 CTCs per mL of blood). Further, Chen et al. designed a nanoroughened surface using reactive ion etching (RIE), which takes advantage of the differential adhesion preference between tumor cells and other blood cells to capture CTCs with high capture efficiency (> 90%) (Fig. 13A) [86].

In 2023, Wang et al. combined size-based enrichment and invasiveness-based analysis, providing a fetal bovine serum (FBS) ingredient to isolate and analyze the metastasis potential of CTCs (Fig. 13B) [87]. Their equipment showed excellent capture efficiency ($74.00 \pm 14.05\%$ ~ $88.17 \pm 9.10\%$) and purity ($83.93 \pm 0.63\%$) in spiking experiments of gastric cancer cell line (SGC-7901) as well as good cell viability. Furthermore, their clinical results demonstrated that CTCs ($EpCAM^+$, $DAPI^+$, and $CD45^-$) were detected in 28 out of 28 colorectal cancer patients (range: 1 ~ 13 CTCs per 1.5 mL of blood). They also found that CTCs from metastatic patients migrated longer distance than other patients without metastasis, which indicates that CTCs can be used as a predicted marker of cancer metastasis. Likewise, Liu et al. took advantage of similar principle and designed the CTC-Race assay to separate a small percentage of CTCs (11.5%) of high motility with excellent purity (97.85%) and viability (> 96%) (Fig. 13C) [88]. To be specific, CTCs were categorized into three types: epithelial types ($EpCAM^+$, Vim^-, $DAPI^+$, and $CD45^-$), mesenchymal type ($EpCAM^-$, Vim^+, $DAPI^+$, and $CD45^-$), and mixed epithelial and mesenchymal type ($EpCAM^+$, Vim^+, $DAPI^+$, and $CD45^-$). They found that CTCs of mesenchymal type showed high migration speed than other two types.

In summary, physical-based isolation methods do not rely on specific biomarkers of CTCs and separate them with high throughput and little damage, allowing for downstream analysis and culture. However, the recovery rate and purity are compromised due to the overlap of some physical properties between CTCs and other non-target cells. Therefore, it is necessary and hence become more effective to combine physical-based approaches and biological-based approaches, for the purpose of compensating the inherent drawbacks of each method and thus enabling the precise isolation and detection of various CTCs [92].

Combined isolation technologies

Combined isolation methods, which constantly spring up in the CTCs research, leverage the advantages of both biological-based and physical-based techniques to improve the specificity, sensitivity, and throughput of CTCs isolation and detection. In this section, we list some combined technologies (Table 5), as well as their advantages and disadvantages (Table 6).

In 2010, Gleghorn et al. designed a geometrically enhanced differential immunocapture (GEDI) chip, which utilizes staggered obstacle arrays modified with anti-PSMA to create size-dependent particle trajectories and isolate CTCs from castrate-resistant prostate cancer (CRPC) patients [95]. The GEDI chip achieved high capture efficiency (> 80%) and good purity (> 60%) and captured CTCs ($PSMA^+$) in 18 of 20 CRPC patients (average: 27 ± 4 per mL of blood).

In addition, Ozkumu et al. developed an inertial focusing–enhanced microfluidic CTCs capture platform (CTC-iChip), which combines (1) DLD to remove RBCs and platelets, (2) inertial focusing to align WBCs and CTCs, and (3) magnetophoresis to deflect magnetically tagged cells (CTCs or WBCs) (Fig. 14A) [96]. The CTC-iChip successfully achieved high capture efficiency (77 ~ 98%) in spiking experiments and captured 0.5 ~ 610 CTCs mL^{-1} of blood

Table 5 Summary of combined CTCs isolation technologies

Technology	Company	Principle	Capture efficiency	Recovery	Purity	Viability	Throughput	Cancer type	Sample volume (mL)	Positive rate of patients	Range (n)	Definition
RosetteSep™ [54, 94]	Stemcell Technologies	antibody cocktail density	N/A	50.7 ± 3.5%; 70%	N/A	viable	N/A	PDAC; HNSCC	7.5; N/A	59% (13/22); 64.0% (16/25)	N/A; 0 ~ 3	CK^+, $CD45^-$, $DAPI^+$
Geometrically enhanced differential immunocapture chip [95]	N/A	PSMA size	85 ± 5%	N/A	68 ± 6% in spiked tests 62 ± 2% in clinical tests	N/A	1 mL/h	CRPC	1	90% (18/20)	27 ± 4	$PSMA^+$
CTC-iChip [96]	N/A	EpCAM/CD45 size	77 ~ 98%	N/A	Positive: > 3.5 log depletion negative: > 2.5 log depletion	viable	8 mL/h	prostate	10	90% (37/41)	0.5 ~ 610/mL	CK^+, $CD45^-$, $DAPI^+$
Monolithic Chip [50]	N/A	CD45, CD16 and CD66b size	N/A	99.5%	N/A	N/A	0.5 mL/min	Melanoma Lung Prostate breast	N/A	100% (39/39)	0.9 ~ 1.5/mL 0.1 ~ 63/mL 7 and 906 0.3 ~ 62.1/mL	$DRAQ5^+$, $CD45/CD66/CD16^-$, $EpCAM^+$ for lung, prostate or breast cancer or $CD146^+/NG2^+$ for melanoma
^{LP}CTC-iChip [97]	N/A	CD45, CD16, CD3, CD45RA and CD66b size	N/A	89.2 ± 5.7% 86.1 ± 0.6%	WBCs (3.35 ± 0.17 log10 depletion) 0.3%	viable	168 mL/h	N/A	N/A	N/A	N/A	N/A
Aptamer-tailed Octopus chip [98]	N/A	EpCAM size	74.2 ~ 84.4%	(74.2 ~ 84.4%) * 80%	N/A	95.8%	1 mL/h	prostate colorectal	1	100% (38/38)	8.3 ± 5.0 2 ~ 20	CK^+, $EpCAM^+$, $CD45^-$, $DAPI^+$
ApTDN-Chip [99]	N/A	EpCAM size	85.4% for MCF-7 73% for SW480	(85.4% or 73%) * 83%	3.1 log10-depletion	90.8%	N/A	adenocarcinoma	1	100% (12/12)	2 ~ 16/mL	CK^+, $CD45^-$, $DAPI^+$
FLASH-Chip [100]	N/A	EpCAM size	> 70%	N/A	N/A	97.6%	N/A	adenocarcinoma	1	100% (17/17)	4 ~ 10/mL	CK^+, $CD45^-$, $Hoechst^+$

Table 5 (continued)

Technology	Company	Principle	Capture efficiency	Recovery	Purity	Viability	Throughput	Cancer type	Sample volume (mL)	Positive rate of patients	Range (n)	Definition
PillarX [101]	N/A	EpCAM size	75 ~ 84%	N/A	N/A	> 70%	N/A	breast	0.5	100% (6/6)	single: 12 ~ 79 cluster: 5 ~ 16	CK^+, $CD45^-$, $DAPI^+$

Abbreviations: *PSMA*, prostate-specific membrane antigen, *EpCAM* epithelial cell adhesion molecule, *PDAC* pancreatic ductal adenocarcinoma, *HNSCC* head and neck squamous cell carcinoma, *CRPC* castrate-resistant prostate cancer, *N/A* not available. All CTC definitions were conducted by immunofluorescence staining

Table 6 Strengths and limitations of combined CTCs isolation technologies

Technology	Strengths	Limitations
RosetteSep™ [54, 94]	higher purity than Ficoll® high throughput inexpensive post-CTC detection and analysis is possible	low recovery rate causing inherent cell loss and morphologic changes platelet contamination
GEDI chip [95]	high capture efficiency high purity low blood volumes need	Expensive 1 mL blood might not contain CTCs not applicable for pan-cancer
CTC-iChip [96]	high capture efficiency high throughput high cell viability for downstream analysis applicable to all cancers	long set up times low purity due to some leukocytes may be captured complicated fabrication expensive
Monolithic Chip [50]	Automated fully integrated high recovery high throughput applicable to all cancers	CTCs expressing CD45 maybe remove from the sample low purity due to some leukocytes may be captured complicated fabrication expensive
^{LP}CTC-iChip [97]	ultrahigh-throughput processing a large concentrate of blood cells without clogging CTCs have preserved viability and molecular integrity applicable to all cancers	CTCs expressing CD45 maybe remove from the sample low purity due to some leukocytes may be captured complicated fabrication expensive lack of clinical data support
Aptamer-tailed Octopus chip [98]	high capture efficiency high specificity gentle release of CTCs high cell viability for downstream analysis	omitting CTCs expressing low levels of EpCAM expensive low throughput 1 mL blood might not contain CTCs
ApTDN-Chip [99]	high capture efficiency high specificity gentle release of CTCs high cell viability for downstream analysis	omitting CTCs expressing low levels of EpCAM expensive low throughput 1 mL blood might not contain CTCs
FLASH-Chip [100]	high capture efficiency high specificity gentle release of CTCs high cell viability for downstream analysis high purity	omitting CTCs expressing low levels of EpCAM expensive low throughput 1 mL blood might not contain CTCs
PillarX [101]	high capture effiency sorting CTCs and clusters based on size, epithelial expression, and deformability	omitting CTCs expressing low levels of EpCAM low throughput complicated fabrication 0.5 mL blood might not contain CTCs

($DAPI^+$, $CD45^-$, CK^+) in 37 out of 41 CRPC patients. Later, to curtail set up time and improve the throughput, Fachin et al. made use of similar principle and developed an automated monolithic chip with 128 multiplexed DLD, double inertial focusing stage and magnetically-activated cell sorting stage, which achieved outstanding recovery rate (99.5%) in spiking tests (Fig. 14B) [50]. Moreover, their clinical results demonstrated that 2561 putative CTCs ($DRAQ5^+$, $CD45/CD66/CD16^-$, $EpCAM^+$ for lung, prostate or breast cancer or $CD146^+/NG2^+$ for melanoma) were found in 39 out of 39 melanoma, lung, prostate, and breast cancer samples. Furthermore, the ^{LP}CTC-iChip, designed by Mishra et al., removes RBCs and platelets by size-based inertial separation, depletes WBCs with a mixture of biotinylated antibodies targeting CD45, CD16, CD3, CD45RA, CD66b by magnetic sorter chip, and finally recovers CTCs with good capture efficiency (> 85%) and ultrahigh throughput (168 mL/h) in 65 mL leukapheresis samples (Fig. 14C) [97].

Besides antibodies, Song et al. designed an aptamer-tailed octopus chip (AP-Octopus-Chip), which uses DLD-patterned and aptamer-functionalized Au nanospheres targeting EpCAM to capture CTCs (capture efficiency: 74.2 ~ 84.4%) and takes advantage of the thiol exchange reaction to release CTCs (recovery rate: 80%, viability: 96%) for downstream

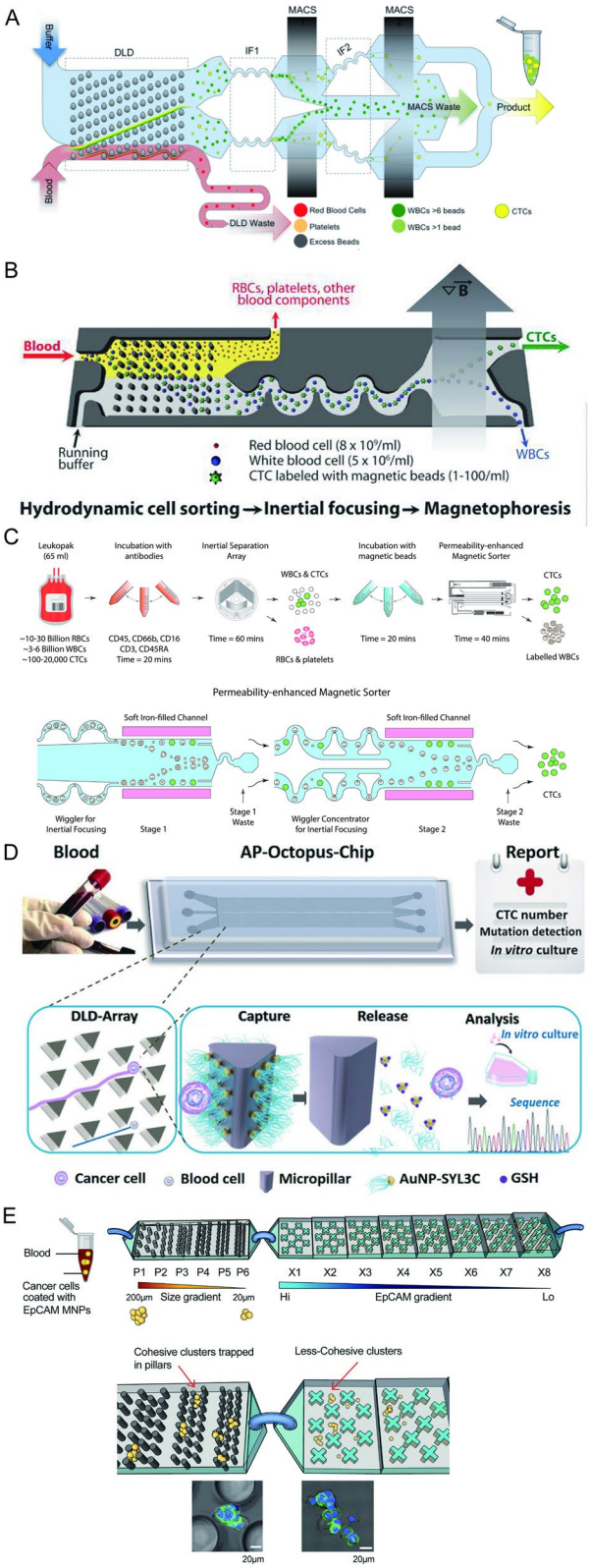
A
Buffer
DLD
IF1
IF2
MACS
MACS
MACS Waste
Product
Blood
DLD Waste
Red Blood Cells
Platelets
Excess Beads
WBCs >6 beads
WBCs >1 bead
CTCs
B
RBCs, platelets, other blood components
Blood
CTCs
Running buffer
WBCs
Red blood cell (8 x 10⁹/ml)
White blood cell (5 x 10⁶/ml)
CTC labeled with magnetic beads (1-100/ml)
Hydrodynamic cell sorting → Inertial focusing → Magnetophoresis
C
Leukopak (65 ml)
Incubation with antibodies
Inertial Separation Array
WBCs & CTCs
Incubation with magnetic beads
Permeability-enhanced Magnetic Sorter
CTCs
~10-30 Billion RBCs
~3-6 Billion WBCs
~100-20,000 CTCs
CD45, CD66b, CD16
CD3, CD45RA
Time = 20 mins
Time = 60 mins
RBCs & platelets
Time = 20 mins
Time = 40 mins
Labelled WBCs
Permeability-enhanced Magnetic Sorter
Soft Iron-filled Channel
Soft Iron-filled Channel
Wiggler for Inertial Focusing
Stage 1
Stage 1 Waste
Wiggler Concentrator for Inertial Focusing
Stage 2
Stage 2 Waste
CTCs
D
Blood
AP-Octopus-Chip
Report
CTC number
Mutation detection
In vitro culture
DLD-Array
Capture
Release
Analysis
In vitro culture
Sequence
Cancer cell
Blood cell
Micropillar
AuNP-SYL3C
GSH
E
Blood
Cancer cells coated with EpCAM MNPs
P1 P2 P3 P4 P5 P6
200μm Size gradient 20μm
X1 X2 X3 X4 X5 X6 X7 X8
Hi EpCAM gradient Lo
Cohesive clusters trapped in pillars
Less-Cohesive clusters
20μm
20μm

Fig. 14 Combined isolation technologies. **A** CTC-iChip [96]. An inertial focusing–enhanced microfluidic CTCs capture platform, which combines (1) deterministic lateral displacement to remove RBCs and platelets, (2) inertial focusing to align WBCs and CTCs, combines (1) deterministic lateral displacement to remove RBCs and platelets, (2) inertial focusing to align WBCs and CTCs, and (3) magnetophoresis to deflect magnetically tagged cells (CTCs or WBCs). Copyright 2013, Science. **B** Monolithic chip [50]. An automated chip with 128 multiplexed deterministic lateral displacement, double inertial focusing stage and magnetically-activated cell sorting stage, which achieved an outstanding recovery rate. Copyright 2017, Springer Nature. **C** LPCTC-iChip [97]. A device, which removes RBCs and platelets by size-based inertial separation, depletes WBCs with a mixture of biotinylated antibodies targeting CD45, CD16, CD3, CD45RA, CD66b by magnetic sorter chip, and finally recovers CTCs with good capture efficiency and ultrahigh throughput in 65 mL leukapheresis samples. Copyright 2020, Proceedings of the National Academy of Sciences of the United States of America. **D** Aptamer-tailed Octopus chip [98]. A chip, which uses DLD-patterned and aptamer-functionalized Au nanospheres targeting EpCAM to capture CTCs and takes advantage of the thiol exchange reaction to release CTCs for downstream sequencing and culture. Copyright 2019, John Wiley and Sons. **E** PillarX [101]. A bimodular microfluidic device which integrates a Pillar device (size- based) and an X-magnetic device (EpCAM expression-based) to profile both single CTCs and clusters. Copyright 2022, John Wiley and Sons

sequencing and culture (Fig. 14D) [98]. For clinical experiments, the AP-Octopus-Chip captured 2 ~ 20 CTCs ($DAPI^+$, $CD45^-$, CK^+) per mL of blood in 38 out of 38 prostate and colorectal cancer samples successfully. Thereafter, this research team also designed the ApTDN-Chip [99] and the FLASH-Chip [100].

Later, in 2022, Green et al. constructed the PillarX device, a bimodular microfluidic device which integrated a Pillar device (size-based) and an X-magnetic device (EpCAM expression-based) to profile both single CTCs and clusters with a mean capture efficiency ranging from 75 ~ 84% and good cell viability (> 70%) in two breast cancer cell lines (MDA-MB-231, MDA-ECAD)(Fig. 14E) [101]. What's more, this technique successfully captured CTCs (12 ~ 79 per 0.5 mL of blood) and clusters (5 ~ 16 per 0.5 mL of blood) in 6 out of 6 breast cancer patients (CTCs were defined as CK^+, $DAPI^+$, $CD45^-$).

In generalization, the combination of biological and physical methods overcomes the limitations of individual technique and improves the sensitivity and specificity of CTCs isolation. However, there are still a few issues that need to be solved. For example, the optimal combination and clinical standardization of those technologies present challenges since different platforms may have varying performance in practice.

Challenges and future perspectives

Since tissue biopsy suffers the drawbacks such as invasiveness, inconvenience, and expensive cost, liquid biopsy has garnered widespread attention in the recent years. As one of the significant markers of liquid biopsy, CTCs have shown their great potential in elucidating the fundamental mechanism of metastasis and providing valuable information in clinical diagnosis and prognosis. However, the rarity and heterogeneity still pose great challenges for the isolation and detection of CTCs. Here, we summarize the challenges and propose the future developments of CTCs related technologies.

Improve the recovery, purity and cell viability

By now, most CTCs isolation technologies have failed to take both recovery and purity into account. Because of the different expression levels of target antigens, biological-based CTCs isolation technologies fail to capture different types of CTCs, leading to a low recovery rate. Hence, though some scientists tried to use multiple epitopes to isolate CTCs, it not only compromises the purity but also increases the cost. As for immunomagnetic negative enrichment methods, some tumor cells are lost since they also have a high expression of CD45, evidenced in a study by Gast et al. where circulating hybridization cells (CHCs) were detected to be positive for both traditional epithelial marker (e.g. CK, EpCAM) and CD45 in tumor-bearing mice and cancer patients [102]. They also found that the number of CHCs was higher than CTCs in pancreatic cancer patients, which means it cannot be overlooked. In brief, depending on surface epitopes of tumor cells or leukocytes will absolutely lose part of CTCs and compromise cell viability as well. Hence, more in-depth researches are needed to discover new biological methods for CTCs separation. For example, Wu et al. used superparamagnetic positively charged nanoparticles to capture CTCs, which are negatively charged due to Warburg effect [103]. Moreover, it is remarkable that a promising method (Datar Cancer Genetics, India), utilizing epigenetically activated media to enrich "apoptosis resistant" tumor cells and also tumor-associated macrophages and fibroblasts, has been granted as 'Breakthrough Designation for Blood Test' by FDA [104]. On the other hand, physical-based CTCs isolation technologies improve the recovery but reduce the purity due to the overlap of physical properties between tumor cells and blood cells. Therefore, it is a good solution to leverage physical-based techniques to enrich CTCs at first, then utilize biological-based methods

to isolate CTCs more accurately. The capture efficiency and detection accuracy will be highly improved if various technologies can be combined and integrated properly.

Furthermore, CTCs are fragile and prone to damage during the process of isolation and detection with current techniques. Consequently, researchers are supposed to improve current technologies, optimize experiment conditions, or design new strategies for CTCs analysis in order to keep them intact and viable. It is meaningful to obtain not only the enumeration of CTCs but also mutation information of key genes with subsequent analysis technologies, such as quantitative PCR [34, 35, 43, 53, 58, 59, 96] and digital PCR [94, 97, 99, 105–108] so as to instruct clinical medicine. Furthermore, live CTCs can be cultured and used to established CTCs-derived tumor xenograft models and organoids, which are suitable for drug screening and efficacy testing, providing personalized medicine suggestions for patients [109, 110]. Moreover, since there is crosstalk between CTCs and other blood cells, including platelets, researchers can simulate patient's tumor microenvironment and explore the interaction and metastatic mechanism in a co-culture organoid model [111, 112]. Thus, the cell viability of CTCs should be maintained well during isolation and detection process so as to showcase more potential in cancer research.

Increase throughput and reduce cost

Most techniques for CTCs isolation and detection are limited by low throughput, which cannot handle a large number of blood samples rapidly. Meanwhile, the cost cannot be ignored as well, which restricts their clinical practice. Until now, in most cases, CTCs are still detected using CellSearch® system by manual evaluation of thumbnail fluorescent pictures. This, however, undoubtedly requires a large amount of time and manpower, and also introduces biases among different operators. Therefore, the automation of whole process is very important for the clinical practice of CTCs. In 2019, Aguilar-Avelar et al. constructed an automated high-throughput fluorescence microscope, which can identify CTCs labeled by immunofluorescence staining accurately and efficiently without human operation [113]. Similarly, Juan et al. also integrated a membrane-based microfiltration device with a sample processing unit and a machine-vision-enabled imaging system to isolate, label, and detect CTCs from blood automatically [114].

Furthermore, in recent years, artificial intelligence (AI) and neural networks have emerged as promising technologies and already demonstrated extraordinary data analysis and image processing capabilities, which have been widely used in all walks of life. In fact, there have been some researches using deep learning method for CTCs detection with the purpose of enhancing the throughput and also reducing the cost. For instance, Zeune et al. have designed a deep-learning based CTCs detection technologies, which combined autoencoding convolutional neural networks (CNN) with advanced visualization techniques, allowing more convenient analysis than classical image techniques [115]. Their network could classify fluorescent images of five different classes, including CTCs, WBCs, tumor-derived extracellular vesicles (tdEVs), bare nuclei and other objects with excellent accuracy, sensitivity and specificity (> 96%). Moreover, to overcome the challenges of uneven microfilter surfaces and make all cells in focus during scanning, Shen et al. developed an auto-focusing principle fittingly combined with a deep-learning-based identification to automatically detect mimic CTC (mCTC) and cancer-associated fibroblasts (CAFs) [116]. Their technology solved the problem of focus plane variations which are ill-addressed by currently available commercial slide scanners and further demonstrated that the deep learning method outperformed conventional computer vision (CV) models in the performance testing of mCTC and CAFs recognition. Noteworthily, the research of Akashi et al. showed that though they made training sets of KYSE520 cell lines with high expression of EpCAM for CNN-based AI detection system, yet AI can also accurately identify KYSE30 cell lines (EpCAM-negative), suggesting that AI does not just rely on the expression of traditional biomarker to distinguish CTCs from blood cells [117]. It can be speculated that AI can discover some unknown and invisible features such as cell morphology or any tiny differences of nucleus structure for CTCs identification. In addition, Guo et al. [118] and Xu et al. [119] also utilized CNN method to automatically detect CTCs based on FISH detection system, improving its sensitivity and specificity.

Taken together, it is imperative and promising to employ AI in CTCs studies to enhance detection accuracy and efficiency, reduce cost and eliminate human subjectivity. Nevertheless, the criteria of AI-aided CTCs detection are still a black box, which makes it hard to explain clearly the underlying mechanism(s), if there is any. Additionally, substantial high-quality clinical CTCs images and data are required for improving the robustness and reliability of neural networks. Nonetheless, we anticipate that AI and neural networks will ultimately replace manual labor and become the key power of CTCs research in the near future.

Establish label-free detection system of CTCs

In addition to the time and manpower cost, and the biases among different operators, there are also many other shortcomings for CellSearch® immunofluorescence identification method: (1) Due to fluorescent spectrum overlap and crosstalk, the number of alternative markers is limited. (2) The EMT process leads to the heterogenous expressions of common markers. Meanwhile, the existence of CHCs makes

the definitions of CTCs and white blood cells vague. Both of them lead to low detection rate of CTCs. (3) The staining process is complicated, time-consuming and detrimental to cell viability, which is not conductive to subsequent analysis and culture. Consequently, there is an urgent need to develop a label-free CTCs detection system, which does not rely on any surface antigens of CTCs. For example, Wang et al. [120] and Moallem et al. [121] took advantage of CNN and machine learning algorithm to identify CTCs based on bright field microscopy images. This method achieved high accuracy on the identification and enumeration of CTCs without any advanced devices or experts. What's more, imaging flow cytometry has also been integrated with AI for CTC label-free detection. For instance, Hiroyuki Konno and Hiroya Takeuchi team utilized computer vision technology to identify target cells, based on quantitative phase microscopy (QPM) images, comparing the differences of subcellular structures and optical path length between CTCs and other blood cells rather than the cellular outline used in conventional methods [123–125]. Similarly based on the differences of cells' refractive index or optical path length, Pietro Ferraro team designed an AI-aided tomographic phase imaging flow cytometry system, which can provide high-throughput 3D phase-contrast tomograms of single cell to detect CTCs [126, 127]. Moreover, Abani Patra and Irene Georgakoudi team combined confocal backscatter and fluorescence flow cytometry for label-free detection of CTC clusters and accuracy assessment with machine learning or deep learning for peak detection/classification [128, 129].

In summary, label-free methods can enhance the sensitivity of CTCs detection without complicated and time-consuming staining process, keeping good cell viability for further downstream analysis and culture. However, current label-free CTCs detection models were mostly developed and validated by a few types of tumor cell lines, which could not reflect the enormous tumor heterogeneity. To address this issue, Piansaddhayanon et al. established the patient liver tissue derived organoids, consisting of various cell types and represent complex genotype and phenotype of cancer subtype [122]. Then, they constructed a dataset of bright field images of organoid-derived cancer cells and other blood cell and made a deep learning model to distinguish them. Even so, there are still some differences between CTCs and tumor cells derived from primary tissue in molecular characteristics, cell morphology and their living environments. Therefore, a large amount of actual patient-derived CTCs data is needed to establish a more efficient and accurate AI detection model concerning CTCs, where two main challenges should be considered. Firstly, as excellent AI models require a large dataset of CTCs images, but due to the low number of CTCs in patient blood, patient samples and blood volumes are demanded in substantial quantities that will absolutely cost a lot of time, efforts and money. Secondly, a positive standard or valid ground truth is essential for supervised machine learning-based models. Hence, it is necessary to find or develop a reliable and convenient method, such as next-generation sequencing, as the gold standard of label-free CTCs detection, and then input real CTCs data to optimize the performance of AI model continuously. In addition to these challenges, current label-free methods are limited by low throughput. To resolve this issue, larger multichannel with high flow rates and more sophisticated data analysis algorithms are needed. Taken together, we value the potential of label-free methods and speculate that they may replace traditional immunofluorescence staining and establish a new clinical standard in years to come. Achieve single cell isolation and sequencing of CTCs.

Currently, most techniques of CTCs are confined to obtain genomic information from batch analysis of dozens or hundreds of CTCs. However, the distinguishing information between individual CTC may be overlooked [91]. Since the heterogeneity of inter- and intra-patients and complex physiological environment lead to highly diverse CTCs, it is necessary to isolate single CTC and study the molecular and phenotypic differences of each CTC with single cell isolation platforms, including automated micromanipulation, fluorescence-activated cell sorting (FACS), nanowell systems, droplet generators, dielectrophoresis and optofluidics [130], and also multi-omics analysis, such as genomic, epigenomics, transcriptomic, and proteomic [131]. Single cell analysis of CTCs not only helps scientists reveal the biological mechanism of metastasis, understand cancer evolution process, but also provides more information for patient risk stratification, therapeutic target discovery, and tissue origin identification in clinical practice [132]. For example, Cheng, et al. developed Hydro-Seq, a massively parallel CTCs analysis platform, which combines size-based capture and single cell whole-transcriptome sequencing [133]. Their results presented the both inter- and intra-patient heterogeneity of CTC subtypes in some important genes about proliferation, metastasis, therapy, and stemness. Hence, it is of vital importance to coordinate isolation and detection methods of CTCs with single cell analysis techniques.

Promote CTCs to clinical application

Up to now, CTCs have been included into the fifth edition of the *WHO Classification of Tumours*: *Breast Tumours* and the seventh edition of the *AJCC Cancer Staging Manual* as a new classification, cM0(i+), which indicates that no overt metastasis but tumor cells have been detected in blood, bone marrow or lymph nodes [134]. Moreover, according to ClinicalTrials.gov, there have been a lot of clinical trials and researches related to CTCs. Not only the enumeration, but also the molecular characterization of CTCs has shown enormous potential in the clinical practice of melanoma

[135] and various solid tumors, including breast cancer [6, 136, 137], lung cancer [138–141], colorectal cancer [142–145], prostate cancer [146–148], gastric cancer [149–151], hepatocellular carcinoma [152–155], pancreatic cancer [156, 157], head and neck cancer [158, 159], renal cell carcinoma [160, 161], thyroid cancer [162, 163], and ovarian cancer [164]. In fact, the enumeration was the first step of CTCs clinical application, which has mainly been used for real-time treatment monitoring, tumor progression evaluation, minimal residual disease monitoring, prognosis and recurrence prediction [165]. Furthermore, as intact and viable cells, CTCs can be utilized to offer more molecular information by different technologies from bulk analysis to single cell sequencing. The molecular subtyping of CTCs based on key therapeutic targets, such as AR-V7 (prostate cancer endocrine therapy), HER-2/EGFR/KRAS (targeted therapy), PD-L1 (immunotherapy), is meaningful to guide treatment decisions and indicate therapy efficacy [166]. Additionally, CTCs are considered as an early event of cancer progression, meaning that it can be used for early detection of cancer [5].

However, there are still many obstacles in the clinical application of CTCs. First, patients of early stage have limited number CTCs, which means small-volume blood samples may not contain any CTC, leading to false negative result. Hence, it is recommended to increase sample volumes especially for patients at an early stage. Second, it is extremely difficult to judge the clinical utility of various CTCs isolation and detection methods since different technologies using different cancer cell lines demonstrated different performances with different definitions of CTCs. What's more, the cut-off value of positive patient is hard to define due to the differences of various technologies and the lack of enough clinical evidence. As a result, after the introduction and performance evaluation of a CTCs analysis technology, it is recommended that researchers should conduct large-scale, multi-center pre-clinical studies to clarify the validity and definite standard for all detailed information in order to make it clearer for clinical assessment and approval. Last but not least, good quality management of blood samples is also a prerequisite for subsequent CTCs analysis, including standardized patient preparation, sample collection, pre-treatment, storage, and transportation. Sample collection involves but not limited to collection time, volume, vessel site, anticoagulant type, etc. In fact, Diamantopoulou et al. have illustrated the circadian rhythm on CTCs release and shown that highest counts of CTCs were detected during sleep in both mouse models and breast cancer patients owing to hormone levels [167]. As for the vessel site of blood withdrawal, Sun et al. revealed the spatial heterogeneity of CTCs between different blood collection sites, including hepatic vein (HV), peripheral artery (PA), peripheral vein (PV) and portal vein (PoV) using single-cell full-length RNA sequencing in HCC patients [168]. Therefore, scientists and clinicians can choose different schemes depending on different purposes, but the conditions must be fixed during the whole research process to make sure the reliability of their results. Furthermore, the preservation and transportation of blood samples also require standardized and appropriate conditions to maintain the viability and integrity of CTCs over time. It is generally recommended that blood samples should be sent for analysis as soon as possible after collection.

In short, due to the complexity of hematology and the heterogeneity of CTCs, more convictive data, studies and trials are needed to explain the ambiguous relevance and prove the clinical validity and utility of CTCs. Even though most clinicians have still been inclined to trust the result of pathological examination during clinical practice for many years, CTCs and liquid biopsy are considered as a blueprint for the future of cancer research especially after utilizing AI, which is the cornerstone to achieve automation and fully exert the clinical value of CTCs. Moreover, single cell sequencing of CTCs is able to uncover intra-patient heterogeneity, providing more details about tumor subtypes and evolution. Therefore, developing more affordable sequencing methods for clinical application will be another direction of CTCs development for the time to come.

Conclusion

Cancer is a common, complex and intractable disease affecting people all over the world. As one of valuable biomarkers of liquid biopsy, CTCs hold immense potential for cancer early detection, prognosis, and treatment guidance. Despite the challenges in the isolation and detection technologies of CTCs, ongoing researches and future advances by refining existing techniques, combining different strategies, and leveraging the imaging and AI approaches, will allow CTCs to play a crucial role in forthcoming precision medicine. Moreover, persistent interdisciplinary efforts and collaborations between biology, engineering, materials science, chemistry, clinical medicine and other related fields, are critical to translate new progress into clinical practice and ultimately embrace the era of precision medicine.

Acknowledgements The authors would like to acknowledge the helpful discussions with Dr.Fan Li, Dr. Baoliang Ge, Dr. Ziling Wu, Dr. Xiaogang Wang, Zhuo Chen, Yuchen Wang.

Authors' contributions Z.G. and W.X. conceived the idea and framework; Z.G. wrote the original manuscript; W.X. edited and revised the manuscript; Z.G. and W.X. read and approved the final version.

Funding This work is supported by National Key Research and Development Program of China (2022YFC2702703 to W. X.), Science and

Technology Commission of Shanghai Municipality (21ZR1433100 to W.X.), Open Project of National Facility for Translational Medicine (Shanghai) (TMSK-2021–139 to W.X.), SJTU funding (YG2022ZD016 to W.X.).

Data availability Not applicable.

Declarations

Ethics approval and consent to participate Not applicable.

Consent for publication Not applicable.

Competing interests The authors declare that they have no competing interests.

References

1. Singh D, et al. Global estimates of incidence and mortality of cervical cancer in 2020: a baseline analysis of the WHO Global Cervical Cancer Elimination Initiative. Lancet Glob Health. 2023;11:e197–206. https://doi.org/10.1016/s2214-109x(22)00501-0.
2. "Cancer." World Health Organization, World Health Organization, 2022. https://www.who.int/zh/news-room/fact-sheets/detail/cancer. Accessed 10 Mar 2024.
3. Siegel RL, Miller KD, Fuchs HE, Jemal A. Cancer statistics, 2022. CA Cancer J Clin. 2022;72:7–33. https://doi.org/10.3322/caac.21708.
4. Li W, et al. Liquid biopsy in lung cancer: significance in diagnostics, prediction, and treatment monitoring. Mol Cancer. 2022;21:25. https://doi.org/10.1186/s12943-022-01505-z.
5. Lawrence R, Watters M, Davies CR, Pantel K, Lu YJ. Circulating tumour cells for early detection of clinically relevant cancer. Nat Rev Clin Oncol. 2023;20:487–500. https://doi.org/10.1038/s41571-023-00781-y.
6. Cani AK, Hayes DF. Breast cancer circulating tumor cells: current clinical applications and future prospects. Clin Chem. 2024;70:68–80. https://doi.org/10.1093/clinchem/hvad191.
7. He Y, et al. Circulating tumor cells as a biomarker to assist molecular diagnosis for early stage non-small cell lung cancer. Cancer Manag Res. 2020;12:841–54. https://doi.org/10.2147/cmar.S240773.
8. Allard WJ, et al. Tumor cells circulate in the peripheral blood of all major carcinomas but not in healthy subjects or patients with nonmalignant diseases. Clin Cancer Res. 2004;10:6897–904. https://doi.org/10.1158/1078-0432.Ccr-04-0378.
9. Effenberger KE, et al. Improved risk stratification by circulating tumor cell counts in pancreatic cancer. Clin Cancer Res. 2018;24:2844–50. https://doi.org/10.1158/1078-0432.Ccr-18-0120.
10. Miltenyi S, Müller W, Weichel W, Radbruch A. High gradient magnetic cell separation with MACS. Cytometry. 1990;11:231–8. https://doi.org/10.1002/cyto.990110203.
11. Talasaz AH, et al. Isolating highly enriched populations of circulating epithelial cells and other rare cells from blood using a magnetic sweeper device. Proc Natl Acad Sci U S A. 2009;106:3970–5. https://doi.org/10.1073/pnas.0813188106.
12. Deng G, et al. Single cell mutational analysis of PIK3CA in circulating tumor cells and metastases in breast cancer reveals heterogeneity, discordance, and mutation persistence in cultured disseminated tumor cells from bone marrow. BMC Cancer. 2014;14:456. https://doi.org/10.1186/1471-2407-14-456.
13. Gorges TM, et al. Improved detection of circulating tumor cells in metastatic colorectal cancer by the combination of the cell search® system and the adnatest®. PLoS One. 2016;11:e0155126. https://doi.org/10.1371/journal.pone.0155126.
14. Danila DC, et al. Clinical validity of detecting circulating tumor cells by adnatest assay compared with direct detection of tumor mrna in stabilized whole blood, as a biomarker predicting overall survival for metastatic castration-resistant prostate cancer patients. Cancer J. 2016;22:315–20. https://doi.org/10.1097/ppo.0000000000000220.
15. Xiong K, et al. Biomimetic immuno-magnetosomes for high-performance enrichment of circulating tumor cells. Adv Mater. 2016;28:7929–35. https://doi.org/10.1002/adma.201601643.
16. Wu X, et al. Neutrophil membrane-coated immunomagnetic nanoparticles for efficient isolation and analysis of circulating tumor cells. Biosens Bioelectron. 2022;213:114425. https://doi.org/10.1016/j.bios.2022.114425.
17. Huang XY, et al. A clinically feasible circulating tumor cell sorting system for monitoring the progression of advanced hepatocellular carcinoma. J Nanobiotechnol. 2023;21:25. https://doi.org/10.1186/s12951-023-01783-9.
18. Feely N, et al. Targeting mucin protein enables rapid and efficient ovarian cancer cell capture: role of nanoparticle properties in efficient capture and culture. Small. 2023;19:e2207154. https://doi.org/10.1002/smll.202207154.
19. Liu Z, et al. Negative enrichment by immunomagnetic nanobeads for unbiased characterization of circulating tumor cells from peripheral blood of cancer patients. J Transl Med. 2011;9:70. https://doi.org/10.1186/1479-5876-9-70.
20. Tong B, et al. Prognostic significance of circulating tumor cells in non-small cell lung cancer patients undergoing chemotherapy. Oncotarget. 2017;8:86615–24https://doi.org/10.18632/oncotarget.21255
21. Yu H, et al. Significant diagnostic value of circulating tumour cells in colorectal cancer. Oncol Lett. 2020;20:317–25. https://doi.org/10.3892/ol.2020.11537.
22. Drucker A, et al. Comparative performance of different methods for circulating tumor cell enrichment in metastatic breast cancer patients. PLoS One. 2020;15:e0237308. https://doi.org/10.1371/journal.pone.0237308.
23. Chen Y, et al. Regenerative nanooctopus based on multivalent-aptamer-functionalized magnetic microparticles for effective cell capture in whole blood. Anal Chem. 2019;91:4017–22. https://doi.org/10.1021/acs.analchem.8b05432.
24. Chen Y, et al. Non-invasive isolation of rare circulating tumor cells with a DNA mimic of double-sided tape using multimeric aptamers. Nanoscale. 2019;11:5879–83. https://doi.org/10.1039/c9nr00364a.
25. Ding C, Zhang C, Cheng S, Xian Y. Multivalent aptamer functionalized Ag 2 S Nanodots/Hybrid cell membrane-coated magnetic nanobioprobe for the ultrasensitive isolation and detection

of circulating tumor cells. Adv Funct Mat. 2020;30:1909781. https://doi.org/10.1002/adfm.201909781.
26. Vajhadin F, et al. MXene-based cytosensor for the detection of HER2-positive cancer cells using CoFe(2)O(4)@Ag magnetic nanohybrids conjugated to the HB5 aptamer. Biosens Bioelectron. 2022;195:113626.https://doi.org/10.1016/j.bios.2021.113626
27. Wang S, et al. Three-dimensional nanostructured substrates toward efficient capture of circulating tumor cells. Angew Chem Int Ed Engl. 2009;48:8970–3. https://doi.org/10.1002/anie.200901668.
28. Zhang N, et al. Electrospun TiO2 nanofiber-based cell capture assay for detecting circulating tumor cells from colorectal and gastric cancer patients. Adv Mater. 2012;24:2756–60. https://doi.org/10.1002/adma.201200155.
29. Zhao L, et al. High-purity prostate circulating tumor cell isolation by a polymer nanofiber-embedded microchip for whole exome sequencing. Adv Mater. 2013;25:2897–902. https://doi.org/10.1002/adma.201205237.
30. Zhang P, et al. Programmable fractal nanostructured interfaces for specific recognition and electrochemical release of cancer cells. Adv Mater. 2013;25:3566–70. https://doi.org/10.1002/adma.201300888.
31. Sun N, et al. A cellular compatible chitosan nanoparticle surface for isolation and in situ culture of rare number CTCs. Small. 2015;11:5444–51. https://doi.org/10.1002/smll.201501718.
32. Sun N, et al. A multiscale TiO2 nanorod array for ultrasensitive capture of circulating tumor cells. ACS Appl Mater Interfaces. 2016;8:12638–43. https://doi.org/10.1021/acsami.6b02178.
33. Zhai TT, Ye D, Zhang QW, Wu ZQ, Xia XH. Highly efficient capture and electrochemical release of circulating tumor cells by using aptamers modified gold nanowire arrays. ACS Appl Mater Interfaces. 2017;9:34706–14. https://doi.org/10.1021/acsami.7b11107.
34. Harb W, et al. Mutational analysis of circulating tumor cells using a novel microfluidic collection device and qPCR assay. Transl Oncol. 2013;6:528–38. https://doi.org/10.1593/tlo.13367.
35. Winer-Jones JP, et al. Circulating tumor cells: clinically relevant molecular access based on a novel CTC flow cell. PLoS One. 2014;9:e86717. https://doi.org/10.1371/journal.pone.0086717.
36. Poudineh M, et al. Tracking the dynamics of circulating tumour cell phenotypes using nanoparticle-mediated magnetic ranking. Nat Nanotechnol. 2017;12:274–81. https://doi.org/10.1038/nnano.2016.239.
37. Nora Dickson M, et al. Efficient capture of circulating tumor cells with a novel immunocytochemical microfluidic device. Biomicrofluidics. 2011;5:34119–3411915. https://doi.org/10.1063/1.3623748.
38. Mayer JA, et al. FISH-based determination of HER2 status in circulating tumor cells isolated with the microfluidic CEE™ platform. Cancer Genet. 2011;204:589–95. https://doi.org/10.1016/j.cancergen.2011.10.011.
39. Nagrath S, et al. Isolation of rare circulating tumour cells in cancer patients by microchip technology. Nature. 2007;450:1235–9. https://doi.org/10.1038/nature06385.
40. Adams AA, et al. Highly efficient circulating tumor cell isolation from whole blood and label-free enumeration using polymer-based microfluidics with an integrated conductivity sensor. J Am Chem Soc. 2008;130:8633–41. https://doi.org/10.1021/ja8015022.
41. Stott SL, et al. Isolation of circulating tumor cells using a microvortex-generating herringbone-chip. Proc Natl Acad Sci U S A. 2010;107:18392–7. https://doi.org/10.1073/pnas.1012539107.
42. Wang S, et al. Highly efficient capture of circulating tumor cells by using nanostructured silicon substrates with integrated chaotic micromixers. Angew Chem Int Ed Engl. 2011;50:3084–8. https://doi.org/10.1002/anie.201005853.
43. Yoon HJ, et al. Sensitive capture of circulating tumour cells by functionalized graphene oxide nanosheets. Nat Nanotechnol. 2013;8:735–41. https://doi.org/10.1038/nnano.2013.194.
44. Sheng W, et al. Capture, release and culture of circulating tumor cells from pancreatic cancer patients using an enhanced mixing chip. Lab Chip. 2014;14:89–98. https://doi.org/10.1039/c3lc51017d.
45. Sheng W, et al. Aptamer-enabled efficient isolation of cancer cells from whole blood using a microfluidic device. Anal Chem. 2012;84:4199–206. https://doi.org/10.1021/ac3005633.
46. Zhao L, et al. Enhanced and differential capture of circulating tumor cells from lung cancer patients by microfluidic assays using aptamer cocktail. Small. 2016;12:1072–81. https://doi.org/10.1002/smll.201503188.
47. Park MH, et al. Enhanced isolation and release of circulating tumor cells using nanoparticle binding and ligand exchange in a microfluidic chip. J Am Chem Soc. 2017;139:2741–9. https://doi.org/10.1021/jacs.6b12236.
48. Saucedo-Zeni N, et al. A novel method for the in vivo isolation of circulating tumor cells from peripheral blood of cancer patients using a functionalized and structured medical wire. Int J Oncol. 2012;41:1241–50. https://doi.org/10.3892/ijo.2012.1557.
49. Whitesides GM. The origins and the future of microfluidics. Nature. 2006;442:368–73. https://doi.org/10.1038/nature05058.
50. Fachin F, et al. Monolithic chip for high-throughput blood cell depletion to sort rare circulating tumor cells. Sci Rep. 2017;7:10936. https://doi.org/10.1038/s41598-017-11119-x.
51. Vona G, et al. Isolation by size of epithelial tumor cells : a new method for the immunomorphological and molecular characterization of circulatingtumor cells. Am J Pathol. 2000;156:57–63. https://doi.org/10.1016/s0002-9440(10)64706-2.
52. Tamminga M, et al. Detection of Circulating tumor cells in the diagnostic leukapheresis product of non-small-cell lung cancer patients comparing cell search(®) and ISET. Cancers (Basel). 2020;12:896. https://doi.org/10.3390/cancers12040896.
53. Desitter I, et al. A new device for rapid isolation by size and characterization of rare circulating tumor cells. Anticancer Res. 2011;31:427–41.
54. Kulasinghe A, et al. Impact of label-free technologies in head and neck cancer circulating tumour cells. Oncotarget. 2016;7:71223–34. https://doi.org/10.18632/oncotarget.12086.
55. Bobek V, Kacprzak G, Rzechonek A, Kolostova K. Detection and cultivation of circulating tumor cells in malignant pleural mesothelioma. Anticancer Res. 2014;34:2565–9.
56. Bobek V, Gurlich R, Eliasova P, Kolostova K. Circulating tumor cells in pancreatic cancer patients: enrichment and cultivation. World J Gastroenterol. 2014;20:17163–70. https://doi.org/10.3748/wjg.v20.i45.17163.
57. Adams DL, et al. The systematic study of circulating tumor cell isolation using lithographic microfilters. RSC Adv. 2014;9:4334–42. https://doi.org/10.1039/c3ra46839a.
58. Hvichia GE, et al. A novel microfluidic platform for size and deformability based separation and the subsequent molecular characterization of viable circulating tumor cells. Int J Cancer. 2016;138:2894–904. https://doi.org/10.1002/ijc.30007.
59. Kim TH, et al. FAST: size-selective, clog-free isolation of rare cancer cells from whole blood at a liquid-liquid interface. Anal Chem. 2017;89:1155–62. https://doi.org/10.1021/acs.analchem.6b03534.
60. Tan SJ, Yobas L, Lee GY, Ong CN, Lim CT. Microdevice for the isolation and enumeration of cancer cells from blood. Biomed Microdevices. 2009;11:883–92. https://doi.org/10.1007/s10544-009-9305-9.
61. Tan SJ, et al. Versatile label free biochip for the detection of circulating tumor cells from peripheral blood in cancer patients.

Biosens Bioelectron. 2010;26:1701–5. https://doi.org/10.1016/j.bios.2010.07.054.
62. Xu T, Lu B, Tai YC, Goldkorn A. A cancer detection platform which measures telomerase activity from live circulating tumor cells captured on a microfilter. Cancer Res. 2010;70:6420–6. https://doi.org/10.1158/0008-5472.Can-10-0686.
63. Hosokawa M, et al. Size-selective microcavity array for rapid and efficient detection of circulating tumor cells. Anal Chem. 2010;82:6629–35. https://doi.org/10.1021/ac101222x.
64. Yagi S, et al. Development of an automated size-based filtration system for isolation of circulating tumor cells in lung cancer patients. PLoS One. 2017;12:e0179744.https://doi.org/10.1371/journal.pone.0179744
65. Zhou MD, et al. Separable bilayer microfiltration device for viable label-free enrichment of circulating tumour cells. Sci Rep. 2014;4:7392. https://doi.org/10.1038/srep07392.
66. Rosenberg R, et al. Comparison of two density gradient centrifugation systems for the enrichment of disseminated tumor cells in blood. Cytometry. 2002;49:150–8. https://doi.org/10.1002/cyto.10161.
67. Riebensahm C, et al. Clonality of circulating tumor cells in breast cancer brain metastasis patients. Breast Cancer Res. 2019;21:101. https://doi.org/10.1186/s13058-019-1184-2.
68. Campton DE, et al. High-recovery visual identification and single-cell retrieval of circulating tumor cells for genomic analysis using a dual-technology platform integrated with automated immunofluorescence staining. BMC Cancer. 2015;15:360. https://doi.org/10.1186/s12885-015-1383-x.
69. van der Toom EE, et al. Analogous detection of circulating tumor cells using the AccuCyte(®) -CyteFinder(®) system and ISET system in patients with locally advanced and metastatic prostate cancer. Prostate. 2018;78:300–7. https://doi.org/10.1002/pros.23474.
70. Loutherback K, et al. Deterministic separation of cancer cells from blood at 10 mL/min. AIP Adv. 2012;2:42107. https://doi.org/10.1063/1.4758131.
71. Park ES, et al. Continuous flow deformability-based separation of circulating tumor cells using microfluidic ratchets. Small. 2016;12:1909–19. https://doi.org/10.1002/smll.201503639.
72. Au SH, et al. Microfluidic isolation of circulating tumor cell clusters by size and asymmetry. Sci Rep. 2017;7:2433. https://doi.org/10.1038/s41598-017-01150-3.
73. Lee Y, Guan G, Bhagat AA. ClearCell® FX, a label-free microfluidics technology for enrichment of viable circulating tumor cells. Cytometry A. 2018;93:1251–4. https://doi.org/10.1002/cyto.a.23507.
74. Wong VC, Ko JM, Lam CT, Lung ML. Succinct workflows for circulating tumor cells after enrichment: From systematic counting to mutational profiling. PLoS One. 2017;12:e0177276.https://doi.org/10.1371/journal.pone.0177276
75. Warkiani ME, et al. Slanted spiral microfluidics for the ultra-fast, label-free isolation of circulating tumor cells. Lab Chip. 2014;14:128–37. https://doi.org/10.1039/c3lc50617g.
76. Lin E, et al. High-throughput microfluidic labyrinth for the label-free isolation of circulating tumor cells. Cell Syst. 2017;5:295–304.e294. https://doi.org/10.1016/j.cels.2017.08.012.
77. Sollier E, et al. Size-selective collection of circulating tumor cells using Vortex technology. Lab Chip. 2014;14:63–77. https://doi.org/10.1039/c3lc50689d.
78. Che J, et al. Classification of large circulating tumor cells isolated with ultra-high throughput microfluidic vortex technology. Oncotarget. 2016;7:12748–60. https://doi.org/10.18632/oncotarget.7220.
79. Zhou J, et al. Isolation of circulating tumor cells in non-small-cell-lung-cancer patients using a multi-flow microfluidic channel. Microsyst Nanoeng. 2019;5:8. https://doi.org/10.1038/s41378-019-0045-6.
80. Gupta V, et al. ApoStream(™), a new dielectrophoretic device for antibody independent isolation and recovery of viable cancer cells from blood. Biomicrofluidics. 2012;6:24133. https://doi.org/10.1063/1.4731647.
81. O'Shannessy DJ, Davis DW, Anderes K, Somers EB. Isolation of circulating tumor cells from multiple epithelial cancers with ApoStream(®) for Detecting (or Monitoring) the expression of folate receptor alpha. Biomark Insights. 2016;11:7–18. https://doi.org/10.4137/bmi.S35075.
82. Di Trapani M, Manares N, Medoro G. DEPArray™ system: An automatic image-based sorter for isolation of pure circulating tumor cells. Cytometry A. 2018;93:1260–6. https://doi.org/10.1002/cyto.a.23687.
83. Rossi T, et al. Single-Cell NGS-based analysis of copy number alterations reveals new insights in circulating tumor cells persistence in early-stage breast cancer. Cancers (Basel). 2020;12:2490. https://doi.org/10.3390/cancers12092490.
84. Li M, Anand RK. High-throughput selective capture of single circulating tumor cells by dielectrophoresis at a wireless electrode array. J Am Chem Soc. 2017;139:8950–9. https://doi.org/10.1021/jacs.7b03288.
85. Lu J, et al. Isolation of circulating epithelial and tumor progenitor cells with an invasive phenotype from breast cancer patients. Int J Cancer. 2010;126:669–83. https://doi.org/10.1002/ijc.24814.
86. Chen W, et al. Nanoroughened surfaces for efficient capture of circulating tumor cells without using capture antibodies. ACS Nano. 2013;7:566–75. https://doi.org/10.1021/nn304719q.
87. Wang J, et al. A novel microfluidic system for enrichment of functional circulating tumor cells in cancer patient blood samples by combining cell size and invasiveness. Biosens Bioelectron. 2023;227:115159. https://doi.org/10.1016/j.bios.2023.115159.
88. Liu Y, et al. CTC-race: single-cell motility assay of circulating tumor cells from metastatic lung cancer patients. ACS Nano. 2024;18:8683–93. https://doi.org/10.1021/acsnano.3c09450.
89. Zheng S, et al. Membrane microfilter device for selective capture, electrolysis and genomic analysis of human circulating tumor cells. J Chromatogr A. 2007;1162:154–61. https://doi.org/10.1016/j.chroma.2007.05.064.
90. Holdich R, Kosvintsev S, Cumming I, Zhdanov S. Pore design and engineering for filters and membranes. Philos Trans A Math Phys Eng Sci. 2006;364:161–74. https://doi.org/10.1098/rsta.2005.1690.
91. He S, Wei J, Ding L, Yang X, Wu Y. State-of-the-arts techniques and current evolving approaches in the separation and detection of circulating tumor cell. Talanta. 2022;239:123024. https://doi.org/10.1016/j.talanta.2021.123024.
92. Descamps L, Le Roy D, Deman AL. Microfluidic-based technologies for CTC isolation: a review of 10 years of intense efforts towards liquid biopsy. Int J Mol Sci. 2022;23:1981. https://doi.org/10.3390/ijms23041981.
93. Gonda MA, Aaronson SA, Ellmore N, Zeve VH, Nagashima K. Ultrastructural studies of surface features of human normal and tumor cells in tissue culture by scanning and transmission electron microscopy. J Natl Cancer Inst. 1976;56:245–63. https://doi.org/10.1093/jnci/56.2.245.
94. Buscail E, et al. High Clinical value of liquid biopsy to detect circulating tumor cells and tumor exosomes in pancreatic ductal adenocarcinoma patients eligible for up-front surgery. Cancers (Basel). 2019;11:1656. https://doi.org/10.3390/cancers11111656.
95. Gleghorn JP, et al. Capture of circulating tumor cells from whole blood of prostate cancer patients using geometrically enhanced differential immunocapture (GEDI) and a prostate-specific antibody. Lab Chip. 2010;10:27–9. https://doi.org/10.1039/b917959c.
96. Ozkumur E, et al. Inertial focusing for tumor antigen-dependent and -independent sorting of rare circulating tumor cells. Sci

Transl Med. 2013;5:179ra147.https://doi.org/10.1126/scitranslmed.3005616
97. Mishra A, et al. Ultrahigh-throughput magnetic sorting of large blood volumes for epitope-agnostic isolation of circulating tumor cells. Proc Natl Acad Sci U S A. 2020;117:16839–47. https://doi.org/10.1073/pnas.2006388117.
98. Song Y, et al. Bioinspired engineering of a multivalent aptamer-functionalized nanointerface to enhance the capture and release of circulating tumor cells. Angew Chem Int Ed Engl. 2019;58:2236–40. https://doi.org/10.1002/anie.201809337.
99. Zhang J, et al. DNA Nanolithography enables a highly ordered recognition interface in a microfluidic chip for the efficient capture and release of circulating tumor cells. Angew Chem Int Ed Engl. 2020;59:14115–9. https://doi.org/10.1002/anie.202005974.
100. Wu L, et al. Fluidic multivalent membrane nanointerface enables synergetic enrichment of circulating tumor cells with high efficiency and viability. J Am Chem Soc. 2020;142:4800–6. https://doi.org/10.1021/jacs.9b13782.
101. Green BJ, et al. PillarX: a microfluidic device to profile circulating tumor cell clusters based on geometry, deformability, and epithelial state. Small. 2022;18:e2106097. https://doi.org/10.1002/smll.202106097.
102. Gast CE, et al. Cell fusion potentiates tumor heterogeneity and reveals circulating hybrid cells that correlate with stage and survival. Sci Adv. 2018;4:eaat7828. https://doi.org/10.1126/sciadv.aat7828.
103. Wu S, et al. Rapid label-free isolation of circulating tumor cells from patients' peripheral blood using electrically charged Fe(3)O(4) nanoparticles. ACS Appl Mater Interfaces. 2020;12:4193–203. https://doi.org/10.1021/acsami.9b16385.
104. Akolkar D, et al. Circulating ensembles of tumor-associated cells: A redoubtable new systemic hallmark of cancer. Int J Cancer. 2020;146:3485–94. https://doi.org/10.1002/ijc.32815.
105. Zhang Q, et al. Isolation of circulating tumor cells and detection of EGFR mutations in patients with non-small-cell lung cancer. Oncol Lett. 2019;17:3799–807. https://doi.org/10.3892/ol.2019.10016.
106. Strati A, et al. Development and analytical validation of a reverse transcription droplet digital PCR (RT-ddPCR) Assay for PD-L1 transcripts in circulating tumor cells. Clin Chem. 2021;67:642–52. https://doi.org/10.1093/clinchem/hvaa321.
107. Ntzifa A, Kotsakis A, Georgoulias V, Lianidou E. Detection of EGFR mutations in plasma cfDNA and paired CTCs of NSCLC patients before and after osimertinib therapy using crystal digital PCR. Cancers (Basel). 2021;13:276. https://doi.org/10.3390/cancers13112736.
108. Vismara M, et al. Single-cell phenotypic and molecular characterization of circulating tumor cells isolated from cryopreserved peripheral blood mononuclear cells of patients with lung cancer and sarcoma. Clin Chem. 2022;68:691–701. https://doi.org/10.1093/clinchem/hvac019.
109. Zhu Z, Hu E, Shen H, Tan J, Zeng S. The functional and clinical roles of liquid biopsy in patient-derived models. J Hematol Oncol. 2023;16:36. https://doi.org/10.1186/s13045-023-01433-5.
110. Kahounová Z, et al. Circulating tumor cell-derived preclinical models: current status and future perspectives. Cell Death Dis. 2023;14:530. https://doi.org/10.1038/s41419-023-06059-6.
111. Pereira-Veiga T, Schneegans S, Pantel K, Wikman H. Circulating tumor cell-blood cell crosstalk: Biology and clinical relevance. Cell Rep. 2022;40:111298. https://doi.org/10.1016/j.celrep.2022.111298.
112. Huang L, et al. Next-Generation Preclinical Functional Testing Models in Cancer Precision Medicine: CTC-Derived Organoids. Small Methods. 2024;8:e2301009.https://doi.org/10.1002/smtd.202301009
113. Aguilar-Avelar C, et al. High-throughput automated microscopy of circulating tumor cells. Sci Rep. 2019;9:13766. https://doi.org/10.1038/s41598-019-50241-w.
114. Yee-de León JF, et al. Characterization of a novel automated microfiltration device for the efficient isolation and analysis of circulating tumor cells from clinical blood samples. Sci Rep. 2020;10:7543. https://doi.org/10.1038/s41598-020-63672-7.
115. Zeune LL, et al. Deep learning of circulating tumour cells. Nature Machine Intelligence. 2020;2:124–33. https://doi.org/10.1038/s42256-020-0153-x.
116. Shen C, et al. Automatic detection of circulating tumor cells and cancer associated fibroblasts using deep learning. Sci Rep. 2023;13:5708. https://doi.org/10.1038/s41598-023-32955-0.
117. Akashi T, et al. The use of an artificial intelligence algorithm for circulating tumor cell detection in patients with esophageal cancer. Oncol Lett. 2023;26:320. https://doi.org/10.3892/ol.2023.13906.
118. Guo Z, et al. Circulating tumor cell identification based on deep learning. Front Oncol. 2022;12:843879. https://doi.org/10.3389/fonc.2022.843879.
119. Xu X, et al. Attention Mask R-CNN with edge refinement algorithm for identifying circulating genetically abnormal cells. Cytometry A. 2023;103:227–39. https://doi.org/10.1002/cyto.a.24682.
120. Wang S, et al. Label-free detection of rare circulating tumor cells by image analysis and machine learning. Sci Rep. 2020;10:12226. https://doi.org/10.1038/s41598-020-69056-1.
121. Moallem G, Pore AA, Gangadhar A, Sari-Sarraf H, Vanapalli SA. Detection of live breast cancer cells in bright-field microscopy images containing white blood cells by image analysis and deep learning. J Biomed Opt. 2022;27:076003.https://doi.org/10.1117/1.Jbo.27.7.076003
122. Piansaddhayanon C, et al. Label-free tumor cells classification using deep learning and high-content imaging. Sci Data. 2023;10:570. https://doi.org/10.1038/s41597-023-02482-8.
123. Ozaki Y, et al. Label-free classification of cells based on supervised machine learning of subcellular structures. PLoS One. 2019;14:e0211347. https://doi.org/10.1371/journal.pone.0211347.
124. Yamada H, et al. Label-free imaging flow cytometer for analyzing large cell populations by line-field quantitative phase microscopy with digital refocusing. Biomed Opt Express. 2020;11:2213–23. https://doi.org/10.1364/boe.389435.
125. Hirotsu A, et al. Artificial intelligence-based classification of peripheral blood nucleated cells using label-free imaging flow cytometry. Lab Chip. 2022;22:3464–74. https://doi.org/10.1039/d2lc00166g.
126. Pirone D, et al. Label-free liquid biopsy through the identification of tumor cells by machine learning-powered tomographic phase imaging flow cytometry. Sci Rep. 2023;13:6042. https://doi.org/10.1038/s41598-023-32110-9.
127. Borrelli F, et al. AI-aided holographic flow cytometry for label-free identification of ovarian cancer cells in the presence of unbalanced datasets. APL Bioeng. 2023;7:026110.https://doi.org/10.1063/5.0153413
128. Vora N, Shekhar P, Esmail M, Patra A, Georgakoudi I. Label-free flow cytometry of rare circulating tumor cell clusters in whole blood. Sci Rep. 2022;12:10721. https://doi.org/10.1038/s41598-022-14003-5.
129. Vora N, Shekar P, Esmail M, Patra A, Georgakoudi I. Deep learning-enabled, detection of rare circulating tumor cell clusters in whole blood using label-free, flow cytometry. bioRxiv. 2023. https://doi.org/10.1101/2023.08.01.551485.
130. Radfar P, et al. Single-cell analysis of circulating tumour cells: enabling technologies and clinical applications. Trends Biotechnol. 2022;40:1041–60. https://doi.org/10.1016/j.tibtech.2022.02.004.

131. Visal TH, den Hollander P, Cristofanilli M, Mani SA. Circulating tumour cells in the -omics era: how far are we from achieving the "singularity"? Br J Cancer. 2022;127:173–84. https://doi.org/10.1038/s41416-022-01768-9.
132. Keller L, Pantel K. Unravelling tumour heterogeneity by single-cell profiling of circulating tumour cells. Nat Rev Cancer. 2019;19:553–67. https://doi.org/10.1038/s41568-019-0180-2.
133. Cheng YH, et al. Hydro-Seq enables contamination-free high-throughput single-cell RNA-sequencing for circulating tumor cells. Nat Commun. 2019;10:2163. https://doi.org/10.1038/s41467-019-10122-2.
134. Ring A, Nguyen-Strauli BD, Wicki A, Aceto N. Biology, vulnerabilities and clinical applications of circulating tumour cells. Nat Rev Cancer. 2023;23:95–111. https://doi.org/10.1038/s41568-022-00536-4.
135. Shoji Y, Bustos MA, Gross R, Hoon DSB. Recent developments of circulating tumor cell analysis for monitoring cutaneous melanoma patients. Cancers (Basel). 2022;14:859. https://doi.org/10.3390/cancers14040859.
136. Fabisiewicz A, Szostakowska-Rodzos M, Zaczek AJ, Grzybowska EA. Circulating tumor cells in early and advanced breast cancer; biology and prognostic value. Int J Mol Sci. 2020;21:1671. https://doi.org/10.3390/ijms21051671.
137. Kotsifaki A, Maroulaki S, Armakolas A. Exploring the immunological profile in breast cancer: recent advances in diagnosis and prognosis through circulating tumor cells. Int J Mol Sci. 2024;25:1832. https://doi.org/10.3390/ijms25094832.
138. Kejík Z, et al. Circulating Tumour Cells (CTCs) in NSCLC: From prognosis to therapy design. Pharmaceutics. 2021;13:1879. https://doi.org/10.3390/pharmaceutics13111879.
139. Hamilton G, Rath B, Stickler S. Significance of circulating tumor cells in lung cancer: a narrative review. Transl Lung Cancer Res. 2023;12:877–94.https://doi.org/10.21037/tlcr-22-712
140. Andrikou K, et al. Circulating tumour cells: detection and application in advanced non-small cell lung cancer. Int J Mol Sci. 2023;24:16085. https://doi.org/10.3390/ijms242216085.
141. Wang X, Bai L, Kong L, Guo Z. Advances in circulating tumor cells for early detection, prognosis and metastasis reduction in lung cancer. Front Oncol. 2024;14:1411731. https://doi.org/10.3389/fonc.2024.1411731.
142. Tsai KY, et al. Current applications and future directions of circulating tumor cells in colorectal cancer recurrence. Cancers (Basel). 2024;16:2316. https://doi.org/10.3390/cancers16132316.
143. Petrik J, et al. Circulating tumor cells in colorectal cancer: detection systems and clinical utility. Int J Mol Sci. 2022;23:13582. https://doi.org/10.3390/ijms232113582.
144. Hu M, et al. Circulating tumor cells in colorectal cancer in the era of precision medicine. J Mol Med (Berl). 2022;100:197–213. https://doi.org/10.1007/s00109-021-02162-3.
145. Jiang M, et al. Detection and clinical significance of circulating tumor cells in colorectal cancer. Biomark Res. 2021;9:85. https://doi.org/10.1186/s40364-021-00326-4.
146. Enikeev D, Morozov A, Babaevskaya D, Bazarkin A, Malavaud B. A systematic review of circulating tumor cells clinical application in prostate cancer diagnosis. Cancers (Basel). 2022;14:3802. https://doi.org/10.3390/cancers14153802.
147. Cieślikowski WA, Antczak A, Nowicki M, Zabel M, Budna-Tukan J. Clinical relevance of circulating tumor cells in prostate cancer management. Biomedicines. 2021;9:1179. https://doi.org/10.3390/biomedicines9091179.
148. Lu L, Hu W, Liu B, Yang T. Insights into circulating tumor cell clusters: a barometer for treatment effects and prognosis for prostate cancer patients. Cancers (Basel). 2022;14:3985. https://doi.org/10.3390/cancers14163985.
149. Asawa S, Nüesch M, Gvozdenovic A, Aceto N. Circulating tumour cells in gastrointestinal cancers: food for thought? Br J Cancer. 2023;128:1981–90. https://doi.org/10.1038/s41416-023-02228-8.
150. Thanhhuong P, et al. Emerging role of circulating tumor cells in gastric cancer. Cancers (Basel). 2020;12:695. https://doi.org/10.3390/cancers12030695.
151. Konczalla L, et al. Clinical significance of circulating tumor cells in gastrointestinal carcinomas. Diagnostics (Basel). 2020;10:192. https://doi.org/10.3390/diagnostics10040192.
152. Salehi M, et al. Circulating Tumor Cells as a Promising Tool for Early Detection of Hepatocellular Carcinoma. Cells. 2023;12:2260. https://doi.org/10.3390/cells12182260.
153. Teng PC, et al. Circulating tumor cells: A step toward precision medicine in hepatocellular carcinoma. J Gastroenterol Hepatol. 2022;37:1179–90. https://doi.org/10.1111/jgh.15886.
154. Ahn JC, et al. Detection of circulating tumor cells and their implications as a biomarker for diagnosis, prognostication, and therapeutic monitoring in hepatocellular carcinoma. Hepatology. 2021;73:422–36. https://doi.org/10.1002/hep.31165.
155. Zhang Q, et al. Circulating tumor cells in hepatocellular carcinoma: single-cell based analysis, preclinical models, and clinical applications. Theranostics. 2020;10:12060–71. https://doi.org/10.7150/thno.48918.
156. Ko SW, Yoon SB. Clinical implications and perspectives of portal venous circulating tumor cells in pancreatic cancer. World J Gastrointest Oncol. 2023;15:632–43. https://doi.org/10.4251/wjgo.v15.i4.632.
157. Yeo D, et al. Exploring the clinical utility of pancreatic cancer circulating tumor cells. Int J Mol Sci. 2022;23:1671. https://doi.org/10.3390/ijms23031671.
158. Aktar S, Baghaie H, Islam F, Gopalan V, Lam AK. Current status of circulating tumor cells in head and neck squamous cell carcinoma: a review. Otolaryngol Head Neck Surg. 2023;168:988–1005. https://doi.org/10.1002/ohn.186.
159. Rao VU, et al. Circulating tumour cells in head and neck cancers: Biological insights. J Oral Pathol Med. 2020;49:842–8. https://doi.org/10.1111/jop.13075.
160. Couto-Cunha A, Jerónimo C, Henrique R. Circulating tumor cells as biomarkers for renal cell carcinoma: ready for prime time? Cancers (Basel). 2022;15:287. https://doi.org/10.3390/cancers15010287.
161. Palmela Leitão T, et al. Circulating tumor cell detection methods in renal cell carcinoma: a systematic review. Crit Rev Oncol Hematol. 2021;161:103331. https://doi.org/10.1016/j.critrevonc.2021.103331.
162. Zeyghami W, et al. Liquid biopsies in thyroid cancers: a systematic review and meta-analysis. Endocr Relat Cancer. 2023;30:e230002.https://doi.org/10.1530/erc-23-0002
163. Wang W, Zheng Z, Lei J. CTC, ctDNA, and exosome in thyroid cancers: a review. Int J Mol Sci. 2023;24:13767. https://doi.org/10.3390/ijms241813767.
164. Jou HJ, Ling PY, Hsu HT. Circulating tumor cells as a "real-time liquid biopsy": Recent advances and the application in ovarian cancer. Taiwan J Obstet Gynecol. 2022;61:34–9. https://doi.org/10.1016/j.tjog.2021.11.008.

165. Salu P, Reindl KM. Advancements in circulating tumor cell research: bridging biology and clinical applications. Cancers (Basel). 2024;16:1213. https://doi.org/10.3390/cancers16061213.
166. Vasseur A, Kiavue N, Bidard FC, Pierga JY, Cabel L. Clinical utility of circulating tumor cells: an update. Mol Oncol. 2021;15:1647–66. https://doi.org/10.1002/1878-0261.12869.
167. Diamantopoulou Z, et al. The metastatic spread of breast cancer accelerates during sleep. Nature. 2022;607:156–62. https://doi.org/10.1038/s41586-022-04875-y.
168. Sun YF, et al. Dissecting spatial heterogeneity and the immune-evasion mechanism of CTCs by single-cell RNA-seq in hepatocellular carcinoma. Nat Commun. 2021;12:4091. https://doi.org/10.1038/s41467-021-24386-0.